LABORATORY STUDIES OF AFTERGLOW SPECTRA

FOR

MOLECULAR GASES

by

AJAI KUMAR

A THESIS

SUBMITTED FOR THE DEGREE OF

DOCTOR OF PHILOSOPHY

OF THE

GUJARAT UNIVERSITY

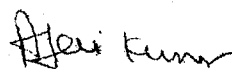AUGUST 1984

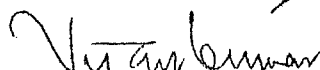PHYSICAL RESEARCH LABORATORY

AHMEDABAD 380 009

INDIA

TO MY PARENTS

CERTIFICATE

I hereby declare that the work presented in this thesis is original and has not formed the basis for the award of any degree or diploma by any University or Institution.

Ajai Kumar

Certified by:

Vijay Kumar

Professor-in-charge

Physical Research Laboratory

Ahmedabad 380 009, India

STATEMENT

The basic aim of the work presented in this thesis, is to study the afterglow spectra of molecular gases like nitrogen and oxygen as a function of pressure, temperature and carrier gas. This will contribute to the knowledge about the possible population mechanisms of the emitting states, and also about the quenching of emitting states by carrier gas. A high resolution afterglow spectrometer which includes gas purification system, discharge region, observation vessel, high speed pumping system, monochromator, highly sensitive light detector and data acquisition system has been designed and fabricated in the laboratory. The novel feature of the experimental set up is the Wrede-Harteck gauge which has been incorporated in the system. The Wrede-Harteck gauge has been used to measure absolute atomic concentration under various experimental conditions.

The afterglow spectra of nitrogen is studied at $77^{\circ}K$ and $300^{\circ}K$ in the spectral range from 1900 to 8000 $\overset{\circ}{A}$. The relative vibrational intensities for the first positive system have been computed from the afterglow spectra at both the temperatures. The pressure dependence of intensities of various bands have been investigated at pressures between 2 and 7 Torr while the effect of diluent like argon has been studied at a fixed argon pressure of 5 Torr and varying nitrogen pressure from 0.2 to 3 Torr. The mechanisms for populating the different vibrational levels of B $^3\Pi_g$ state have been discussed in the light of new results obtained in the present

experiment and previous measurements reported in the literature.

For the first time, quenching rates of (12,8) and (11,7) vibrational bands of the first positive system of nitrogen by nitric oxide, observed in the afterglow, have been measured for temperatures varying from about $87^\circ K$ to $90^\circ K$. Also, the quenching rates for vibrational level $v' = 12, 11, 10$ of the first positive system of nitrogen by argon have been studied at room temperature.

High resolution afterglow spectra for molecular nitrogen have been obtained, for the first time, for the (12,8), (12,9), (11,7) and (11,8) vibrational bands of the first positive system (B $^3\Pi_g \rightarrow$ A $^3\Sigma_u^+$) and studied at $300^\circ K$ and $77^\circ K$. The rotational transitions corresponding to P, Q, R branches have been unambiguously identified in the afterglow spectra. From these results, dissociation energy corresponding to the lowest dissociation limit of nitrogen has been computed and result obtained has been compared with that reported by others in relatively recent times.

The afterglow spectra of oxygen corresponding to Herzberg I system have been studied at $300^\circ K$ in the spectral region from about 2400 to 4250 $\overset{o}{A}$ at various oxygen pressures ranging from 2 to 7 Torr. Practically no laboratory measurements have been made to study quantitatively, the deactivation of A $^3\Sigma_u^+$ state by O_2 so far. The deactivation of O_2(A $^3\Sigma_u^+$) state by oxygen itself has been studied in detail and the quenching rates for some of the vibrational bands of Herzberg I system have been calculated. The afterglow spectra of oxygen have also

been studied in the presence of diluents like argon and helium at oxygen pressure ranging from 0.2 to 1 Torr. The quenching rates for some bands of Herzberg I system by argon and helium have also been measured.

ACKNOWLEDGEMENTS

CONTENTS

CHAPTER I

INTRODUCTION

I. Afterglow

An afterglow can be described as a light emission process
which persists in some gases even after the excitation agency has been
interrupted. The term afterglow is used to describe the system in
which electronically excited molecules are formed by the combination
of free atoms either with each other or with molecules. This is one of
the important phenomena occurring in planetary atmospheres during night
time. Hence the data obtained in laboratory on afterglow will be
important in studying the neutral dynamics of planetary atmospheres.
Afterglow data also provide various details of the atomic and molecular
collision processes like electronic quenching, vibrational relaxation
and reaction kinetics. Also, it gives information about the

dissociation energies of molecules corresponding to first or/and higher dissociation limits. Afterglows are mainly useful for studying excited states which are not readily populated by photon or electron bombardment.

When the electrical discharge through a gas is switched on, it gives rise to glow in the discharge region. This glow is due to direct excitation mechanism. When an electrical discharge through the gas is switched off or the discharged gas is pumped from the discharge region to other region which is optically isolated from the discharge region, it is found that the glow still exists in some gases.

The processes responsible for light emission in afterglow can be divided into two distinct classes: two body and three body recombination of active species. In case of two body recombination, the combining species approach along a potential curve from which radiation can occur to another electronic state. In the three body process, the initial step is stabilization of the recombining species by a third body. Molecules in these stabilized states undergo colli-sion-induced radiationless transition, near the intersection of the respective potential curves, to emitting states. The molecules in these emitting states will radiate giving rise to a glow. Wavelength versus intensity analysis of this glow is called afterglow spectrum.

The vibrational intensity distribution of emission due to direct excitations will be different from the vibrational intensity distribution of afterglow. This is because the emitting states of these two types of emission are populated by different mechanism. In direct emission, molecules are populated to higher state by absorption

of energy from an interacting electron or from incident photon whereas
in afterglow, molecules in higher states are populated by recombination
of active species by two body or three body processes.

I.1. Nature of the active species in afterglow

When an electrical discharge is switched on through a mole-
cular gas, it either

a   ionizes the gaseous molecules

b   or dissociates the gas molecules into atoms

c   or excites the gas molecules to some metastable state

d   or excites the gas molecules to some higher excited state

It would be interesting to know the type of active species, responsible
for starting the afterglow, which are present as discharged products,
when the electrical discharge is switched off. Any of four types of
discharged products proposed above could be responsible for the after-
glow. This type of study was first done on the nitrogen afterglow.
Using a microwave cavity, Benson (1952) measured the electron density
in active nitrogen. He compared the available recombination energy of
N_2^+ ions and electrons with the energy content of active nitrogen which
can be measured by the heat released during its decay on a copper
surface. It was found that concentration of charged species was about
10^{-8} or less than that of neutral molecules, and that the available
recombination energy was approximately 10^{-6} times the heat content of
active nitrogen. So it rules out the possibility of N_2^+ being the
active species in afterglow. Mass spectrometric analysis by
Berkowitz et al. (1956) showed that nitrogen atom (N^{14}) in ground

state $N(^4S)$ was present in much larger quantities in active nitrogen than in ordinary undischarged nitrogen. It was also shown by them that in active nitrogen, at constant pressure and flow rate, the visible afterglow intensity was proportional to $[N]^2$ for both the (11,7) and (6,3) vibrational bands of the positive system of nitrogen afterglow.

These results clearly indicate that much of the activity of the discharged nitrogen is due to $N(^4S)$ atoms and to a number of collision processes in which the ground state atoms are actively involved. Similar type of study has been done in the oxygen afterglow also. It has been found (Broida and Gaydon (1954)) that oxygen after-glow owes its origin to the recombination of two ground state oxygen atoms in the presence of a third body.

I.2. Afterglow in Combination Processes

The most familiar reaction in gases involve the association of free atoms to form electronically excited diatomic molecules. Some-times, the association of free atoms with diatomic molecules could lead to the formation of triatomic molecules. These reactions are commonly observed by subjecting gases to a pulsed electric discharge or by flowing gases through a discharge.

The processes responsible for light emission in afterglow as mentioned previously can be divided into two distinct classes:

a   Two body recombination

b   Three body recombination

1.2.1. Two body recombination

A recombination of atom A with atom B or atom A with molecule B can be represented by the process

$$A + B \underset{k_{-1}}{\overset{k_1}{\rightleftarrows}} AB^* \overset{k_2}{\longrightarrow} AB + h\nu \qquad 1.1$$
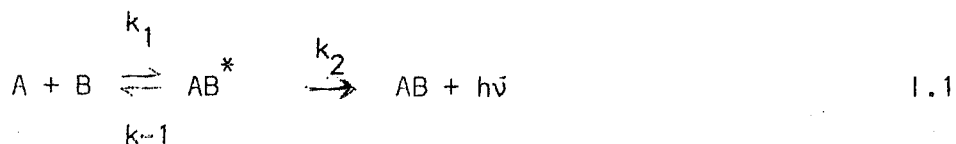
AB^* is molecule formed in excited state due to recombination of A and B. If the life time of AB^* is short, then the intensity of emission observed because of de-excitation of AB^* will be given by the relation

$$I = I^0 \, [A] \, [B] \qquad 1.2$$

where [A], [B] are concentrations of A and B. Sometimes, radiation can occur directly from a potential curve which correlates with the combining species A and B. This process is known as the reverse of direct photo-dissociation in a region of continuous absorption. Here AB^* has no real existence as a molecule and simply represents the number of collision pair lying in a specified region of the appropriate potential curve. In other case, AB^* represents a bound excited state of the molecule which is formed by the inverse predissociation. So two body combination can be grouped into two classes:

1) Two body processes in which the emitting state is formed adiabati-cally (Direct two body recombination)

2) Two body processes in which the emitting state is populated by a nonadiabatic transition between two potential curve (Two body recombination with curve-crossing).

1.2.1.1. Direct two-body recombination

Two-body recombination without crossing between potential curves takes two forms:

a   Emission occurs from a repulsive curve to a bound lower state which is the reverse of photochemical dissociation of a molecule. The best studied example is the radiative recombination of halogen atoms at high temperature. Here continuous emission in the visible region from repulsive states to the bound ground state arises from the molecular electronic transition $\sigma_u \rightarrow \Pi_g$.

b   Two body emissions are also observed in a system where the atomic transition is forbidden but the molecular transition is allowed. Such a situation has been reported in the helium afterglow by Nickerson (1935) and Tanaka and Yoshino (1963). Here the emission extends from about 60 n.m. to the long wavelength side of the forbidden atomic transition, $He(1s\ 2s\ {}^1S) \rightarrow (1s^2\ {}^1S)$. This is due to the allowed molecular transition from the bonding ${}^1\Sigma_u^+$ state of He_2, arising from $He(1s\ 2s\ {}^1S) + He(1s^2\ {}^1S)$, to the repulsive ${}^1\Sigma_g^+$ ground state of He_2, formed from $2\ He(1s^2\ {}^1S)$ atoms.

Theoretical calculation for halogen emission intensity I^0 was done classically by Bates (1951) and by applying statistical mechanics to the equilibrium between A, B and the quasi-molecule AB^* by Palmer (1967). Smith and Meriwether (1965) and Chow and Smith (1971) have done theoretical calculation for the spectral distribution of helium afterglow.

1.2.1.2. <u>Two-body recombination with curve crossing (Preassociation)</u>

Here two atoms approach each other on one potential surface/ curve and then make a radiationless transition to the emitting state at the point of intersection of the two curves. Such a process is called inverse of predissociation (or preassociation). Inverse predissociation has been discussed in Appendix I.

This process can be represented by equation (I.1). The steady state expression for the intensity of emission from the molecular level of angular momentum quantum number J, gives

$$I_J^O = (\frac{k_1 k_2}{k_{-1}+k_2})_J$$
$$1.3$$

using equilibrium statistical mechanics, the statistical mechanical equilibrium constant K_J between the atoms A and B and a state of AB^* having angular momentum J and energy E_J relative to separated atoms is given by (Carrington (1972)).

$$K_J = \frac{q_{AB}^\dagger}{q_A^\dagger q_B^\dagger} (2J + 1) \exp(\frac{-E_J}{kT})$$
$$1.4$$

where $q_A^\dagger = (2\pi m_A kT)^{3/2}/h^3$ etc. are normal translational partition function. For process given by equation (I.1), K_J can be defined as

$$K_J = (k_1/k_{-1})_J$$
$$1.5$$

so equation (I.3) can be written as

$$I_J^O = k_2 K_J/(1+k_2/k_{-1}) = (k_{-1}k_2/(k_{-1} + k_2))K_J$$
$$1.6$$

I^O is the sum of I^O_J over all the levels of AB^* which can contribute to two body emission. For the transitions which are dealt in afterglow, k_2 can be identified with A, the Einstein coefficient for spontaneous emission, and can be treated as constant over the levels concerned. Expression for I^O will be

$$I^O = \sum_J I^O_J = k_2 \sum_J \frac{K_J}{(1+k_2/k_{-1})} \qquad 1.7$$

which shows that all thermally accessible levels for which the rate of predissociation, k_{-1}, approaches or exceeds the rate of radiation will contribute. In other words, the condition that a level lying just above the predissociation threshold should contribute fully to two body emission, is that the rate of predissociation, k_{-1}, should be fast compared with rate of radiation, k_2.

For a diatomic molecule, the vibrational but not the rotational spacing is normally much greater than kT. If all the rotational levels of one vibrational state are accessible ($k_{-1} \gg k_2$) and lie above the dissociation limit, that is,

$$E_J = E_o + J(J+1)h^2/8\pi^2 I \qquad 1.8$$

where E_o is the energy of the lowest rotational level relative to free atom. Using this expression for E_J and substituting the value of K_J in equation (1.7) for I^O

$$I^O = k_2 \sum_J \frac{q^+_{AB}}{q^+_A q^+_B}(2J+1) \exp\left(\frac{-J(J+1)h^2}{8\pi^2 I \, kT}\right) \exp\left(\frac{-E_o}{kT}\right) \qquad 1.9$$

This expression gives the maximum rate of two-body radiative recombination through a particular vibrational state.

Predissociation (preassociation) can be divided into three classes (Herzberg 1950, 1966):

Class I - This involves crossing to another electronic state in which the predissociation is caused by either a bound state crossing below the dissociation threshold or by the intersection which occurs above the dissociation limit. When predissociation is caused by a bound state crossing below the dissociation threshold, predissociation can be observed in the spectrum as soon as the dissociation threshold is reached. In this case E_o in equation (1.9) is zero if there is a vibrational level of the bound state at or just below the dissociation limit since the density of rotational levels of a diatomic molecule is independent of the rotational energy unless the spacing is much greater than kT. If the emitting vibrational level is wholly above the dissociation limit than E_o is the energy of its lowest rotational level above the dissociation threshold.

For the allowed predissociation, that is one obeying the selection rules, discussed in Appendix I, will be so strong that $k_{-1} \gg k_2$ and attention must be focussed on forbidden predissociation. In that case, k_{-1} is often of the order of 10^8 sec^{-1} (for allowed transition $k_2 \simeq 10^6 - 10^8$ sec^{-1}) and has to compete with radiation. Examples of such behaviour are the predissociation of $N_2(B^3\Pi_g)$ and $N_2(a^1\Pi_g)$ by the $^5\Sigma_g^+$ state arising from ground state atoms for which selection rule $\Delta S \neq \pm 1$ is violated.

10

Class II - Predissociation by vibration

Here redistribution of vibrational energy can enable a molecule to pass from a stable region of a potential curve/surface to a dissociation limit.

Class III - Predissociation by rotation

This is confined to weakly bound states where the need to conserve angular momentum can produce a barrier to dissociation in a state which does not have a potential maximum.

1.2.2. Three-body emission

In most afterglow, the bulk of the emission comes from bound vibrational levels below the dissociation limit, establishing that some of the energy of the nascent molecule has therefore been removed by a third body. The emitting state does not normally correlate with the ground state atoms from which it has clearly been formed. Kinetically two different processes could yield the observed result:

a   The atoms could approach along a bound potential curve and then be stabilized into the emitting state by an inelastic collision with a third body while they are close to the crossing point.

b   A three-body collision stabilizes the molecule initially and crossing into the emitting state occurs subsequently. The absence of emission from states which correlate directly with ground state atoms does not provide evidence for mechanism a), since such transitions are forbidden in all the relevant afterglow.

Theoretical calculations (Smith (1962) and Shui et al. (1970))
have been able to reproduce the observed rates of three-body recombina-
tion adequately, However, theoretical studies have not so far been
particularly successful in reproducing the considerable dependence of the
rate constant on the nature of third body, which increases with its
molecular complexity. It is clearly a very strong function of the inter-
molecular forces involved. The magnitude of these forces probably deter-
mines the negative temperature coefficients observed for almost every
three-body recombination (Campbell and Thrush (1967) and Clyne and
Stedman (1967). Observed negative temperature coefficient of a three-body
recombination process supports mechanism b) rather than a).

The presence of the negative temperature coefficient and the
dependence on the nature of the third body can provide a useful method
for identifying emission associated with the three-body recombination.
In most of the cases, the emitting state is removed predominantly by
collisional quenching viz. process

$$
\begin{aligned}
A + B + M &\xrightarrow{k_3} AB^* + M \\
AB^* &\xrightarrow{k_2} AB + h\nu \\
\text{or } AB^* + M &\xrightarrow{k_4} AB + M
\end{aligned}
\qquad 1.10
$$
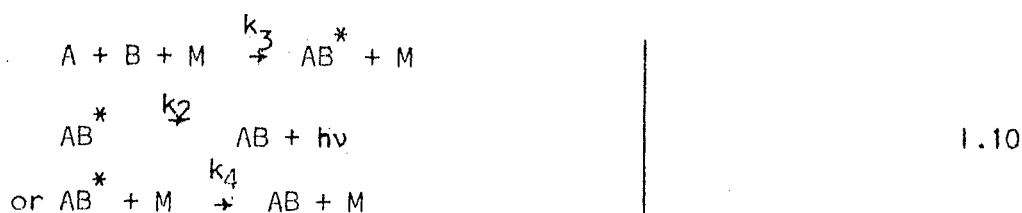
Absolute emission intensity for this process will be

$$
I_3 = I_3^0 [A][B] \qquad 1.11
$$

where $I_3^0 = \dfrac{k_3 \, k_2 [M]}{k_2 + k_4 [M]}$

If $k_2 \ll k_4[M]$ then I^0 will depend on the nature, not on the pressure of third body, M.

If the quenching step were also included in the two-body mechanism given by process (1.1)

$$A + B \overset{k_1}{\underset{k_{-1}}{\rightleftharpoons}} AB^*$$

$$AB^* \overset{k_2}{\rightarrow} AB + h\nu \qquad\qquad 1.12$$

$$AB^* + M \overset{k_5}{\rightarrow} AB + M$$
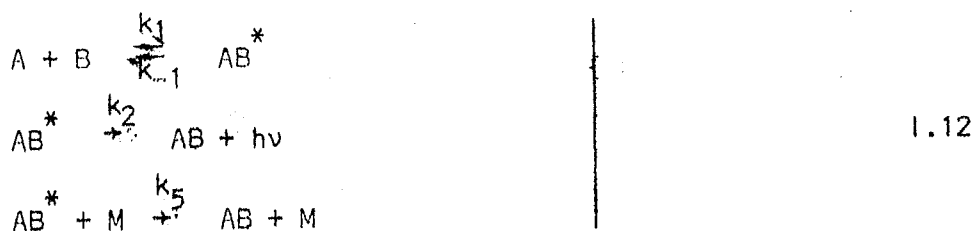
the corresponding expression for an absolute emission intensity would be

$$I_2 = I_2^0 \, [A] \, [B] \qquad\qquad 1.13$$

where $I_2^0 = \dfrac{k_1 \, k_2}{k_{-1}+k_2+k_5[M]}$

Thus experiments over a sufficiently wide range of pressures should be able to distinguish between the types of mechanisms. The three-body emission intensity, I_3, should show a change from a second order to third order at low pressures. For the two body recombination, emission intensity, I_2, will become less than second order at high pressures, because collisional quenching coefficient, $k_5[M]$, will begin to compete with radiation coeffient, k_2, plus predissociation coefficient, k_{-1}, where normally $k_{-1} > k_2$. So the overall order of emission involving three body recombination must be between 2 and 3, depending on whether the emitting state is significantly quenched. This, however, would be irrespective of how many precursor steps are involved, provided that all these steps are collision controlled.

1.3. Afterglow Spectra of Molecular Gases

Most of the experimental as well as theoretical work on afterglow have been confined to molecules of atmospheric significance. These are diatomic molecules like N_2, O_2 and NO, triatomic molecules like H_2O, CO_2, N_2O, NO_2 and inert gas afterglows. Recently, the after-glow studies of all these molecules have been reviewed by Golde and Thrush (1973). Experimental work on all the molecules listed above is far from complete. Most of the theoretical work has been reported only for N_2 and O_2 and this also shows rather poor agreement with experi-mental data. In case of oxygen, data got in laboratory experiments show the order of magnitude difference with the results obtained from atmos-pheric studies. Many mechanisms have been proposed to explain afterglow spectra but these are neither applicable to all molecules uniformly, nor are always self-consistent.

The first and most studied afterglow is that of nitrogen. In 1865, Morren discovered that, when nitrogen at low pressure was subje-cted to an electric discharge, a yellow glow appeared in the gas and persisted even after the discharge was turned off. Lewis (1900) showed that the glow was due to electronic transitions of the nitrogen molecule. Rayleigh (1911) observed the glow gas to be chemically active and coined the term 'active nitrogen'.

Many complex phenomena related to afterglow have been identi-fied. Many mechanisms have been proposed over the years (Berkowitz et al (1956), Bayes and Kistiakowsky (1960), Noxon (1962), Young and Sharpless (1963), Campbell and Thrush (1967), Gross (1968) and Brown (1970)) to

account for selected features of the afterglow. But the lack of adequate
means for sufficiently precise and accurate measurement of low light
intensity and absolute atomic concentration has created a distressing
situation in research on the kinetics and mechanism of nitrogen atom
recombination. Even after more than 50 years of effort, it has not been
possible to write with confidence a tested rate law relating the relative
intensity of a well defined portion of the afterglow spectrum to the
atomic concentration and the concentration of diluent gas. In addition
to that, disagreement exists in the literature about the value of the
homogeneous termolecular overall recombination rate coefficient in pure
nitrogen.

Another well-known afterglow studied in the laboratory is
that of oxygen. The laboratory measurements have proved helpful in
identifying the peaks obtained in night glow spectra. But the experi-
mental results reported show a large disagreement with the results
obtained from atomspheric night airglow. Still lot of work is
required to be undertaken in the laboratory to explain kinetics of
emission of the oxygen afterglow.

1.3.1. Nitrogen Afterglow

The nitrogen afterglow shows many features of interest.
Electronically excited nitrogen molecules are formed by both two-body
and three-body recombination processes. Their subsequent de-excitation
by relaxation, quenching and energy transfer processes with both mole-
cules and atoms is of much current interest and needs to be investigated,
both experimentally and theoretically, in greater details.

It is now agreed that the observed emitting states are populated by two or three-body recombination of ground state nitrogen atoms. The emitting states, with the exception of $N_2(A^3\Sigma_u^+)$, do not correlate with $N(^4S) + N(^4S)$. Initial recombination into both the very shallow $N_2(^5\Sigma_g^+)$ state and the stable $N_2(A^3\Sigma_u^+)$ state followed by curve crossing into the emitting state has been proposed. Thus, for mechanism involving $N_2(^5\Sigma_g^+)$, three-body recombination would imply stabilization of molecule in $v = 0$, believed to lie about 850 cm^{-1} below the dissociation threshold. Molecules in $^5\Sigma_g^+$, $v = 0$ undergo collision-induced radiationless transition, near the intersection of the respective potential curve (Fig. 1.1), into (i) $B^3\Pi_g$, $v = 12$, (ii) $B'\ ^3\Sigma_u^-$, $v = 8$, (iii) $a^1\Pi_g$, $v = 5$ and (iv) $a'\ ^3\Sigma_u^-$, $v = 7$. Molecules in these levels undergo both collision-induced vibrational relaxation to lower v-levels of respective states as well as collision-induced electronic quenching. The subsequent transitions from $B^3\Pi_g$ to $A^3\Sigma_u^+$ state, $B'\ ^3\Sigma_u^-$ to $B^3\Pi_g$ state, $a^1\Pi_g$ to $X^1\Sigma_g^+$ state and $a'\ ^1\Sigma_u^-$ to $X^1\Sigma_g^+$ state give rise to the first positive bands, infrared afterglow bands, Lyman-Birge-Hopfield bands and Wilkinson-Mulliken ultraviolet bands of molecular nitrogen respectively.

In contrast, two body recombination would involve approaching of the atoms along the $^5\Sigma_g^+$ curve with collision-free curve-crossing to the emitting state. As no energy has been lost in this process, emission must arise from very near or above the dissociation threshold. Only in the last decade had the two body emission process been identified. This process arises by association of two ground state nitrogen atoms along the unobserved but, well-established $^5\Sigma_g^+$ curve, followed by inverse
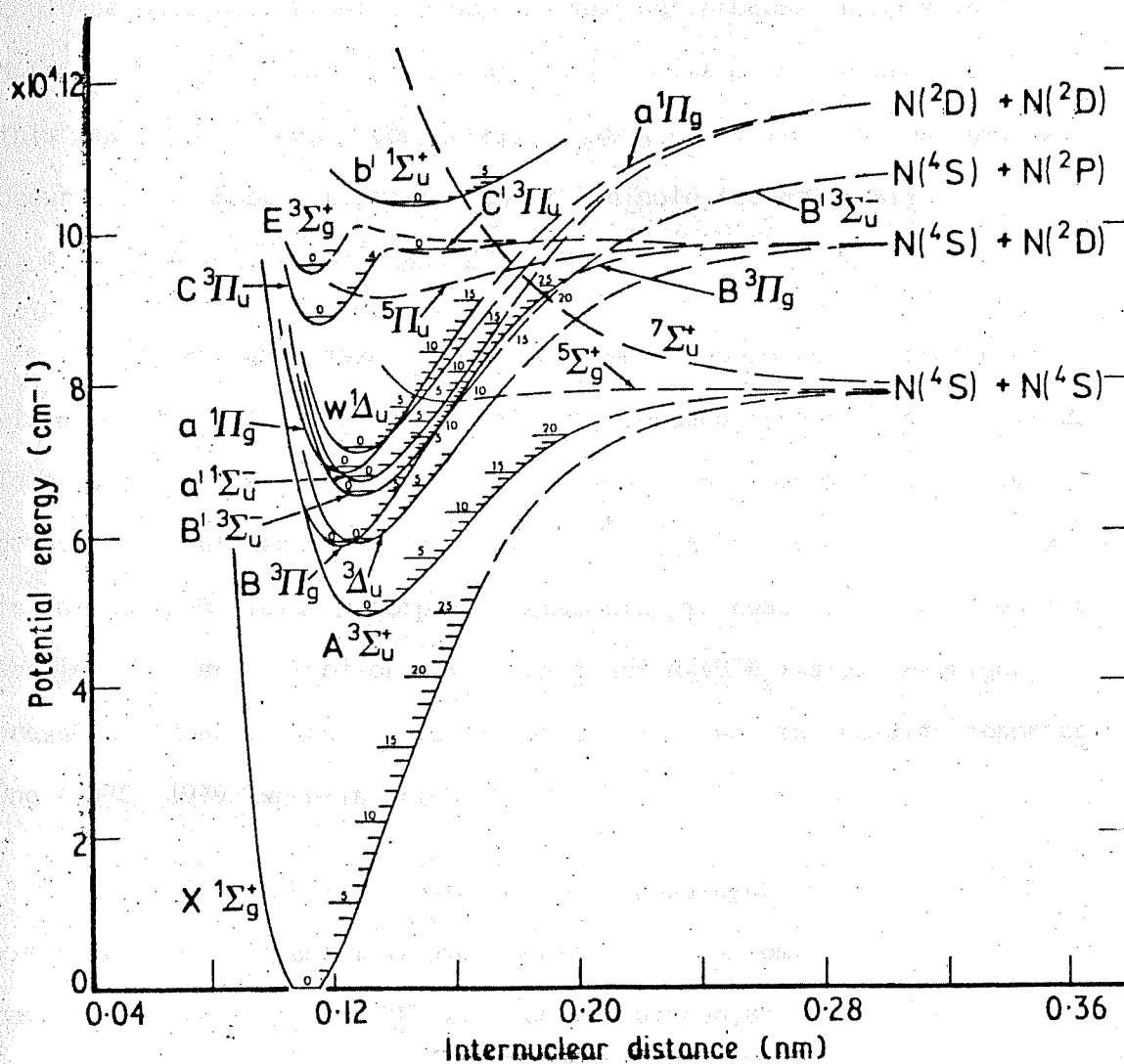
Fig. I.1   Potential energy curves for N_2 (Gilmore, 1965)

predissociation. The vibrational level $v' = 13$ of $N_2(B^3\Pi_g)$ plus high rotational level of $v' = 12$ (Becker et al. 1972), at very low pressures could be populated by this process. Another process, populating $N_2(a^1\Pi_g, v' = 6)$ (Golde and Thrush, 1972) is also of interest since this state itself has a comparatively long radiative life and emission occurs to the ground state by magnetic dipole radiation with $k_2 = 7 \times 10^3$ sec^{-1} (Borst and Zipf, 1971).

But Ung (1976, 1980) reported the observation of the 13th vibrational level of $N_2(B^3\Pi_g)$ state at pressure ranging from 0.5 to 20 Torr under various experimental conditions. He, for the first time, detected the higher vibrational levels of $N_2(B^3\Pi_g)$ state upto $v' = 26$ in the Lewis-Rayleigh afterglow. According to reaction rates, reported earlier, one should not observe $v' = 13$ of $N_2(B^3\Pi_g)$ state at higher pressure. However, now it is almost certain that the results reported by Ung (1976, 1979) were in error.

The kinetics of the strongly populated levels of $N_2(B^3\Pi_g)$, $v = 9$-12 is consistent with the formation of the emitting state at a rate proportional to $[N]^2[M]$ and removal by radiation and collisional quenching. Still there is some controversy about the precursor of $N_2(B^3\Pi_g)$ state. The $N_2(^5\Sigma_g^+)$ and $(A^3\Sigma_u^+)$ states can be formed directly by N atom recombination and cross or lie close to the $B^3\Pi_g$ state near the dissociation limit. These states have been invoked as the precursor of $N_2(B^3\Pi_g)$. Four mechanisms have been proposed for the formation process:

(i) Benson (1968) suggested that $N_2(B^3\Pi_g)$ is populated by inverse predissociation via unbound levels of the $^5\Sigma_g^+$ state into high rotational levels ($N \geq 33$) of $B^3\Pi_g$, $v = 12$, followed by vibrational relaxation to yield lower levels.

(ii) This mechanism was originally proposed by Berkowitz et al. (1956) and recently restated by Becker et al. (1972). According to this mechanism a steady state population of $^5\Sigma_g^+$, $v = 0$ exists and collisions transfer molecules from this level to a range of vibrational levels, $v = 9\text{--}12$, of $N_2(B^3\Pi_g)$. They postulated that the vibrational distribution in these levels depends on the nature of the collision between $^5\Sigma_g^+$, $v = 0$ and M and thus on the nature of M and the temperature.

(iii) Brennen and Shane (1971) and Anketell and Nicholls (1970), considering that direct population of levels $v' < 12$ from $^5\Sigma_g^+$, $v = 0$ would be relatively inefficient because of the increasing energy mismatch involved, favoured initial population predominantly of level $v = 12$ from $^5\Sigma_g^+$, $v = 0$. According to Anketell and Nicholls, lower levels of $B^3\Pi_g$ are populated by vibrational relaxation in this state. Brennen and Shane considered the possibility that collisional crossing between $B^3\Pi_g$ and $A^3\Sigma_u^+$ occurs, with the vibrational relaxation mainly in the latter state.

(iv) Campbell and Thrush (1967) proposed that the steady state population of the shallow $^5\Sigma_g^+$ state would not be large enough to explain the high rate of population of the $B^3\Pi_g$ state and preferred collisional crossing from the $A^3\Sigma_u^+$ state, which lies close to the

$B^3\Pi_g$ state over the relevant energy range.

The mechanism by which an emitting level is populated is deduced from the dependence of its emission intensity on

<u>1</u>   nitrogen atom concentration and pressure

<u>2</u>   added foreign agent

<u>3</u>   temperature

1.3.1.1. <u>Nitrogen atom concentration and pressure dependence</u>

The emission of the first positive bands of nitrogen has been studied extensively. It had been widely suggested that this reaction is third order at pressure less than 1 Torr. But the experimental evidence for this conclusion was contradictory and a completely satisfactory experimental investigation was not reported before the work of Jonathan and Petty (1969) using fast flow system and of Brennen and Shane (1971), using pressure jump experiment. The results from work in the 1-10 Torr region generally agree that here the emission is pressure independent and proportional only to the square of the ^4S nitrogen-atom concentration. So the emission kinetics of the first positive bands showed a change from third-order dependence $(I \alpha [N]^2 \times P)$, at lower pressures, to second-order dependence $(I \alpha [N]^2, \ I$ independent of $P)$ as the pressure was increased. This study indicates that $N_2(B^3\Pi_g)$ state is populated by three-body recombination process. Also the kinetic study of the afterglow provides data regarding how the emitting states are quenched by the carrier gas.

1.3.1.2. Effect of added gas

Both the total intensity and the intensity distribution of the vibrational bands in the afterglow spectrum depend on the presence and nature of any additives present in the glowing gas. At normal pressure, the emission is enhanced by partial replacement of the nitrogen carrier with an inert gas carrier. Measurement of the radiative life of $N_2(B)$ (Jeunehomme (1966)) clearly demonstrates that this effect is due to the quenching by nitrogen. So one can find quenching of $N_2(B)$ state by nitrogen or argon from the emission kinetics.

Partial replacement of nitrogen by most foreign gases (except Ar and He) gives rise to quenching effect on the afterglow, thereby reducing the intensity by more than what would be expected on the basis of a simple dilution effect. Here vibrational distribution of first positive system is characteristic of foreign gas.

1.3.1.3. Temperature Dependence

Study of afterglow spectrum at low temperature will provide the knowledge as to whether the emitting states are populated by two-body recombination or three-body recombination processes. As the temperature decreases, number of collisions will also decrease. At the same pressure but at low temperature, two-body recombination would show less intensity for a particular vibrational band than at higher temperature. If the emitting state is in equilibrium, by means of collision, with a state, which directly correlates with recombination of atoms, than reducing temperature will show an increase in intensity of emission.

As had been found by Campbell and Thrush (1967), three-body volume recombination rate constant had a negative temperature coefficient.

In the first positive system of nitrogen afterglow, the highest vibrational level, $v' = 12$, is populated by curve crossing from $^5\Sigma_g^+$ state of nitrogen, which directly correlates with nitrogen atoms, very near to the dissociation limit. If one can resolve rotational level in the vibrational band corresponding to $v' = 12$ for $\Delta v = 4, 3, 2$ and find out the highest rotational level populated, one could get the dissociation energy of the nitrogen molecule. Cooling the afterglow, at liquid nitrogen temperature, shows increase in intensity; so it will be a better idea to find out highest rotational levels populated at this temperature. Because of better signal and thus better statistics, one may get one or two more rotational levels at low temperatures.

Also quenching of molecular state reduces by reducing the temperature. For example the second positive bands of nitrogen have not been observed in the afterglow at room temperature. If the afterglow chamber is cooled at liquid nitrogen temperature, these bands could be readily observed.

1.3.2. Oxygen Afterglow

There is much less literature available on activen oxygen than on active nitrogen. The main energy source in both the systems is the recombination of atoms. In contrast to nitrogen afterglow where the recombining $N(^4S)$ atoms have access to a considerable manifold of electronic states which may then be populated through curve crossing

mechanisms, no such possibility exists for oxygen. With 5.1 eV recombi-
nation energy, the only bound electronic states accessible to a pair of
$O(^3P)$ atoms are the six states which correlate with the $O(^3P) + O(^3P)$
limit shown in Fig. I.2. The transitions between these states are all
strongly forbidden. Emission from the three upper oxygen states A $^3\Sigma_u^+$,
C $^3\Delta_u$ and C $^1\Sigma_u^-$ are much weaker, with respect to gas phase emission
spectra. Only two transitions, Herzberg I system A $^3\Sigma_u^+ \rightarrow$ X $^3\Sigma_g^-$ (Broida
and Gaydon (1954)) and weak Herzberg II system C $^1\Sigma_u^- \rightarrow$ X $^3\Sigma_g^-$ (Degen
(1968)) had been reported till 1976.

The Herzberg I (A $^3\Sigma_u^+$ – X $^3\Sigma_g^-$) band system of oxygen which
lies in the wavelength range 2500-4900 Å, contributes significantly to
the ultra-violet spectrum of the night airglow. Broida and Gaydon (1954)
were the first to report Herzberg I in afterglow of pure oxygen. They
reported the vibrational intensity distribution of levels populated. In
pure oxygen, this process at low pressures is limited, by diffusion of
the oxygen atoms formed in the driving discharge to the walls of the tube,
and at high pressure by collisional deactivation of metastable A $^3\Sigma_u^+$ by
oxygen atoms and molecules (Barth 1964).

Most of the afterglow studies have been carried out by
mixing small quantities of oxygen with excess argon or helium. These
diluent gases are capable of reducing diffusion and wall effects, and
enhance the recombination process. Degen (1968) was the first to
identify two bands at wavelength 4491 Å (0,7) and 4791 Å (0,8) of
Herzberg II (C $^1\Sigma_u^- \rightarrow$ X $^3\Sigma_g^-$) forbidden system of oxygen in the oxygen-
argon afterglow. The work of Lawrence et al. (1977) established that
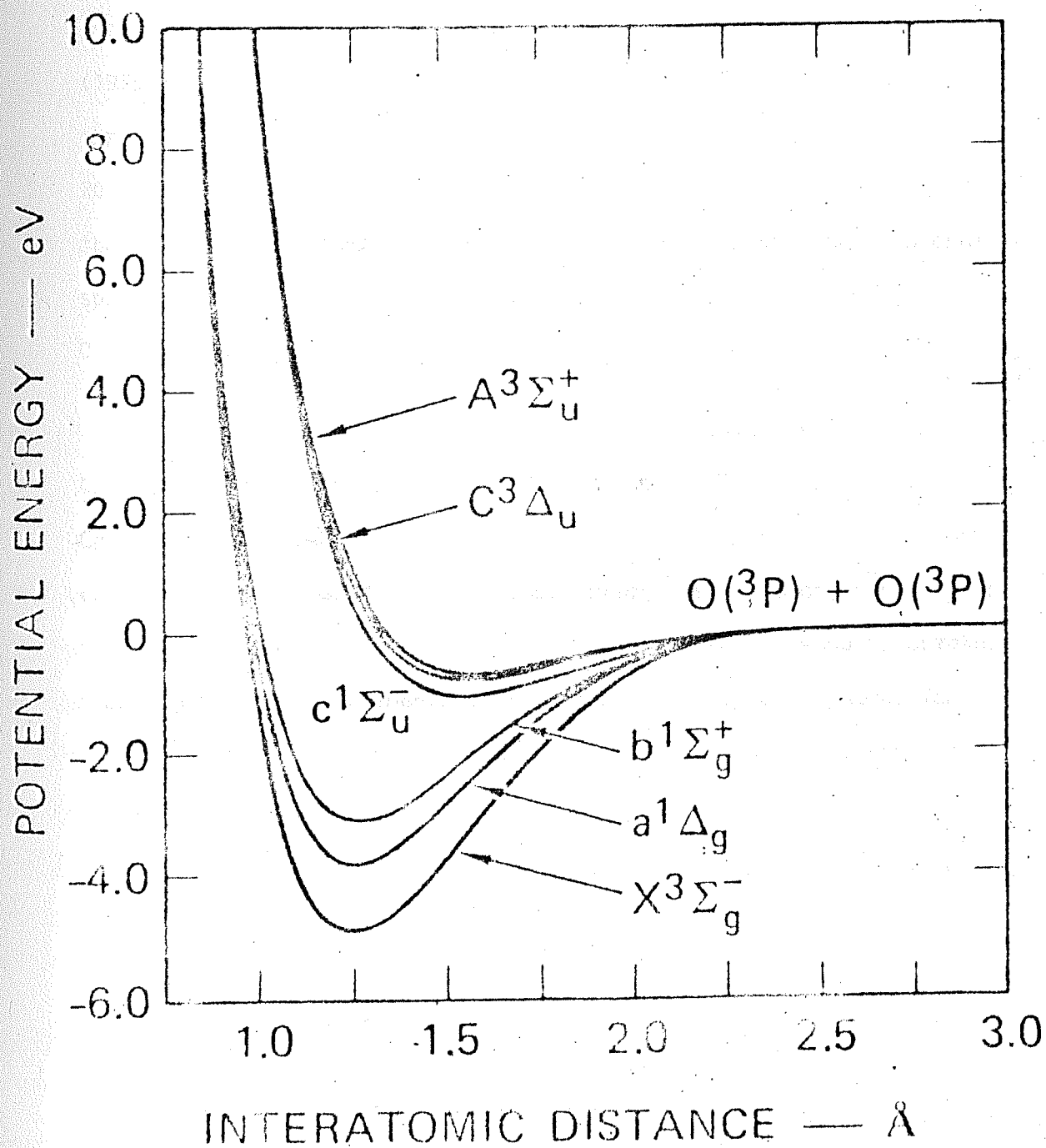
Fig. I.2 Potential energy curves for bound states of O_2
(Saxon and Liu, 1977)

under appropriate conditions, the Herzberg II ($C\ ^1\Sigma_u^- \rightarrow X\ ^3\Sigma_g^-$) system could also be obtained when, downstream the discharge, CO_2 at partial pressure of 10 Torr was added to the stream of oxygen atoms. But Slanger (1978a, 1978b) reported that the $O_2(C\ ^1\Sigma_u^- \rightarrow X\ ^3\Sigma_g^-)$ system could be obtained even in the absence of CO_2, at pressures 38 m. Torr of O_2 and 20 Torr of helium. In addition to this system they have discovered three new band systems, not observed previously in gas phase laboratory spectra. These systems are $C\ ^3\Delta_u \rightarrow a\ ^1\Delta_g$, $C\ ^3\Delta_u \rightarrow X\ ^3\Sigma_g^-$ and $C\ ^1\Sigma_u^- \rightarrow a\ ^1\Delta_g$.

The kinetics of Herzberg I band emission from $O_2(A\ ^3\Sigma_u^+ - X\ ^3\Sigma_g^-)$ had been studied by Young et al. (1963, 1966) and by Campbell and Thrush (1967b). However, it may be pointed out that not enough work has been done in this direction. Half quenching pressures obtained by them are not at all in agreement with the results obtained from night glow measurements (Barth (1964)). Population mechanism of $O_2(A\ ^3\Sigma_u^+)$ state is still not known to good extent and requires further study.

1.4. Present Investigations

The work presented in this thesis has been oriented towards making some studies of nitrogen and oxygen afterglow in the above context. The above discussion very clearly shows the necessity of studying the nitrogen afterglow with high resolution afterglow spectro- meter. Resolving rotational levels of some vibrational bands correspond- ing to different band systems may help in identifying the population mechanisms for the emitting states.

The experimental set-up has been described in details in Chapter II. In the third chapter of the thesis, the results obtained from the study of nitrogen afterglow spectra in the spectral range from 1900 to 8000 $\overset{O}{A}$, at 77° K and 300° K and variation of intensity of various bands of first positive system with pressure (between 2 and 7 Torr) have been presented. The effect of diluent like argon at fixed pressure with nitrogen at pressures varying from 0.2 to 3 Torr has also been studied using high resolution flowing afterglow spectrometer. Also, the mechanisms for populating the different vibrational levels of B $^3\Pi_g$ state are discussed in the light of new results obtained.

The quenching effect on (12,8) and (11,7) vibrational bands of the first positive system of nitrogen by nitric oxide, observed in the afterglow, is discussed in the Chapter IV, for temperature varying from about 87° K to 90° K. The results obtained from high resolution study of (12,8), (12,9), (11,7) and (11,8) vibrational bands of the first positive system, both at 300° K and 77° K are given in the Chapter V. Dissociation energy corresponding to the lowest dissociation limit of nitrogen has been computed and results obtained are given in the same chapter.

Chapter VI deals with the study of afterglow spectra of molecular oxygen in the spectral range from 2400 to 4250 $\overset{O}{A}$. Also, the quenching rates for the vibrational bands (5,4), (4,4) and (4,3) of the Herzberg I system by oxygen, argon and helium are reported.

CHAPTER II

EXPERIMENTAL   SET-UP

II.1.   Introduction

The necessity of studying the afterglow spectra of molecular
gases as a function of pressure, temperature and additives has been
pointed out in the first chapter.   The essential requirements for such a
kind of work are a gas purification system, discharge system, observation
vessel with cooling facility, high speed pumping system, monochromator,
system for measuring absolute atomic concentration, highly sensitive light
detector, fast data acquisition system, etc.   The block diagram for produ-
cing afterglow has been shown in Fig. II.1.   The details regarding the
various sub-systems and performance of the integrated system are presented
in the following section.
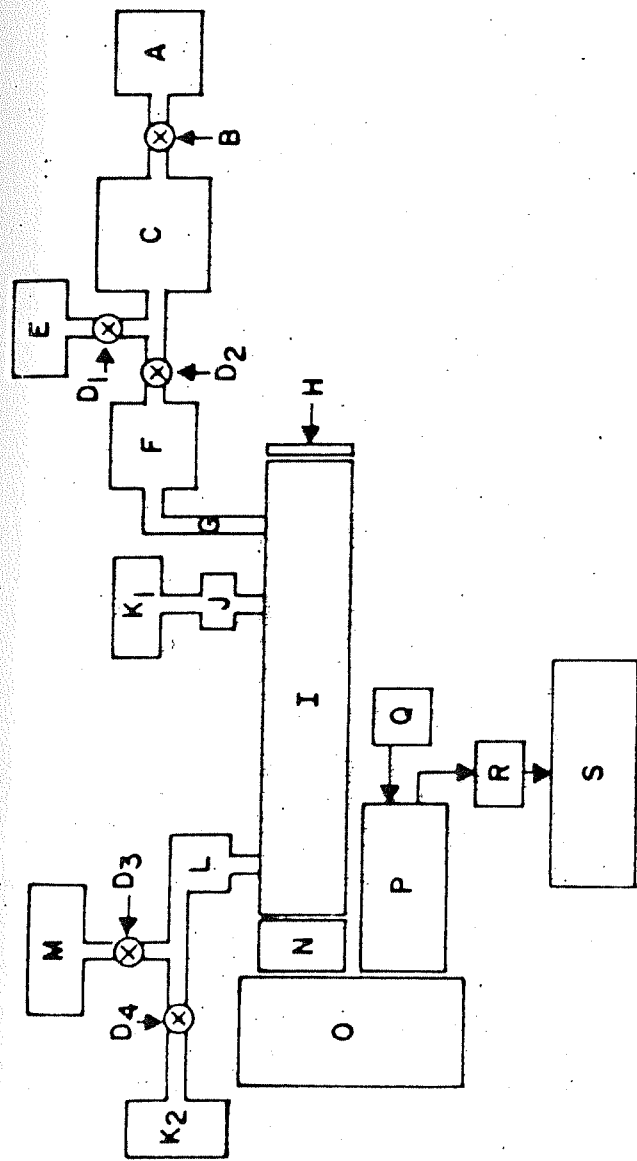
A — PREPURIFIED GAS TANK

B — GRANVILLE – PHILIPS LEAK VALVE

C — PURIFICATION REGION

D_1, D_2, D_3, D_4 – GREASE LESS STOP COCKS

F — DISCHARGE REGION

G — OPTICAL ISOLATING SYSTEM

H — REFLECTING MIRROR

I — OBSERVATION VESSEL

J — WREDE – HARTECK GAUGE

E, K_1, K_2 – OIL DIFFUSION PUMP + ROTARY PUMP

L — DIFFERENTIAL PUMPING STAGE

M — ROOTS PUMP + ROTARY PUMP

N — GLOW FOCUSING SYSTEM

O — SCANNING MONOCHROMATOR

P — COOLED PHOTOMULTIPLIER

Q — STABILIZED NEGATIVE HIGH VOLTAGE SUPPLY

R — PRE AMPLIFIER WITH PULSE HEIGHT DISCRIMINATO

S — DATA ACQUISITION SYSTEM

FIG. II. 1   BLOCK DIAGRAM OF THE AFTERGLOW SPECTROMETER ASSEMBLY

II.2.   Afterglow Spectrometer

II.2.1. Choice of the Afterglow System

Two types of systems can be used to study the afterglow:

a   As pointed out in Chapter I, radiation from afterglow persists even
    when electrical discharge through gas is switched off.   During the
    time immediately after the switching off of the applied energy,
    molecules in excited states are formed by two body or three body
    atomic recombination.   Measurement of the time-dependence of these
    populations provides data from which a variety of reaction rates
    can be calculated with the aid of the kinetics discussed in
    Chapter I.   This is termed as time-dependent afterglow, and is
    sometimes called "Static Afterglow".

b   A flowing afterglow is one in which gas is pumped through the dis-
    charge region continuously and the glow is examined in the gas
    removed from the discharge.   The population of the species under
    study are monitored along the axis of observation tube, so that
    time variation is converted into spatial variation along one
    dimension.

         The advantage of the flowing afterglow derives from the
flexibility with which the rate processes can be controlled.   It is
difficult to avoid unwanted excited species in a time-dependent after-
glow.   In the flowing afterglow, this could be avoided by pumping
discharge products to a long distance before allowing these to enter the
observation region.   During this time, most of the unwanted excited

species would come to ground state. Also, in the flowing afterglow
system, kinetic data are obtained from measuring steady state intensi-
ties as a function of reagent concentration. In static system, the
dependence of the afterglow on the concentration of reacting species
is obtained by comparing the rate of decay of the emission intensity and
the concentration. These advantages have weighed in favour of choosing
the flowing afterglow system for the proposed afterglow studies of mole-
cular nitrogen and molecular oxygen.

II.2.2. Production of the Afterglow

Afterglow is produced by discharge through the parent mole-
cules. Production of afterglow requires gas purification before the
parent molecules enter the discharge region. The gas purification system
and discharge region are being discussed below in great detail.

II.2.2.1. Gas Purification

Gas used for producing afterglow has to be extremely puri-
fied. In case of nitrogen, afterglow is highly sensitive to the purity
of the nitrogen gas. Oxygen as impurity in nitrogen will give very
intense bands of nitric oxide (NO) and will suppress Vegard-Kaplan band
system of nitrogen which lies in the same wavelength region as that for
nitric oxide. Nitric oxide produced in this manner will act as a
quenching agent for nitrogen afterglow and will disturb kinetic study of
pure nitrogen afterglow spectra. Because of this reason, purified gas
from the cylinder has to be further purified.

We have used Iolar-2 nitrogen for producing nitrogen after-glow. This gas was further purified by passing it first through a glass spiral tube maintained at liquid nitrogen temperature. Here, impurities removed will be moisture, CO_2, CO, nitrogen's-oxides, hydro-carbon compounds etc. Impurity left will be like O_2, Ar, H_2. Oxygen is removed by passing gas coming out of first spiral tube to a quartz tube filled with oxygen free copper turning maintained at $700^O C$ (Dodd and Robinson (1957)). Surface of copper turning used here is made active by passing hydrogen through this quartz tube maintained at $500^O C$. While making copper surface active, purification part is disconnected from the main system by closing grease less stop cock D_2 (Fig. II.1) and is pumped through pumping system E by opening stop cock D_1. At $700^O C$, active copper surface will absorb oxygen present in the gas. So we will get oxygen free gas which is again passed through another glass spiral tube maintained at liquid nitrogen temperature to remove, if any, impurity left other than argon and hydrogen. These two impurity gases do not react with active species of afterglow. Iolar-2 argon and Iolar-helium were also purified in the same way as nitrogen to remove all impurity. Iolar-2 oxygen was purified further by passing through glass spiral tube maintained at liquid nitrogen temperature. All Iolar gases other than helium were supplied by Indian Oxygen Limited.

II.2.2.2. Discharge Region

High voltage/high current power, microwave and radio frequency power are normally used for producing discharge through the gas. Condensed discharge (high voltage discharge) requires electrodes inside the discharge

region. Electrodeless discharge (microwave discharge and radio frequency discharge) had been preferred over condensed discharge because of the following reasons:

1   Electrodeless discharge does not contaminate the flow gas.

2   Risks involved because of high voltage as in condensed spark discharge are eliminated.

We have preferred microwave discharge over the R.F. discharge. While using R.F. discharge, most of the electronic equipments which are part of the data acquisition system, require R.F. shielding against R.F. pick up. To avoid this, we are using microwave discharge. The main advantage in using this source was in its steady functioning, almost constant intensity of afterglow and ease of operation.

Microwave generator operating at 2450 MHz with a maximum out- put power of 100 watts was used. Power from microwave generator was coupled to the discharge region through an Evenson cavity (Ophthos Instruments, M.D.). This cavity can easily be clamped around the dis- charge tube. The cavity and the discharge region were cooled by passing compressed air through the port provided in the cavity. The tuning of the cavity had to be done by the two tuning stubs provided with the cavity.

The walls of the tube through which the parent gas ready for discharge passes, must be made of material with low dielectric loss and high heat resistance. Fused silica satisfies both the conditions. Tube made of fused silica was used as discharge tube. Internal diameter of

the discharge tube was about 6 mm.

II.2.2.3. Wood's Horn Light Traps

The horn like traps known as wood's trap are used to make discharge region optically isolated from afterglow observation region. Light which comes because of direct excitation of the gas in the discharge region will hit at the curved surface of the wood's horn light trap which is painted black from outside. Some of the light will be absorbed here and some will be reflected to the next curved surface. Again some will be absorbed and some will be reflected further away from the discharge region. After multiple reflections, it will be absorbed more or less completely.

We have used two right angled bends and two wood's horn light traps to prevent stray light reaching observation region from discharge region. All these right angled bends and wood's horn light traps are painted black from outside to protect outside light to go in.

II.2.3. Observation Region

Afterglow arises because of two body or three body atomic recombination. As pressure reduces, number of collisions also reduces. If one looks at a point perpendicular to the direction of gas flow, there will be small number of atoms which will be recombining in that region and giving a glow. Intensity of this glow will be very weak. It will be very difficult to make spectral analysis of this glow at such a low signal level. Signal level could be increased by increasing the area of the observation region. The area can be enlarged into cylindrical

or spherical form. In the present afterglow system, cylindrical observation vessel has been used. Cylindrical observation vessel has certain advantages over spherical observation vessel. Firstly, in cylindrical vessel, glow can be focussed easily; secondly mixing of added gases takes place faster than in the spherical vessel.

Cylindrical observation vessel made of quartz has been used in the present set-up. It is shown in Fig. II.2. Internal diameter of this tube is 2.2 cm, outer diameter 2.6 cm and length 55 cm. Flat quartz windows were fused on each end of tube. The end of the tube near the discharge region was equipped with a reflecting mirror, to increase the total light intensity going to the entrance slit of the monochromator. This observation vessel had an outer jacket of quartz tube of internal diameter 4.5 cm and length 50 cm. Space between these two tubes could be filled with liquid nitrogen, so as to maintain the system at a temperature of $77^{O}K$ approximately. Except for the windows, the exterior of the outer tube was painted black to prevent external light to get in.

The distance between the discharge and observation vessel was approximately 50 cm and was optically isolated by two right angled bends and two wood's light traps. When discharged gas with all the discharged products traversed this path, most of molecules in metastable states will de-excite to ground state because of collisions. It takes about 15 second for discharged gas to reach the observation vessel.
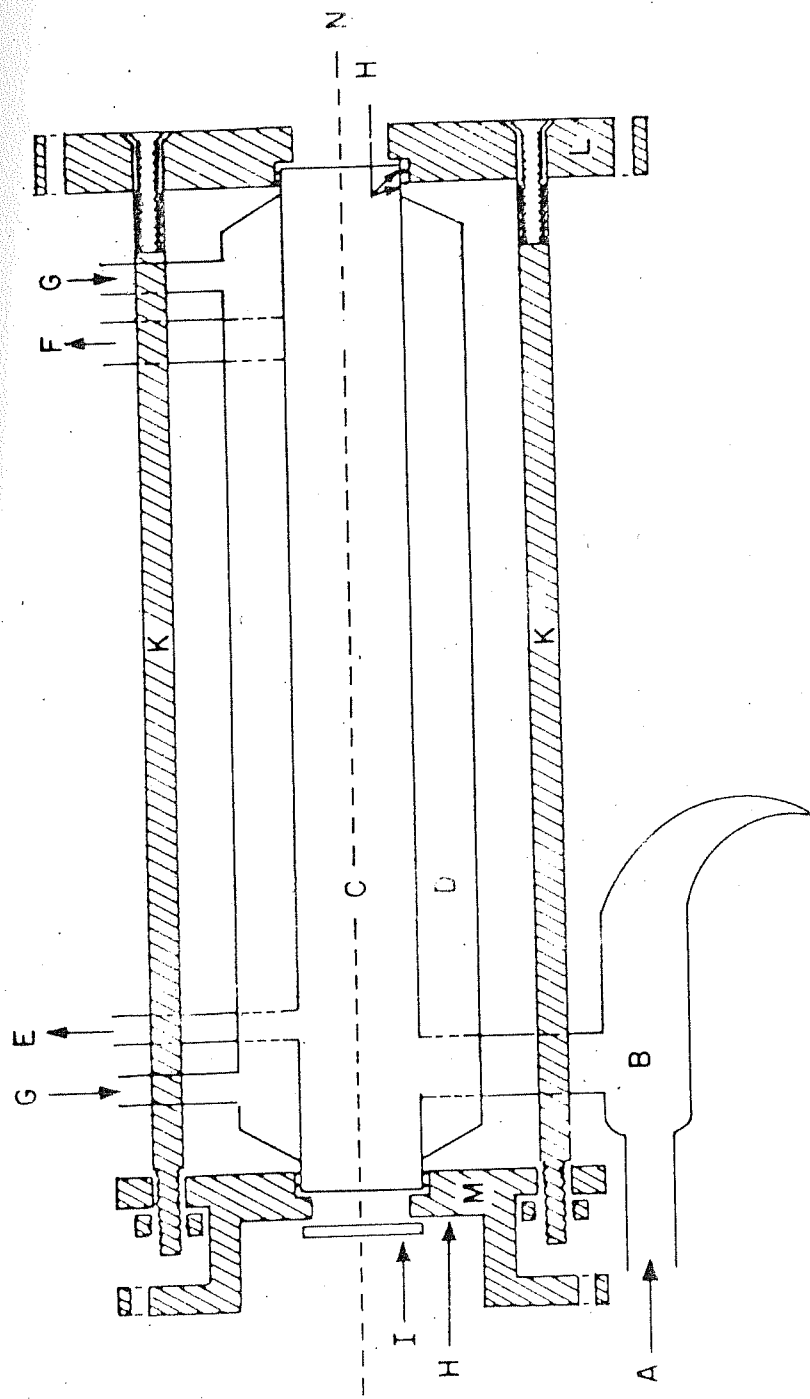
A — DISCHARGED PRODUCTS
B — WOOD'S HORN LIGHT TRAP
C — OBSERVATION VESSEL
D — JACKET TO OBSERVATION VESSEL
E — WREDE-HARTECK GAUGE
F — VACUUM SYSTEM

G — LIQUID NITROGEN
H — NEOPRENE 'O' RING
I — REFLECTING MIRROR
K — ALUMINIUM ROD
L,M — ALUMINIUM FLANGE

FIG. II.2   OBSERVATION VESSEL WITH COOLING JACKET MOUNTING SYSTEM

Observation vessel with cooling jacket is mounted between two flanges with the help of two neoprene '0' rings. These flanges are coupled with each other through four aluminium rods. This is shown in Fig. II.2. Flange L is mounted on the exit slit of monochromator. This mounting helped to align the monochromator-optical-axis with the axis of observation tube. Space provided, in flange M can be used for mounting reflected mirror or mounting interference filter if and when desired.

II.2.3.1. <u>Vacuum System</u>

To avoid quenching of emitting excited state with another molecule in ground state or by atom and to reduce wall recombination, one had to pump the discharged gas fast. Gas is pumped by roots pump (Leybold-Heraeus) backed by a rotary pump with pumping speed of 750 litres/min. The roots pump had a speed of 40 litres/sec and could give an ultimate vacuum of 10^{-3} Torr. To begin with, the whole system is evacuated to a pressure of 10^{-6} Torr by 4" oil diffusion pump backed by a rotary pump. Roots pump and oil diffusion pump were connected to the observation vessel through T connection. One end of T was connected to observation vessel and the other was connected to roots pump through a 4" butterfly valve. Third end was connected to the oil diffusion pump through a 1" diaphragm valve. For oil diffusion pump vacuum, butterfly valve was closed and diaphragm valve was opened. For pumping gas at high pressure, diaphragm valve was closed and butterfly valve was opened.

The speed of the roots pump is 40 litres/sec. upto a pressure of 10^{-1} Torr. Below this pressure, its pumping speed will reduce. So

as to maintain 7 Torr in observation vessel, one had to introduce

impedence to reduce the pumping speed. Pyrex tube of internal diameter

6 mm and length 35 cm was introduced between observation region and

pumping line.

II.2.3.2. <u>Maintenance of the Discharge Flow System</u>

It is known that impurities increase the wall recombination

occurring at the surface of the tube. Also some impurities like carbon

compounds would react with the active species of afterglow and will give

rise to bright glow characteristic of the compound. The reaction kinetics

of the afterglow would also be disturbed. So it was necessary to clean

the inner surfaces of all the glass tubes and other connections used in

the afterglow system. All the glass system was first cleaned with deter-

gent to remove oil and other sticky impurities. Then it was cleaned

with 10% hydrofloric acid and was finally washed by triple distilled water.

The impedence tube which was introduced between the observa-

tion vessel and pumping line, was made in U-form. The U-form impedence

tube was dipped in liquid nitrogen temperature. This protected the obser-

vation vessel against diffusion pump and roots pump oil vapour. Both the

oil diffusion pumps were used with liquid nitrogen traps.

It was found that all types of greases, if used, in the

vacuum system including the Apiezon vacuum grease, react with the active

species of the afterglow and emit their characteristic radiation. Also,

it reduces the atomic concentration by means of wall recombination. To

avoid this, we have used grease-less Kontes hi vacuum teflon stop-cocks.

These stop-cocks can stand a pressure upto 10^{-6} Torr and can be baked upto 200°C. Also no conical joints have been used in the system.

II.2.4. Measurement of Atomic Concentration in Discharge Flow System

Free atoms in discharge-flow system can be detected by a variety of techniques like calorimetry, mass spectrometry, electron paramagnetic resonance (E.P.R.), line absorption spectroscopy and by Wrede-Harteck gauge. The subject has been discussed in detail by Jennings (1961). Mass spectrometer and E.P.R. have been much used in studies of atom-atom reaction.

For hydrogen and halogen atoms, absolute concentration is conveniently obtained using an isothermal calorimeter, which effectively measures the heat released by atomic recombination at a metal probe inserted into the gas stream. Calorimetric probes are unsuitable for measuring nitrogen atom concentrations in the nitrogen afterglow because vibrationally excited nitrogen molecules (Kaufman and Kelso, 1958) will contribute to the heat released at the probe. Similarly discharge through oxygen produce metastable $O_2(^1\Delta_g)$ as well as oxygen atoms, which preclude the use of calorimetric probe in this system.

During the last twenty years, several gas phase titration reactions have been developed, which give absolute concentration of atoms in flow system. These titrations involve adding a known flow of a gas which reacts rapidly and stoichiometrically with the atoms in question. The usefulness of this technique depends on being able to detect the end point of titration. Titration end point is measured in

the following way. The nitrogen atom concentration can be measured by nitric oxide (NO) titration technique (Kaufman and Kelso, 1957).

$$N + NO = N_2 + O \qquad\qquad II.1$$

As it is clear from the above equation, addition of nitric oxide will consume nitrogen atoms and thus will lower the intensity of the yellow nitrogen afterglow. However, in the presence of oxygen atoms the blue nitric oxide afterglow is produced. This afterglow reaches a maximum at a flow of nitric oxide equal to half of the initial nitrogen atoms flow, and then decreases at higher nitric oxide flow. When intensity of nitric oxide afterglow is maximum, it indicates that the end point of titration has reached.

These gas phase titration reactions have two drawbacks:

<u>1</u>   One cannot measure atomic concentration at the same time when one is measuring intensity of the afterglow.

<u>2</u>   Once nitric oxide is introduced into the system for measuring atomic concentration this contaminates the system. Removing this contamination require pumping for long time and baking of the system.

There are only three methods which can be used for measuring atomic concentration at the same time when one is measuring intensity of the afterglow. These are (1) Mass Spectrometer (2) E.P.R., (3) Wrede-Harteck gauge. But problem with mass spectrometer is its interference with the kinetics of reaction. We have choosen Wrede-Harteck gauge over E.P.R. because of its simplicity in construction and sensitivity in performance.

II.2.4.1. Principle of Wrede-Harteck Gauge

The Wrede-Harteck, discussed in detail by Greaves and Linnett (1959), consists of a hole, small compared with the mean-free path, in the wall of the vessel containing the partly atomized gas. Behind this hole is a space, closed except for the hole, containing a catalyst for recombining atoms to molecules. Atoms and molecules enter this space through the hole, but because of catalyst, only molecules are left behind. If the hole is sufficiently small compared to the mean-free path, the atoms and molecules pass through the hole purely by diffusion. Atoms transport mass less effectively than molecules by a factor of $1/\sqrt{2}$ (if the molecules are diatomic) because, though moving, on an average, with $\sqrt{2}$ times the velocity, they are only half the mass. Consequently a pressure difference develops across the orifice.

Let α be the fraction of the gas below the hole which is atomic. Let the total pressure of the gas be P and that above the hole be P'. Then for a mass balance

$$\alpha P/\sqrt{2} + (1 - \alpha)P = P' \qquad\qquad II.2$$

$$\therefore \quad \alpha = 3.41\ \Delta P/P \qquad\qquad II.3$$

where $\Delta P = P - P'$. By measuring P and ΔP, α can be measured.

Knudsen (1910) investigated the flow of gas through small holes as a function of λ/d where d is the hole diameter and λ is mean free path. The deviation from pure diffusion flow was about 0.2% at $\lambda/d =$ 100 and between 1 and 2% at $\lambda/d = 10$. The precise value depends on the

size of the hole. So with a hole for which $\lambda/d = 10$, the atom concentra-
tion estimated by formula will be 1 or 2% lower than the true value. This
much will be the error involved.

In our experiment, a hole of about 25 μm diameter made on a
synthetic sapphire disc 22 mm diameter and 400 μm thick was used. This
synthetic sapphire film with the required hole at the center was provided
by British Diamond Wire Die Company Ltd., Dorset, U.K. The ratio of mean
free path (λ) to the hole diameter (d) varied from 13 at 0.2 Torr to 0.3
at 7 Torr. As a result, the atomic concentration estimated by the above
equation, would be about 1% to about 30% lower than the true value at
0.2 Torr and 7 Torr respectively.

The Wrede-Harteck gauge is incorporated in the afterglow tube.
This system has been shown in Fig. II.3. ΔP as well as P are measured
by M.K.S. Baratron capacitance manometer. P_x arm of M.K.S. Baratron
capacitance manometer head is connected to the higher pressure side that
is to the observation tube and P_R arm is connected to reference side and
is continuously pumped for absolute pressure measurement. For measuring
ΔP, P_R arm is connected to Wrede-Harteck gauge by closing stop-cock A and
opening stop-cock B. So the absolute pressure inside observation tube is
measured when stop-cock A is open and stop-cocks B and C are closed and
difference in pressure developed across the hole is measured by opening
stop-cock B and closing stop-cocks A and C.

II.2.5. Detection of Afterglow Emission

All the phenomena associated with afterglow depend on energy
exchange processes in the gas phase. Spectroscopic investigation can
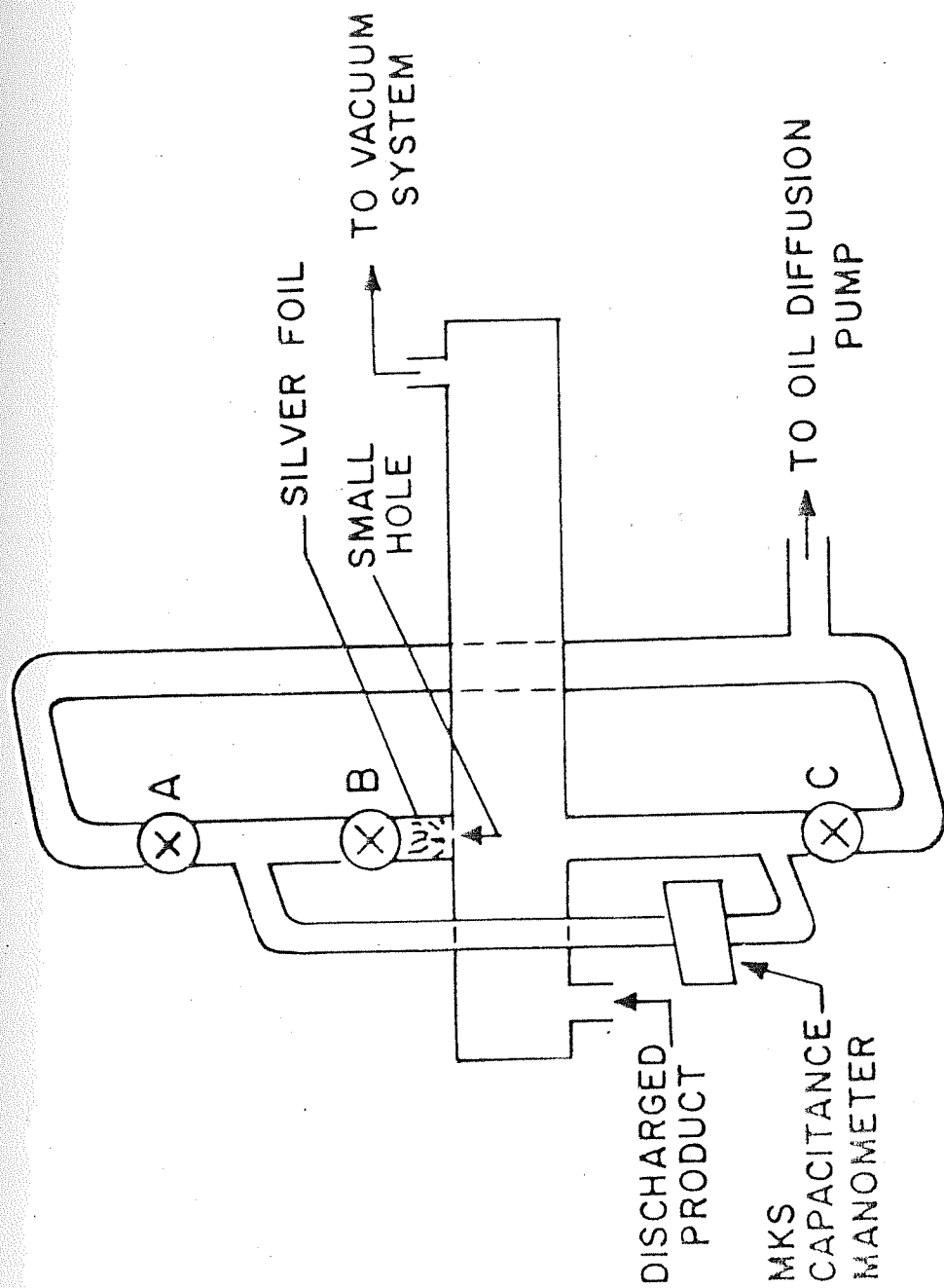
FIG. II. 3 THE AFTERGLOW TUBE WITH WREDE-HARTECK
GAUGE ASSEMBLY

provide sensitive diagnostic tool to study such process. We have used

spectrometric system for energy analysis and detection of afterglow

emission. Spectrometric detection system consists of three parts:

a̲   Monochromator used to disperse afterglow emission.

b̲   Photon detector used to detect low level light signals.

c̲   Data acquisition system.

All these three systems would be discussed in detail in the following

sections.

II.2.5.1. Monochromator

Half-meter vacuum monochromator (model 305-VM, Minuteman

Laboratories, Mass.) used for spectral analysis in this experiment, was a

modified Czerny-Turner spectrometer. This modification essentially

eliminated coma. The model 305-VM was designed to cover the wavelength

region from vacuum ultraviolet (1000 Å) to the infrared (1.2 microns),

using a 1200 lines/m.m. grating (Bausch and Lomb) with a ruled area of

52 x 52 m.m. The normal, linear reciprocal dispersion for the monochro-

mator was approximately 16.7 Å/m.m. and first order half width resolution

better than 0.3 Å. A twelve speed scanning mechanism was provided with

scanning speeds from 0.5 Å/min. to 2000 Å/min. Coupled to this drive

was a digital counter that displayed the wavelength appearing at the exit

slit directly in angstrom units. Both entrance and exit slits were

bilateral and could be adjusted from 0.005 m.m. to 3 m.m. width. Preci-

sion micrometers have been used to open or close the slits.

II.2.5.2. Photon Detector

Below 1.2 microns, the high sensitivity and excellent linearity of photomultiplier tubes make them the most useful photon detectors. In the present experiment, afterglow spectra was studied in the range 1900 to 8000 $\overset{o}{A}$. If one looks at the quantum efficiency curves for all types of photomultipliers, it would be clear that S-20 type with wavelength region extended with quartz window, will be best choice for this range of wavelength. EMI 9558 QB photomultiplier with quartz window has been used in the present system to detect intensity of emission appearing at the exit slit of the monochromator.

An output current could still be obtained at the anode of a photomultiplier even when it is operated in complete darkness. The magnitude of this current sets a limit to the ultimate detectivity and resolution of the device. There are many sources which contribute to the dark current. Principle among these is thermionic emission from the cathode. The thermionic component varies with temperature in accordance with the Richardson equation

$$N = AT^2 \exp(-\phi/kT) \; cm^{-2} \; sec^{-1} \qquad\qquad II.4$$

where ϕ is thermionic work function which ranges from 1 to 1.5 eV for most cathode materials. T is absolute temperature and k is the Boltzman constant.

The background is independent of temperature below a certain critical temperature; for S-20 cathode, negligible background reduction occurs below $-30^{\circ}C$. Thermoelectric refrigerated chamber (Model TE 206-

TSRF, Products for Research, Mass.), which is designed to provide cooling for photomultiplier tube to this temperature was used. The temperature could be maintained in the housing continuously.

Photomultiplier tube is characterised by an ability to generate a discrete electrical output pulse for each photon of excitation. The temperature independent background contains a high proportion of multi electron pulses. The amplitude spectrum for pulse which has arisen from the thermal release of electrons within the dynode structure will generally peak at a lower amplitude than that for a genuine photon event. A useful improvement in output signal-to-noise performance is achieved if these lower amplitude pulses are rejected from the data.

Photomultiplier can be used either in analogue mode or in photon counting mode. In analogue mode, dark current, as measured at the anode, will give a combined contribution of electron emission from the cathode and dynodes together with electrical leakage within the tube. In photon counting mode, contribution of electron emission from dynodes together with electrical leakage within the tube to dark counts can be made zero by using pulse height discriminator. The requirement imposed here is that the top of the pulse should lie above threshold so chosen that the signal to noise ratio is optimum. Photomultiplier tube operated in photon counting mode will provide large signal-to-noise ratio than that in analogue mode for very low light levels. In afterglow, the light level is quite low, that is why the photomultiplier has been used in photon counting mode for afterglow intensity measurement.

The anode dark counts depend on the supply voltage. The
supply voltage of the photomultiplier was so chosen that the ratio between
signal and dark count was as high as possible. For EMI 9558 QB photo-
multiplier with quartz window, this operating voltage was 1300 volts.

II.2.5.3. Data Acuisition System

The data acquisition system included a preamplifier, an
amplifier, a pulse height discriminator and 1024-channel multichannel
analyzer operating in the time mode. The multichannel analyzer was
controlled by a microcomputer. The data display and printing were done by
a cathode ray oscilloscope (C.R.O.) and a teleprinter respectively.
All the data collection system was built in our own laboratory. The
block diagram of the set up is shown in the Fig. II.4.

The anode output from the photomultiplier was capacitively
coupled to a charge sensitive preamplifier with decay time constant of
about 1 µsec. The preamplifier output pulse was amplified through two
stage capacitively coupled amplifier with an overall gain adjusted to
give sufficiently high pulse. This output was fed to a variable threshold
discriminator to cut off the noise and get clean T.T.L. compatible
pulses.

The multichannel analyzer includes the pulse counter, timer,
the master programmer, storage, and the digital to analogue (D/A)
converter for display. The pulses from the variable threshold discrimina-
tor go to the pulse counter and the number of counts for a definite time t
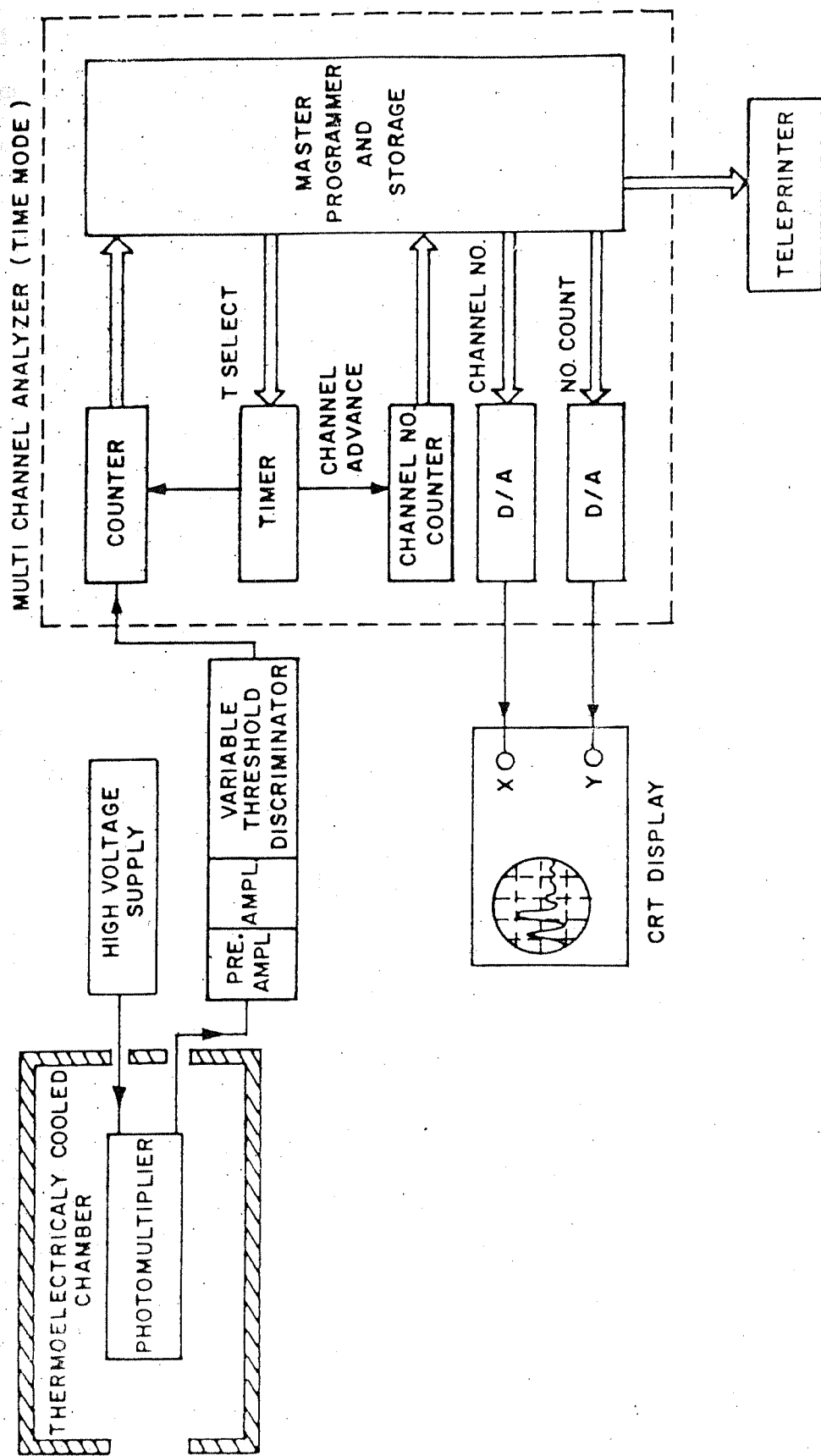is stored in the memory. Here the maximum allowable count rate was about

FIG.II.4: BLOCK DIAGRAM OF THE DATA ACQUISITION SYSTEM

5×10^5. The timer is used to fix the data collection time t for each channel. After each time interval, t, the pulse count is stored in memory in the corresponding channel; and then the channel number is advanced. A repeated fast scan of channel number and corresponding data of pulse counts stored in memory are fed to two D/A converters, output of which were connected to the X and Y inputs of a C.R.O. to display the data distribution. The data at the end of each run is printed and punched out on a paper tape by the teleprinter and plotted on the X-Y recorder.

In our experimental set up, afterglow is scanned by mono-chromator. The wavelength at the exit slit of monochromator is changed linearly by coupling the grating with synchronous motor drive having twelve selectable speeds of scanning. Commands to data acquisition system are given through the teleprinter to select the data collection time t per each channel. The time t can be set from any of the 0.1, 0.2, 1, 2, 10, 20, 100, 200 second intervals. For a particular interval of time t, number of pulses appearing at anode of photomultiplier are counted and are stored in one channel of multichannel analyzer (M.C.A.); at the same time number of that channel is also stored in M.C.A. Then the advanced channel number and number of pulses appearing during time t and 2t are stored in next channel of M.C.A. This way data for 1024 channel can be stored in M.C.A. Now number of pulses stored in one channel for time t is nothing but the average intensity of radiation for particular interval of wavelength. This is displayed on Y-axis of C.R.O. through D/A converter. Each channel number, which corresponds to a certain wavelength at the exit slit is displayed on X-axis of C.R.O.

through another D/A converter. This is how the afterglow spectrum is built and displayed on CRO.

11.3. Performance of the Afterglow Spectrometer

The performance of the afterglow spectrometer was studied under various conditions and the effect of focussing of afterglow emission using one or two cavities was investigated. Also, the effect of impurities on the intensity of afterglow emission was studied in detail. All these aspects along with resolution of the newly built afterglow spectrometer have been discussed in the following sections.

11.3.1. Focussing of Afterglow Emission

We are using cylindrical observation vessel in which atoms are recombining and producing molecules in excited state all over the volume of the vessel. These excited molecules will radiate in all directions. Such an emission could be seen through one of the windows of the observation vessel. This observation vessel will act as a diffuse extended source. Signal level from this extended source could be increased by focussing afterglow at the entrance slit of the monochromator. It may be interesting to study the intensity of some particular vibrational band of the afterglow spectrum both without focussing and after focussing. The intensity of (12,8) and (11,7) vibrational bands of first positive system in nitrogen afterglow was measured first without focussing. Then a quartz lens was used to focus afterglow at the entrance slit of the monochromator. Intensity of the same bands were measured again. Fig. 11.5 shows the effect of focussing very clearly. The intensity in case of focussed spectra is almost twice than that in case of unfocussed
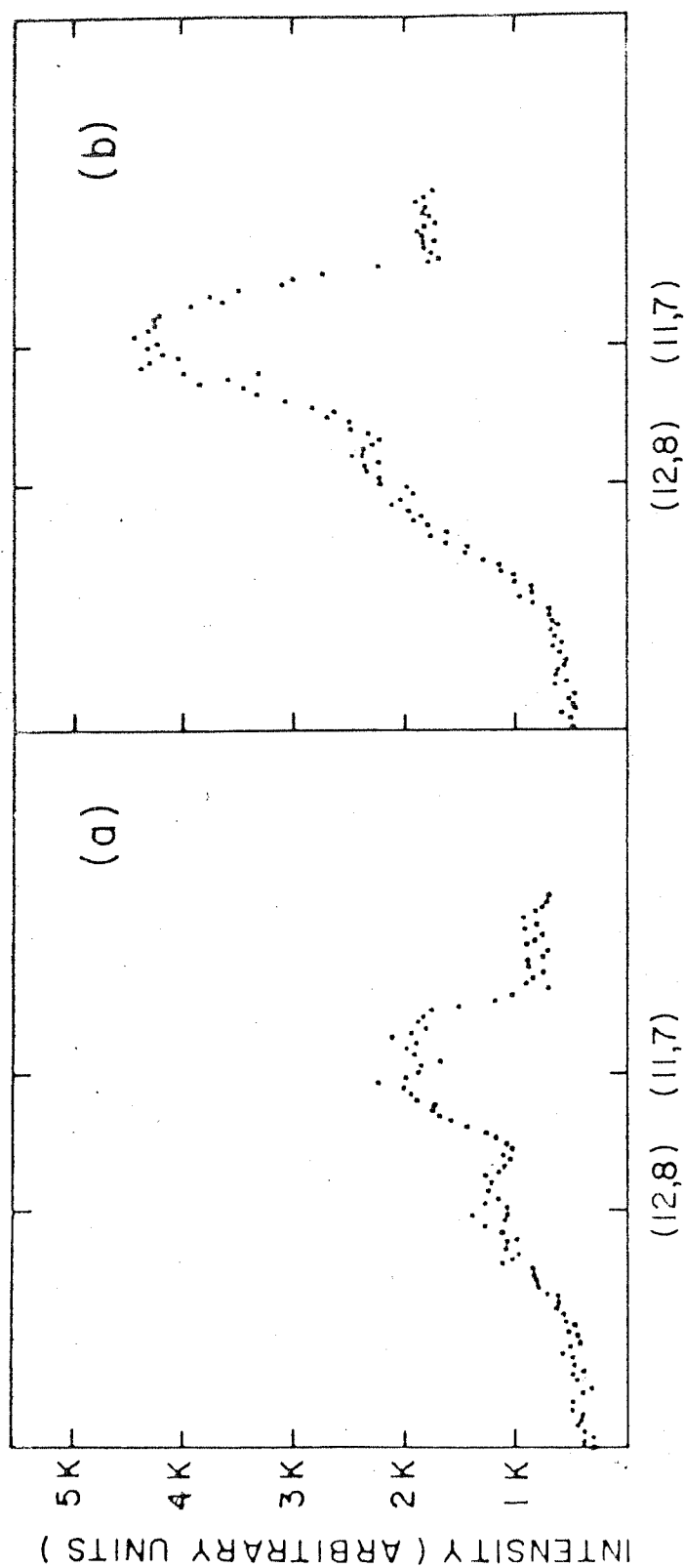
VIBRATIONAL BANDS

FIG. II. 5 CHANGE IN INTENSITY OF (12,8) AND (11,7) VIBRATIONAL BANDS
OF THE FIRST POSITIVE SYSTEM IN NITROGEN AFTERGLOW
(a) WITHOUT USING LENS   (b) AFTER USING LENS ·

spectra. Quartz lens of diameter 2.56 cm and focal length 13 cm was used for this purpose. Effective diameter of the lens used for focussing was 1.8 cm. f-number of lens with effective diameter 18 m.m. and focal length 13 cm matches with f-number, 6.8 for the monochromator. Under this matching condition, the whole grating will be illuminated with afterglow emission.

We have also studied the effect of varying lens position from its focal point. Initially, lens was kept at a distance of focal length from the entrance slit of the monochromator. Distance between this position of lens and observation vessel was 6 cm. Now the distance between the lens and entrance slit was varied from 3 cm towards to 2 cm away from the monochromator. Intensity of (12,8) and (11,7) vibrational bands of first positive system in nitrogen afterglow is monitored for each position and is shown in Fig. II.6. There is some change in intensity as one changes position of lens. But this was found to be much less than what was expected. This is because glow in the observation tube acts as a diffuse extended source. When lens position is varied, some portion of the tube will be focussed and other will be out of focus. Next time some other portion will be focussed and some will be out of focus.

II.3.2. Intensity Versus Time

Discharge through purified gas was switched on and the wavelength at the exit slit of the monochromator was fixed at 5804 $\overset{\circ}{A}$ which corresponded to the peak value of intensity of (11,7) vibrational band of first positive system in nitrogen afterglow. Variation of intensity at this wavelength was monitored with time and is shown in Fig. II.7.

VIBRATIONAL BAND

FIG. II.6   CHANGE IN INTENSITY OF (12,8) AND (11,7) VIBRATIONAL BANDS OF THE
FIRST POSITIVE SYSTEM IN NITROGEN AFTERGLOW

a   LENS POSITION AT 13 cm FROM ENTRANCE SLIT (i.e. AT FOCAL LENGTH)

a+1   LENS POSITION AT 14 cm FROM ENTRANCE SLIT

a+2   LENS POSITION AT 15 cm FROM ENTRANCE SLIT

a−1   LENS POSITION AT 12 cm FROM ENTRANCE SLIT

a−2   LENS POSITION AT 11 cm FROM ENTRANCE SLIT

a−3   LENS POSITION AT 10 cm FROM ENTRANCE SLIT
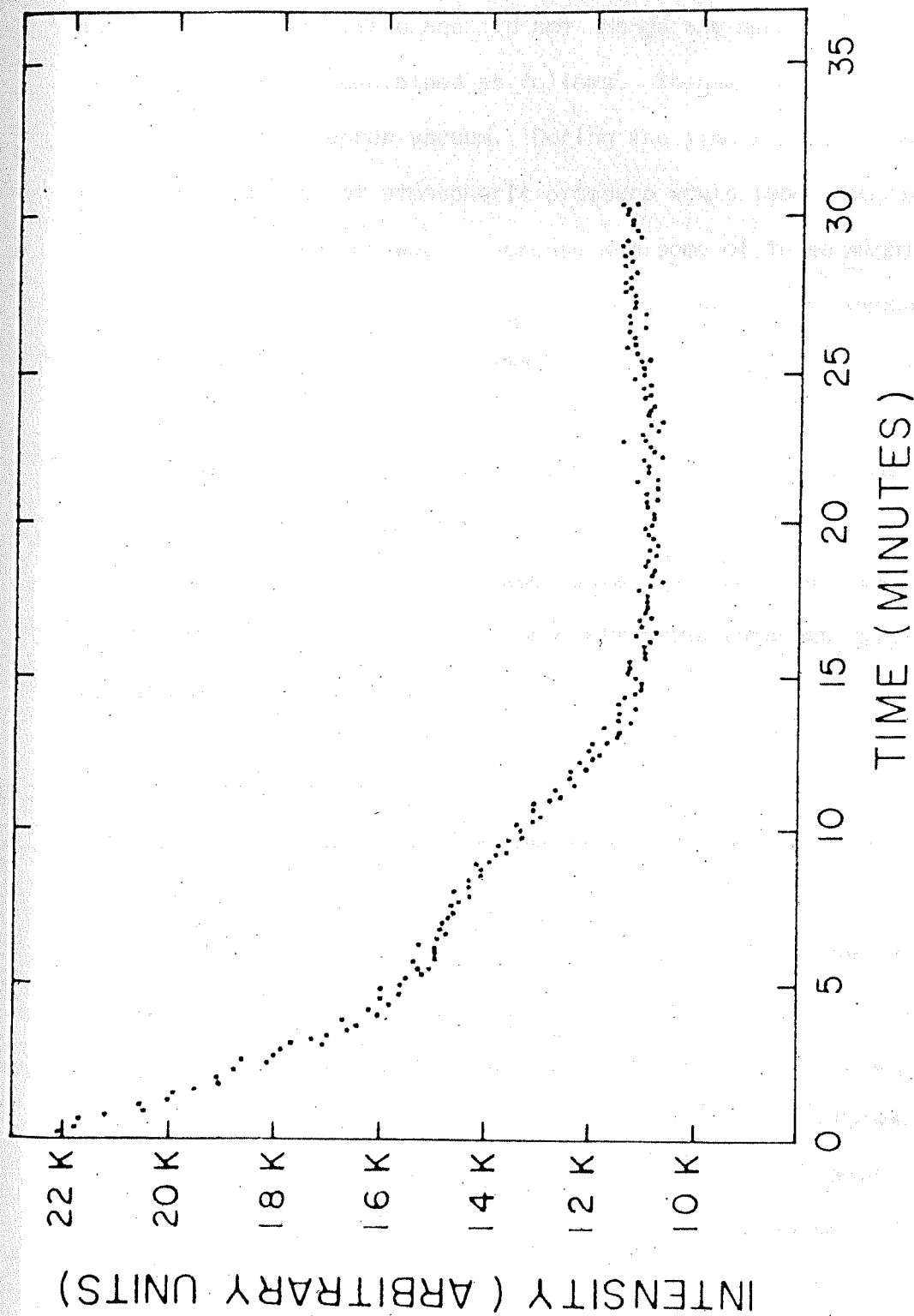
FIG.II.7 CHANGE IN INTENSITY, WHEN WAVELENGTH AT EXIT SLIT WAS FIXED AT 5804 Å, WITH TIME

It was found that in the beginning, the decrease in intensity was quite large but after some time, approximately after 20 minutes, the intensity, more or less, stabilized and did not change any more. The variation in intensity could be explained as follows. Whenever the system was switched off, it was still under vacuum. During the time it is not operated some gases from outside at atmospheric pressure would leak into the system. Impurity concentration would increase and some of these might deposit on the surface of glass tube. Though the whole system was evacuated to 10^{-6} Torr before starting the experiment, it was found that some impurities were still left which gave rise to this problem. Now after 25 minutes, we switched off the discharge and let the gas run continuously at the maintained pressure. The discharge was switched on again after two to three hours. Intensity at the same wavelength was found stabilized. All the observations were taken only after the intensity of the afterglow was completely stabilized.

II.3.3. Effect of Two Cavities

It is known that afterglow comes from two body or three body recombination of atoms forming molecules in excited state. So intensity of the afterglow can be increased by increasing the number of atoms. Microwave discharge is used to dissociate molecules into atoms. It was observed that if two cavities are used in series in place of one cavity, intensity of the first positive system in nitrogen afterglow increased. First using one cavity, intensity of (12,8) and (11,7) vibrational bands of first positive system in nitrogen afterglow was measured and the same was repeated using two cavities. Fig. II.8 a) corresponds to intensity by two cavities and b) corresponds to that by one cavity. It is clear
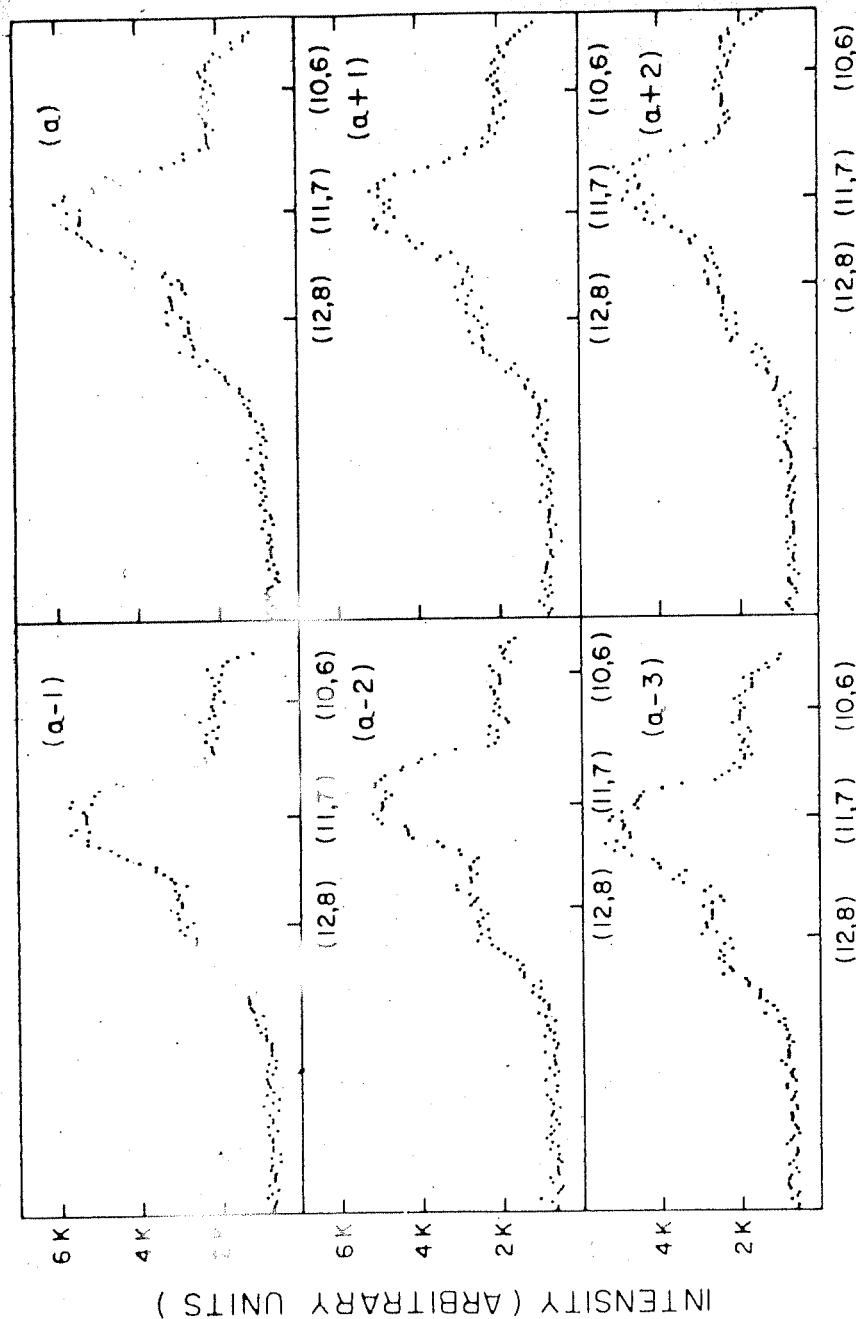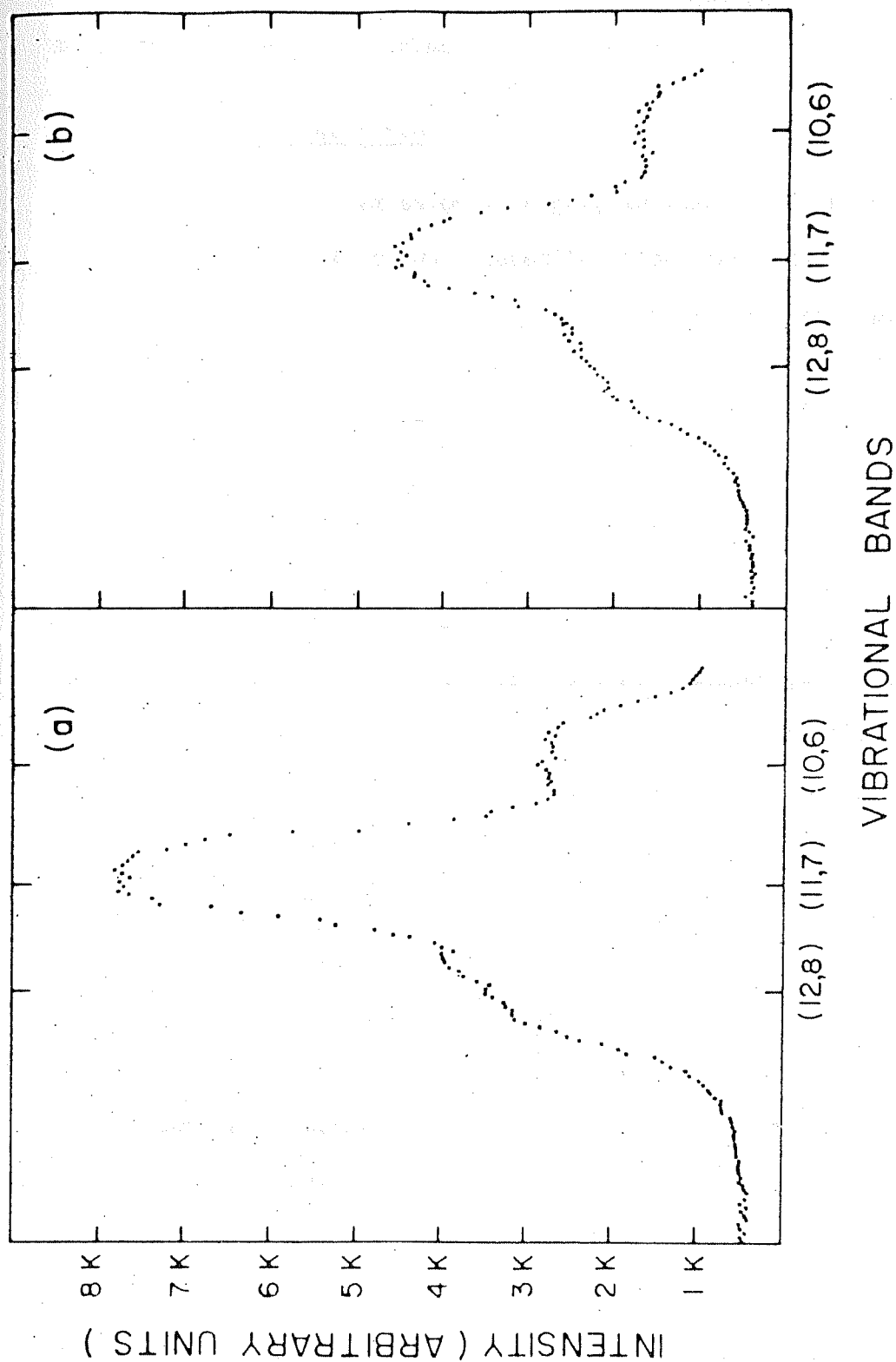
FIG. II.8: CHANGE IN INTENSITY OF (12,8) AND (11,7) VIBRATIONAL BANDS OF
THE FIRST POSITIVE SYSTEM IN NITROGEN AFTERGLOW
(a) WHEN TWO MICROWAVE CAVITY WERE USED
(b) WHEN ONE MICROWAVE CAVITY WAS USED

from the figure that use of two cavities increases the intensity of
these bands by about 1.7 times.

II.3.4. Effect of Impurities

Afterglow emission is highly influenced by impurities. There
are some impurities which when deposited along the walls of the glass
tube from discharge region to observation region, act as a poison to the
afterglow. Most of the emission intensity is lost and practically no
afterglow could be seen coming out of the observation region. Some other
impurities could act as quenching agents to afterglow.

We have come across some impurities which were deposited
on the surface of the flow tubes. One of these impurities was oxides of
copper. For purifying nitrogen gas, ordinary copper turnings were
heated at $700^{\circ}C$ inside a quartz tube as discussed in section II.2.2.1.
Nitrogen gas passing through it has oxygen gas as impurity. Copper's
oxides which were formed inside the quartz tube, came along nitrogen gas
and then passed through the discharge region and were deposited all along
the walls of the observation region. It was found that the intensity of
the first positive system of nitrogen started decreasing with time.
Finally, the intensity decreased to zero. Oil vapours from different
vacuum pumps were another impurity in this class. Oil vapours of the
diffusion/rotary pump could also get deposited on the walls of the system
with the result that glow intensity of the afterglow decreased to zero
after some time. All vacuum greases including the Apiezon grease
(Edwards, U.K.) behaved in the same way and reduction in intensity of the

first positive band was observed. Also any tiny speck of such a grease
if left on the walls of the flow tube, would give a bright blue glow
which is characteristic of its composition. To avoid this, no grease
was used anywhere in the system. No conical joints were used in the
system and greaseless stop-cocks were used wherever necessary. Oil
vapours were trapped using liquid nitrogen traps between the observation
vessel and the pumping line. When ordinary copper turning was replaced
by special pure copper turning, we did not observe the reduction in
intensity of the afterglow.

When Iolar-nitrogen was not purified further we got beta and
gamma band systems of nitric oxide which were very intense. When gas
was further purified by the method discussed earlier, we got very weak beta
and gamma band systems of nitric oxide.

II.3.5. Effect of Varying Slit Heights and Slit Widths of the Monochromator

Resolution of a given monochromator is decided by width and
height of the entrance and exit slits. Slit height controls some of the
optical abervations and therefore contributes to the resolution of the
monochromator only indirectly. If the slit height is reduced, then both
resolution and intensity of the signal are affected. A compromise between
resolution and the intensity throughput would decide the proper slit
height of the monochromator during the experiment.

First of all, height of both entrance and exit slits were
increased equally on both sides from the center of slits. During height
variation slit width was kept constant and lens was kept at its optimum

position. Slit height was increased on both sides of center by 1 mm, 2 mm, 3 mm and 4 mm. For each increase in height, the intensity of (12,8) and (11,7) vibrational bands of the first positive system of nitrogen afterglow were measured. These are shown in Fig. II.9. It is quite clear from Fig. II.9 that when slit height is changed from 1 mm to 2 mm, signal strength increases by a factor of two. But change from 2 mm to 3 mm and from 3 mm to 4 mm shows some nominal increase in the signal strength but the resolution of the monochromator decreases. A 3 mm slit height looks to be a good compromise between resolution and signal strength. Therefore, this slit height was used throughout the experiment.

Effect of variation of slit width was also studied for both resolution and signal strength. Resolving rotational levels requires high resolution and also high signal strength than required for vibrational levels. Slit widths of 300 microns for both entrance and exit slits were chosen for studying the vibrational levels. At these slit widths, most of the vibrational levels were resolved with good signal to noise ratio. Slit widths of 50 microns each was found suitable for studying rotational levels of (12,8) and (11,7) vibrational bands of first positive system of nitrogen. At this slit width, signal to noise ratio was good and some of the rotational levels were resolved. Slit widths of 100 microns each were chosen for rotational levels analysis of (12,9) and (11,8) vibrational bands.

Fast or slow scanning of the monochromator could also affect the apparent resolution to some extent. In our experiment, photon counting technique has been used for intensity measurement. If the
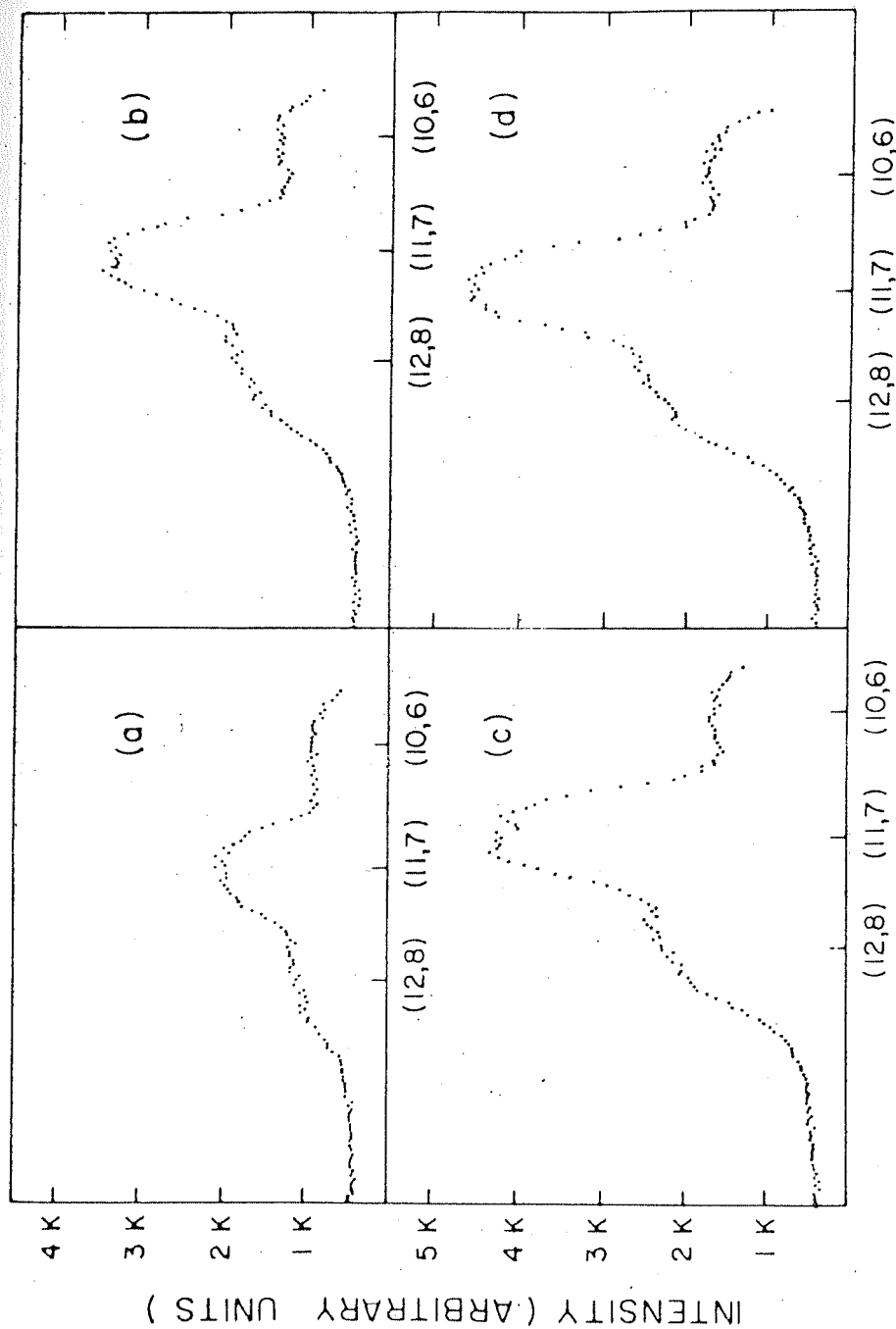
FIG.II.9 CHANGE IN INTENSITY OF (12,8) AND (11,7) VIBRATIONAL BANDS OF THE
FIRST POSITIVE SYSTEM IN NITROGEN AFTERGLOW

(a) AT SLITS HEIGHT 1 m.m. FROM CENTRE OF THE SLIT

(b) AT SLITS HEIGHT 2 m.m. FROM CENTRE OF THE SLIT

(c) AT SLITS HEIGHT 3 mm FROM CENTRE OF THE SLIT

(d) AT SLITS HEIGHT 4 m.m. FROM CENTRE OF THE SLIT

integration of signal is done for time, say x, then during this time, change in wavelength at the exit slit of the monochromator, due to grating rotation, should be less than the wavelength resolution of the system. Though monochromator will be resolving but the resolution at the display of data will show apparently bad resolution. A scanning speed of 20 Å/min. was chosen for vibrational analysis and signal was integrated for 10 second and was stored in a multichannel analyzer. So each channel data will correspond to 3.33 Å. Scanning speed of 2 Å/min. was chosen for rotational levels analysis. Again signal was integrated for 10 second and was stored in multichannel analyzer. So each channel data will correspond to 0.33 Å .

II.3.6. Resolution of the System

Resolution of the system was measured with known intense atomic lines of mercury (Hg) and Cadmium (Cd). For this purpose mercury and cadmium lamps with quartz envelope were used. The lamp was mounted on the flange M (Fig. II.2) of the observation vessel near the quartz window. During this measurement, the reflecting mirror was removed from the quartz window. Resolution of the system was measured using various slit widths.

For 300 micron entrance and exit slit widths, half width (FWHM) of some atomic lines was about 6 to 7 Å in the wavelength region from 2500 to 7600 Å. Beam resolution at 50 and 100 micron slit widths for both entrance and exit slits was about 1.1 and 2.3 Å respectively. Two mercury atomic lines at wavelength 5769.6 Å and 5790.66 Å and cadmium atomic line at wavelength 6438.47 Å were chosen for measuring resolution

of the system at 50 and 100 micron slit widths for both entrance and exit slits.

Effect of vibrations on the resolution of the monochromator was also studied. This effect was studied for the slit width of 50 microns at wavelengths 5769.6 and 5790.6 $\overset{\circ}{A}$. It was found that vibrations due to mechanical pump did not affect the resolution of the system.

II.4. Wavelength Calibration of the Afterglow Spectra

Wavelength analysis of the afterglow emission spectra was done with scanning monochromator. The scanning drive of the monochromator is coupled to a counter that displays the wavelength appearing at the exit slit, directly in angstrom units. The monochromator counter which displays the wavelength, was calibrated with known atomic lines for wavelength calibration of afterglow spectra. Mercury lines at wavelength 2536.52 $\overset{\circ}{A}$, 2847.68 $\overset{\circ}{A}$, 3264.06 $\overset{\circ}{A}$, 3650.15 $\overset{\circ}{A}$, 4046 $\overset{\circ}{A}$, 4358.33 $\overset{\circ}{A}$, 5460.74 $\overset{\circ}{A}$, 5769.6 $\overset{\circ}{A}$ and 5790.66 $\overset{\circ}{A}$ were used for calibration. Cadmium line at wavelength 6438.47 $\overset{\circ}{A}$ and Krypton line at wavelength 7525.40 $\overset{\circ}{A}$ and 7587.41 $\overset{\circ}{A}$ were also used for calibration. It was found that there was a constant difference between the two wavelength scales, one provided by the counter of the monochromator and the other provided by standard atomic lines. This correction was used in the subsequent analysis of the afterglow spectra of nitrogen and oxygen.

CHAPTER III

AFTERGLOW SPECTRA OF NITROGEN AT DIFFERENT TEMPERATURES AND PRESSURES

III.1. Introduction

The importance of studying nitrogen afterglow has been discussed in detail in the first chapter. The afterglow spectrum gives the relative intensity distribution of vibrational peaks corresponding to various electronic states of the molecule. The study of the vibrational intensity in the afterglow spectra at different pressures, temperature and with different diluent gases contributes to the knowledge of population mechanisms of the emitting states and also about quenching of emitting state by the carrier gas.

In this chapter the nitrogen afterglow spectra from 1900 to 8000 Å have been reported at two temperatures, 300°K and 77°K, using experimental system discussed in detail in the second chapter. Relative vibrational intensity for the first positive system have been computed at both the temperatures. The pressure dependence of intensities of various bands has been investigated at pressures between 2 and 7 Torr while the effect of diluent like argon has been studied at a fixed argon pressure of 5 Torr and varying nitrogen pressures from 0.2 to 3 Torr. Finally, the results are discussed in detail.

III.2. Results

III.2.1. Afterglow Spectra

Afterglow spectra of molecular nitrogen was studied from 1900 to 8000 Å at two temperatures, 300°K and 77°K. The spectra observed included, the well known first positive system of nitrogen from around 5000 to 7800 Å, a few Vegard-Kaplan bands from 2300 to 3400 Å and some bands belonging to infra-red afterglow system of nitrogen from 6800 Å to 7400 Å. The beta and gamma bands of nitric oxide, found to be very weak at 300°K but very predominant at 77°K, were observed in the spectral range from around 2000 Å to 4300 Å. Also, some CN bands and bands belonging to second positive system of nitrogen (only at 77°K) were observed in the afterglow spectra of nitrogen. The NI emission line at 3466 Å was observed both at 300°K and 77°K but the OI emission line at 5577 Å was observed in the spectrum at 77°K only.

The afterglow spectrum of nitrogen from 1900 to 4800 Å at 300°K is shown in Fig. III.1. Weak Vegard-Kaplan bands of molecular nitrogen could be identified at the same wavelength as reported by Pearse and Gaydon (1965). Only (0,6), (0,7) and (0,9) bands of the A $^3\Sigma_u^+ \rightarrow$ X $^1\Sigma_g^+$ (Vegard-Kaplan) system were predominant to some extent while other bands were relatively weaker. Some of the beta bands of NO (B $^2\Pi \rightarrow$ X $^2\Pi$) were also observed as impurity spectra. The (0,4) to (0,11) bands were relatively weak and the strongest of these bands was about 25 times less intense than the (11,7) band of first positive system of nitrogen at 300°K (Fig. III.2). The impurity CN bands (B $^3\Sigma \rightarrow$ A $^2\Pi$) corresponding to Δv = 0 and 1 were also observed and were found to be relatively intense. Some other bands were also observed which could not be identified. The NI emission line at 3466 Å corres-ponding to N(^{2}P) $\rightarrow$ N(^{4}S) transition was observed to be as intense as some of the CN bands.

The afterglow spectrum of nitrogen at 7 Torr from 4800 to 8000 Å at 300°K is shown in Fig. III.2. The spectrum covers the first positive system (B $^3\Pi_g \rightarrow$ A $^3\Sigma_u^+$) of nitrogen corresponding to Δv = 6, 5, 4, 3, 2 respectively. The band system corresponding to y' = 12 to 5 for Δv = 4, v' = 12 to 3 for Δv = 3 and v' = 7 to 2 for Δv = 2 are nicely resolved while some bands for Δv = 6 and 5 are barely resolved. The infra-red afterglow system corresponding to (8,2) and (8,3) bands have been observed to be very weak with band heads at 6896 Å and 7780 Å, respectively. These bands were observed to be very predominant at 77°K (Fig. III.6).
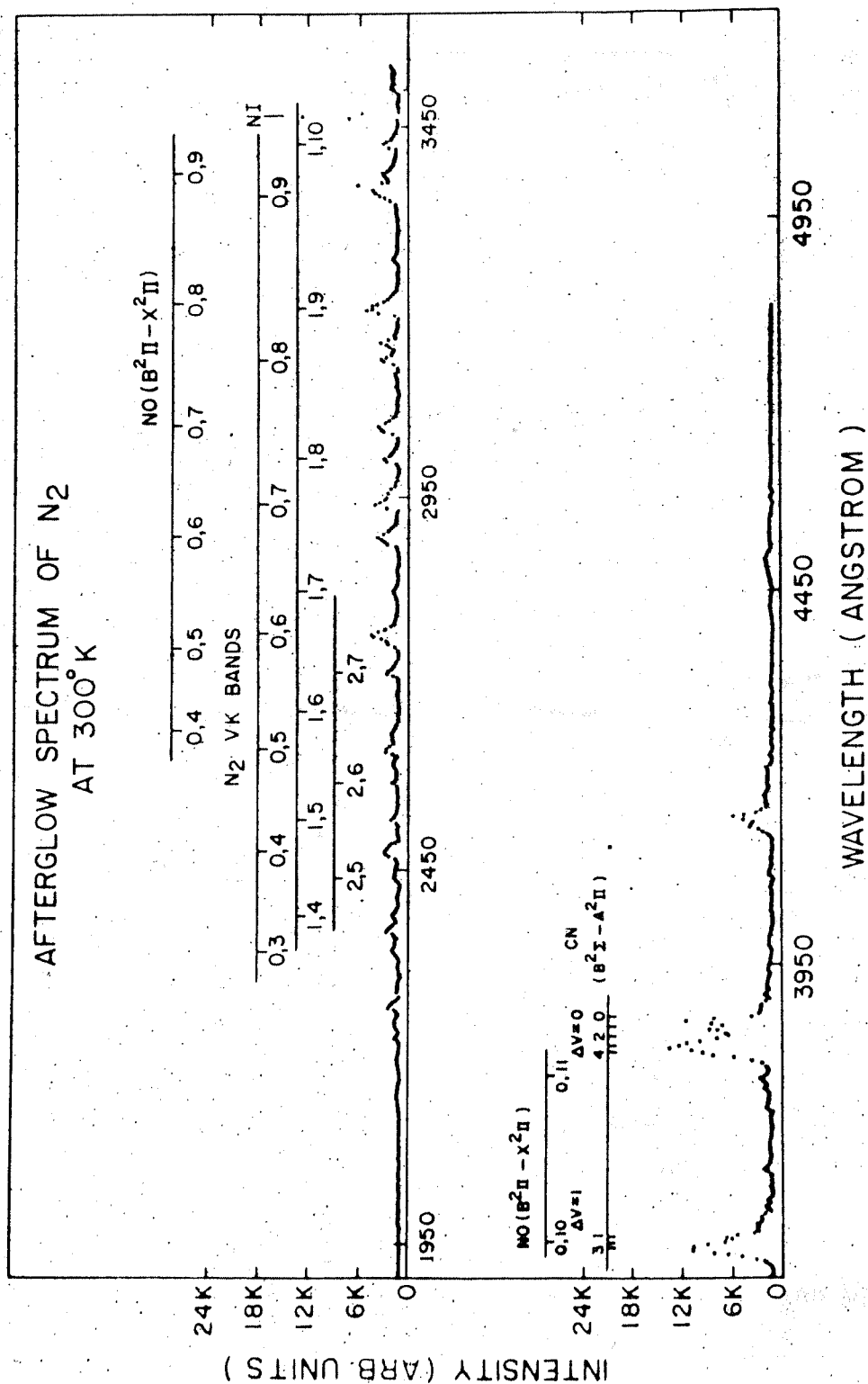
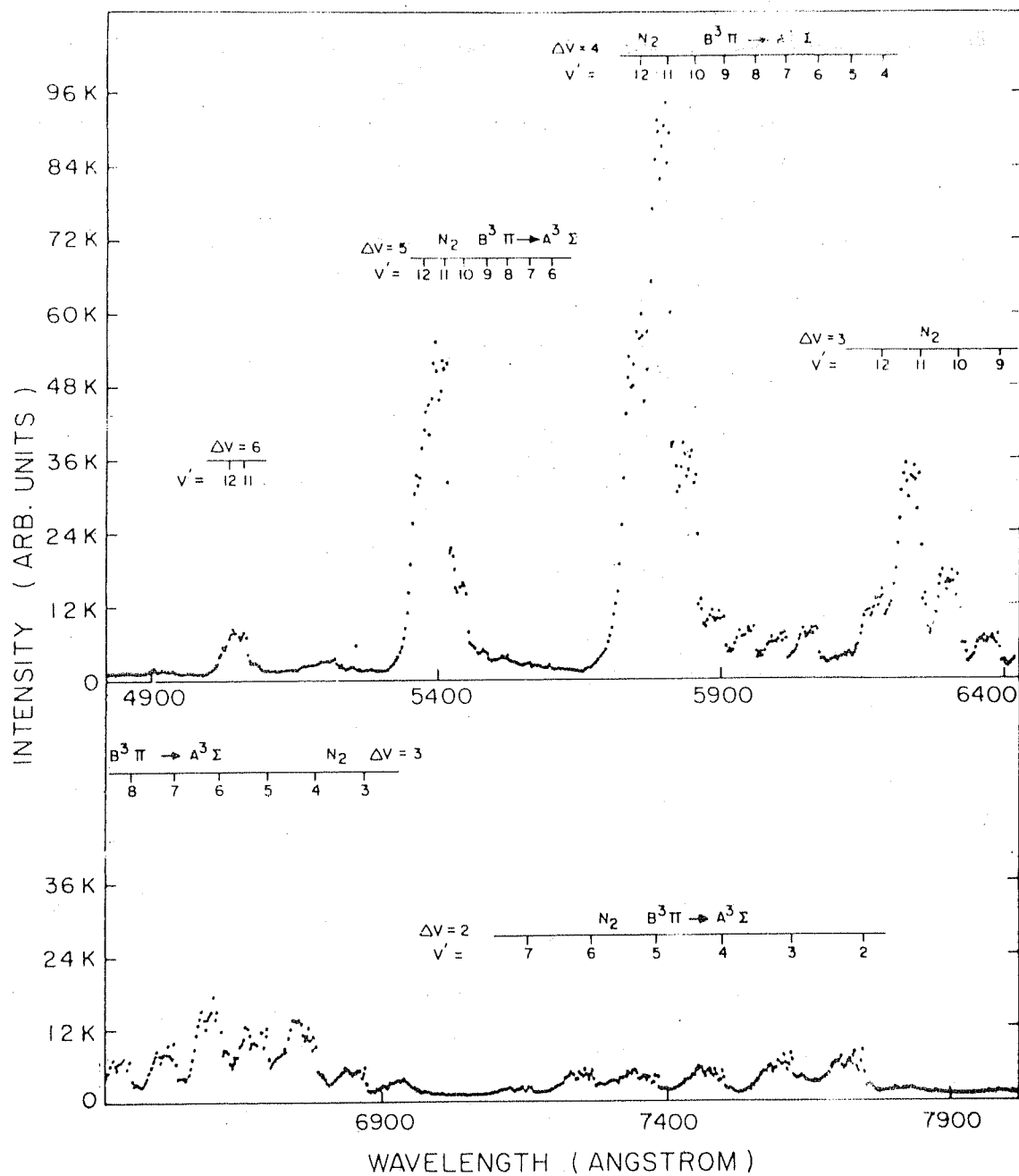Fig. III.1   Afterglow spectra of nitrogen at 300°K from 1900 to 4800 Å.

Fig. III.2   Afterglow spectra of nitrogen at 300°K from 4800 to 8000 Å.

Ung (1976, 1980) observed the vibrational level v' = 13 of $N_2(B\ ^3\Pi_g)$ state, in the first positive system of Lewis-Rayleigh after-glow of nitrogen, at higher pressure range (from 0.5 to 20 Torr). He also reported the detection of higher vibrational levels of the B $^3\Pi_g$ state upto v' = 26. Since v' = 13 lies just above the dissociation limit, it was interpreted as being populated from two-body recombination of N(^{4}S) atoms involving inverse predissociation via the $N_2(^5\Sigma_g^+)$ state. Later on, Brennen and Shuman (1977) in a similar experiment failed to observe emissions from v' ≥ 13 levels in the first positive system of nitrogen afterglow. In the present experiment, at both 300°K (Fig. III.2) and 77°K (Fig. III.6), we did not observe any emission corresponding to v' ≥ 13 level. It appears that in Ung's experiment, there was a likely leakage of light from direct excitation into the afterglow chamber and this leaked light mixed with the afterglow emissions to produce wrong results. Our results therefore, favour the mechanism that $N_2(B\ ^3\Pi_g)$ state is populated through collision-induced transition from a precursor state of nitrogen in the presence of a third body.

From Fig. III.2, the relative populations for the different vibrational levels of the B $^3\Pi_g$ state were measured. Only peak heights were measured and it was assumed that under normal circumstances, the peak heights of different bands were proportional to the areas covered by the peaks. These peak heights were then corrected for the quantum efficiency of the photocathode of EMI 9558 QB photomultiplier, shown in Fig. III.3, which varied with wavelength of the emitted radiation. The vibrational population of the most intense peak ((11,7) in this case)
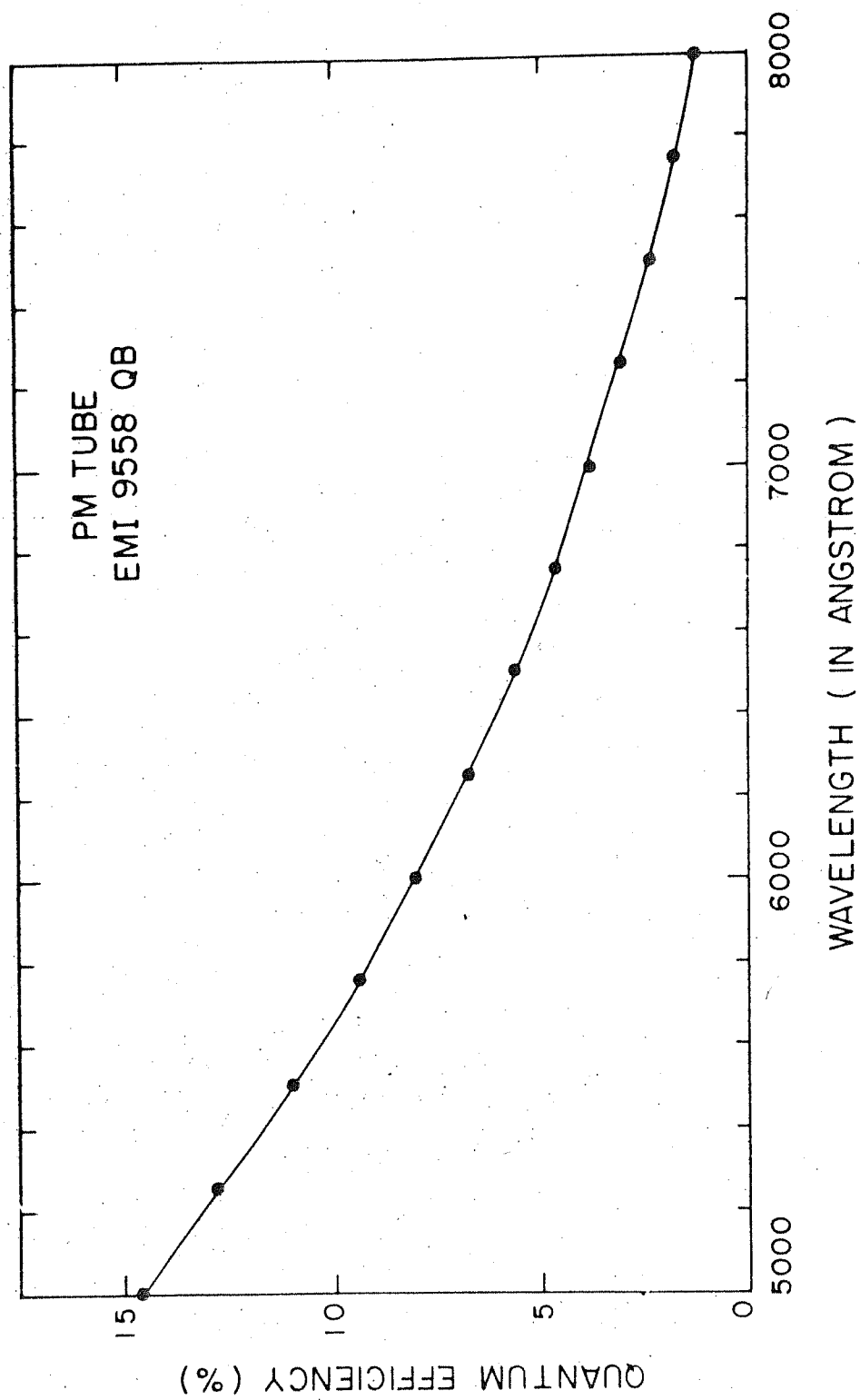
Fig. III.3   Spectral response curve for S-20 type (EMI 9558QB) photomultiplier tube from 5000 to 8000 Å.

was normalized to 100% and the population for other peaks were calculated accordingly. The vibrational populations thus calculated are shown in Fig. III.4. Also shown in this figure are vibrational intensities of the various bands of first positive system of nitrogen as observed from emission spectroscopy (Pearse and Gaydon (1965)). These are normalized in the similar way as in the case of afterglow data. The results for emission spectroscopy show a maxima at $v' = 12, 11, 10$ levels of the B $^3\Pi_g$ state for $\Delta v = 5$, at $v' = 10, 9, 8$ for $\Delta v = 4$, at $v' = 8, 7$ for $\Delta v = 3$ and at $v' = 4, 3$ for $\Delta v = 2$ bands, in accordance with the Franck-Condon principle. In case of afterglow spectra as reported in Fig. III.4, the population maxima occur at $v' = 11$ for $\Delta v = 5$, at $v' = 11, 6$ for $\Delta v = 4$, at $v' = 11, 6$ and 4 for $\Delta v = 3$ and at $v' = 6$ and 2 for $\Delta v = 2$. This is because the emitting states of these two types of emissions are populated by different mechanisms.

Afterglow spectra of nitrogen was also studied at 77^OK in the spectral range between 1900 and 8000 $\overset{O}{A}$. These spectra are shown in Fig. III.5 and Fig. III.6, respectively. In Fig. III.5 is shown the afterglow spectrum observed at 5 Torr nitrogen pressure from 1900 to 4800 $\overset{O}{A}$. Well-defined and very intense bands of nitric oxide have been observed corresponding to B $^2\Pi \rightarrow$ X $^2\Pi$ and A $^2\Sigma^+ \rightarrow$ X $^2\Pi$ transitions. The most intense (0,6) band of NO (B $^2\Pi \rightarrow$ X $^2\Pi$) is almost 1.6 times as intense as (11,7) band of the first positive system of nitrogen observed at 300^OK. The doubly degenerate character of NO beta bands was observed in only some bands like (0,8), (0,9), (0,10), (0,11) etc. Most of the bands corresponding to gamma system of NO have also been identified and
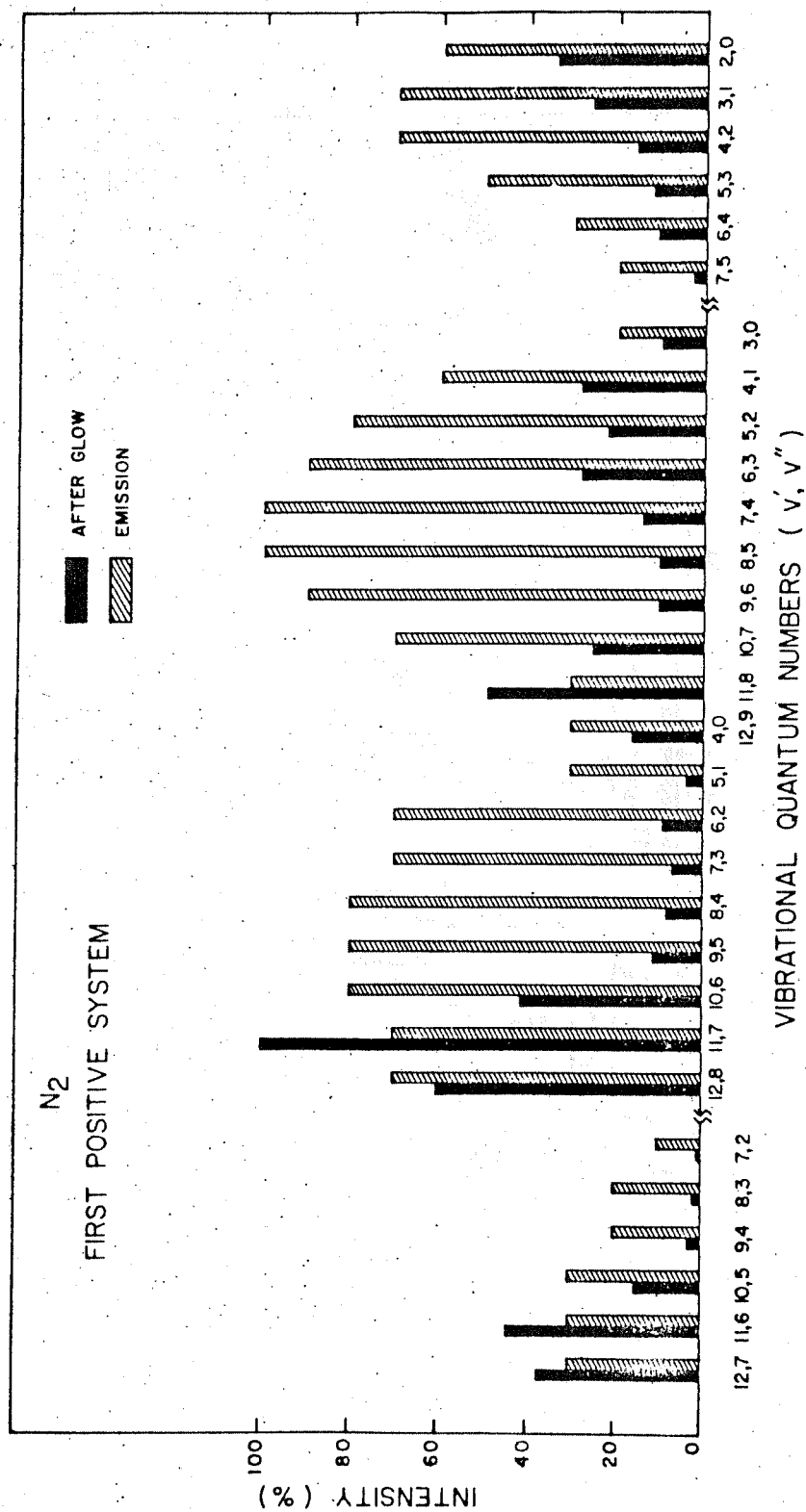
Fig. III.4 The relative intensities of vibrational bands corresponding to first positive system of nitrogen at 300°K. Also shown are intensities of these bands as obtained from emission spectroscopy.
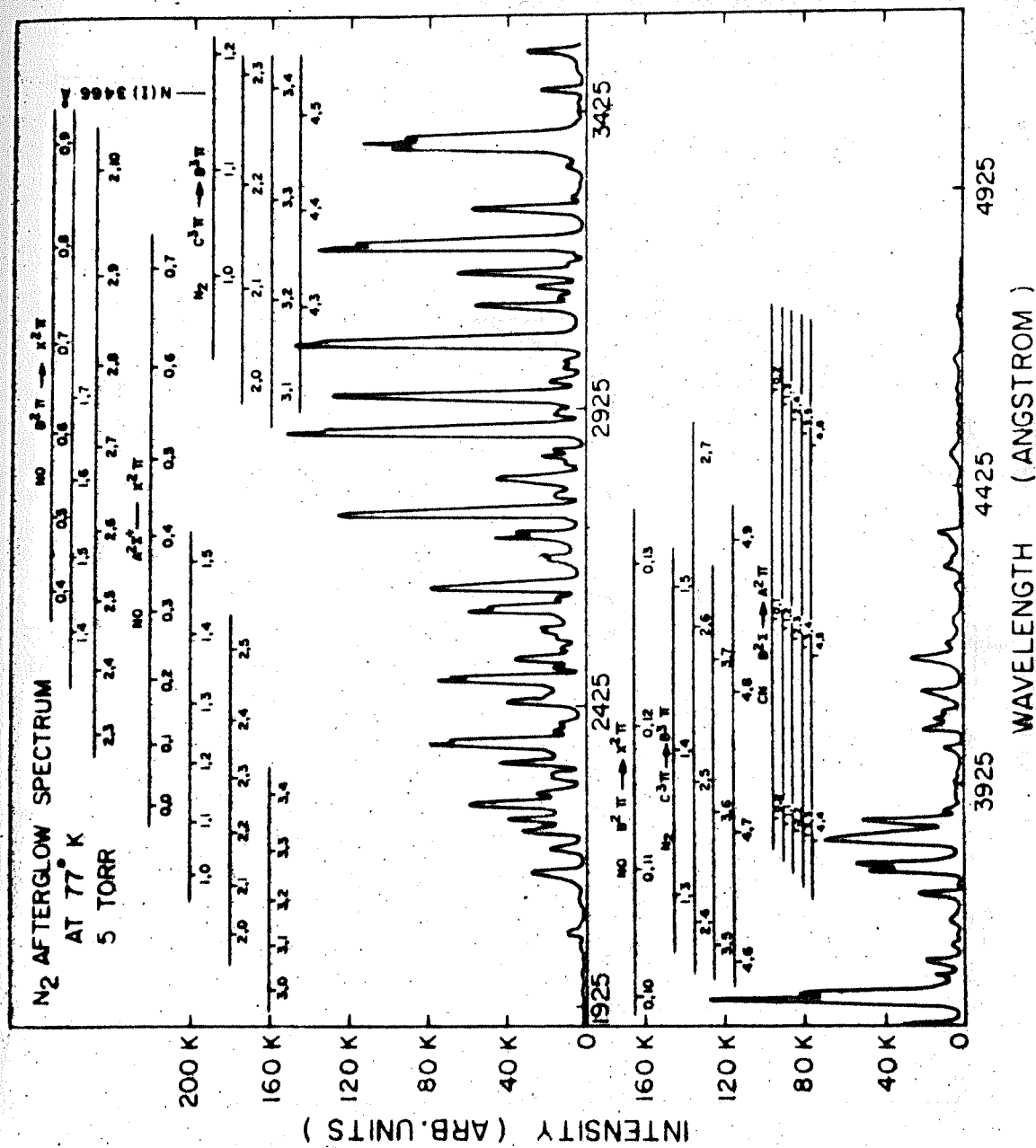
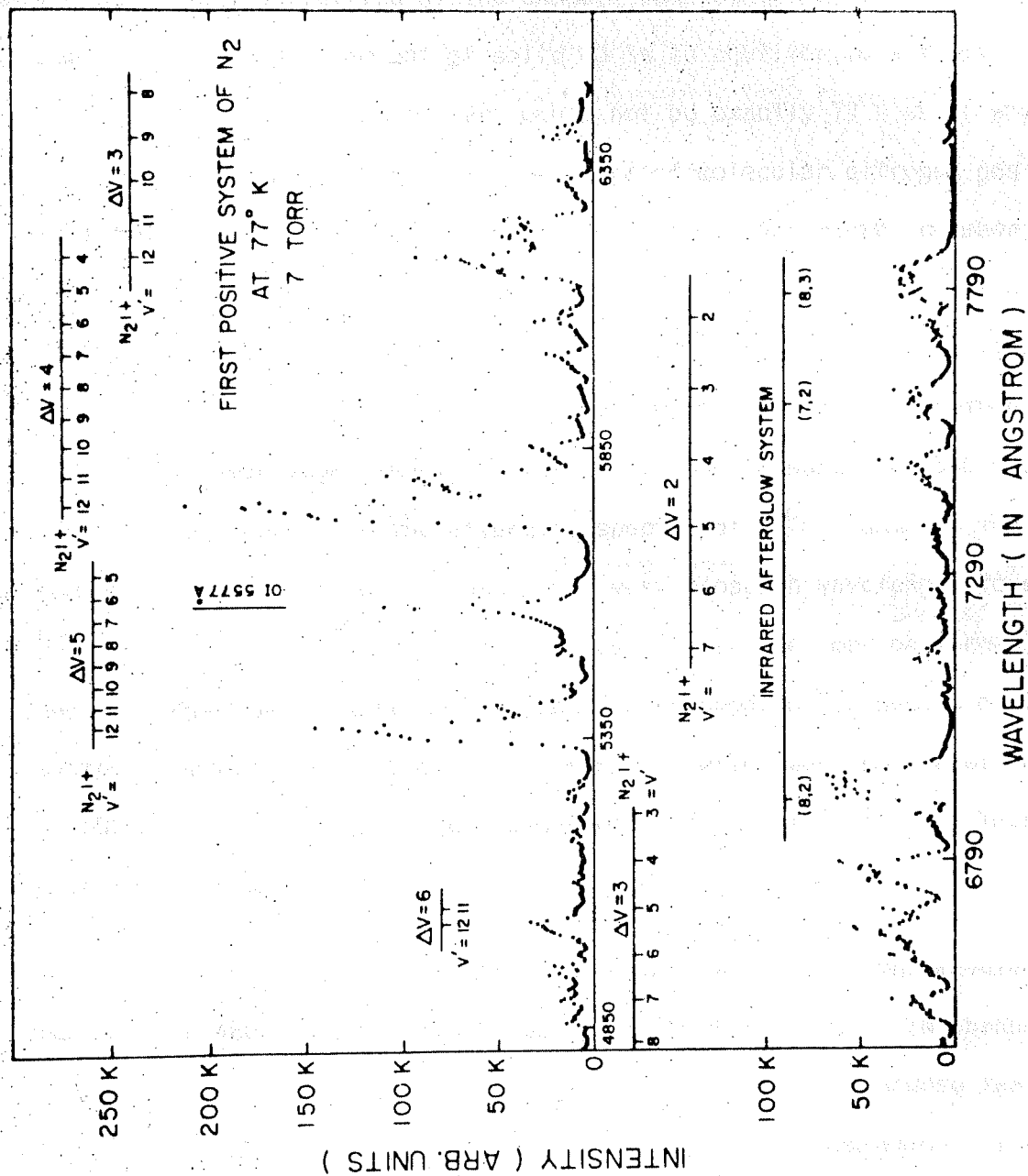Fig. III.5   Afterglow spectra of nitrogen at 77°K from 1900 to 4800 Å.

Fig. III.6   Afterglow spectra of nitrogen at 77°K from 4800 to 8000 Å.

have been shown in Fig. III.5. The NO bands observed as impurity bands.
At 300^OK, these bands are very weak as is evident from Fig. III.1, but
at 77^OK, such bands are highly intense. The reason is that any trace of
NO formed gets solidified at the chamber temperature of 77^OK. After
some time, the large amount of solid NO is in equilibrium with its vapour
at around 77^OK. The temperature would not be exactly 77^OK as it would
vary slightly depending upon the pressure of molecular nitrogen gas in the
afterglow tube. The large amount of NO in the experimental chamber gives
rise to very intense beta and gamma bands. The other impurity afterglow
spectra is of CN. A direct comparison at 77^OK and 300^OK clearly shows
that the B $^3\Sigma \rightarrow$ A $^2\Pi$ bands of CN are much more intense at 77^OK than at
300^OK. The weak Vegard-Kaplan bands of nitrogen observed at 300^OK are
conspicuously absent in the afterglow spectra at 77^OK. Some of the
members of the Vegard-Kaplan bands are very close in wavelength to some
gamma bands of nitric oxide with the result that they may be merged to
show a single peak. A new set of bands corresponding to second positive
system of molecular nitrogen (C $^3\Pi_u \rightarrow$ B $^3\Pi_g$) which were completely absent
at 300^OK (Fig. III.1) have been observed at 77^OK (Fig. III.5). These are
moderately intense bands.

The afterglow spectra of nitrogen at 77^OK in the wavelength
region from 4800 to 8000 $\overset{O}{A}$, has been shown in Fig. III.6. The bands
(12,7), (12,8) and (12,9) were observed to be much more intense than
bands (11,6), (11,7) and (11,8). In comparison, the vibrational level
v' = 11 for the B $^3\Pi_g$ state was found to be much more populated than
the vibrational level v' = 12 in the afterglow spectra at 300^OK. Also,
the most intense band at 77^OK ((12,8) in this case) was observed to be

about 2.2 times more intense than the most intense band (11,7) at 300°K.

In general, the intensity of all bands observed at 77°K is much larger

than for bands studied at 300°K. The infra-red afterglow bands (8,2)

and (8,3) were also very predominant in the spectra at 77°K. Some rela-

tively weak bands in the spectral region from 4850 to 4980 $\overset{O}{A}$, from 5080

to 5300 $\overset{O}{A}$ and around 8070 $\overset{O}{A}$ were also observed but these could not be

identified in an unambiguous manner. Another special feature of the

spectra was the presence of OI emission line at 5577 $\overset{O}{A}$. This emission

line was very intense in the afterglow spectrum at 77°K but was comple-

tely absent in the spectrum at 300°K. It appeared that both at 300°K

and 77°K, an appreciable though small concentration of $O(^1S)$ atoms was

produced by the three body volume recombination of $O(^3P)$ atoms which

in turn, were produced because of discharge of small quantity of impurity

oxygen present in the system. The strong quenching agents of $O(^1S)$

atoms were N_2, N and O_2 ($^1\Delta_g$). It may be noted that O_2 ($^1\Delta_g$) concentra-

tion would be appreciable, though small. We have observed that at a

pressure of 1 Torr of oxygen, O_2 ($^1\Delta_g$) and O (^3P) produced by microwave

discharge were about 24% and 10% respectively of parent molecule.

O_2 ($^1\Delta_g$), though small in concentration, has large quenching rate of about

1.7×10^{-10} cm^3 sec^{-1} for $O(^1S)$ as reported by Slanger and Black (1981).

Thus all the three quenching agents are effective at 300°K where colli-

sions are large. But at 77°K, the number of collisions are appreciably

reduced and therefore, the $O(^1S) \rightarrow O(^1D)$ transition emitting 5577 $\overset{O}{A}$

radiation, could be observed.

The oxygen atoms in $O(^1S)$ state could alternatively be produ-

ced by the following reaction

$$N_2(A \, ^3\Sigma_u^+) + O \, (^3P) \rightarrow N_2 \, (X \, ^1\Sigma_g^+) + O \, (^1S) \qquad III.1$$
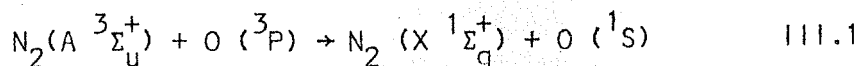
An approximate rate constant of $3.2 \times 10^{-12} \, cm^3 \, sec^{-1}$ as measured in a discharge flow tube, was reported by Meyer et al. (1969). A linear correlation between the intensities of any Vegard-Kaplan band $(A \, ^3\Sigma_u^+ \rightarrow X \, ^1\Sigma_g^+)$ and that of 5577 Å emission would confirm the presence of this reaction. In the present experiment, as stated previously, most of the vibrational bands of Vegard-Kaplan system are masked by NO gamma and beta bands in the afterglow spectra at 77°K. Thus the intensity correlation between the two emissions cannot be studied. In light of the above arguments, it is strongly felt that O (^1S) could be produced by both the reactions mentioned above.

From Fig. III.6, the relative population for the different vibrational levels of the B $^3\Pi_g$ state were measured in the same manner as in the case of measurement of vibrational intensities at 300°K. The vibrational populations were corrected for the quantum efficiency of the photocathode used and were normalized for the most intense peak ((12,8) in this case) to 100%. The populations for the other peaks were computed accordingly. The vibrational populations at 77°K, thus computed are shown in Fig. III.7 alongwith those at 300°K. Intensity maxima were observed at $v' = 12$ for $\Delta v = 5$, at $v' = 12$ and 6 for $\Delta v = 4$, at $v' = 12$, 9, 6 and 4 for $\Delta v = 3$ and at $v' = 7$ and 3 for $\Delta v = 2$.

III.2.2. Pressure Dependence

The afterglow spectra of nitrogen was studied at various pressures ranging from 1 to 7 Torr, both at 300°K and 77°K. All members
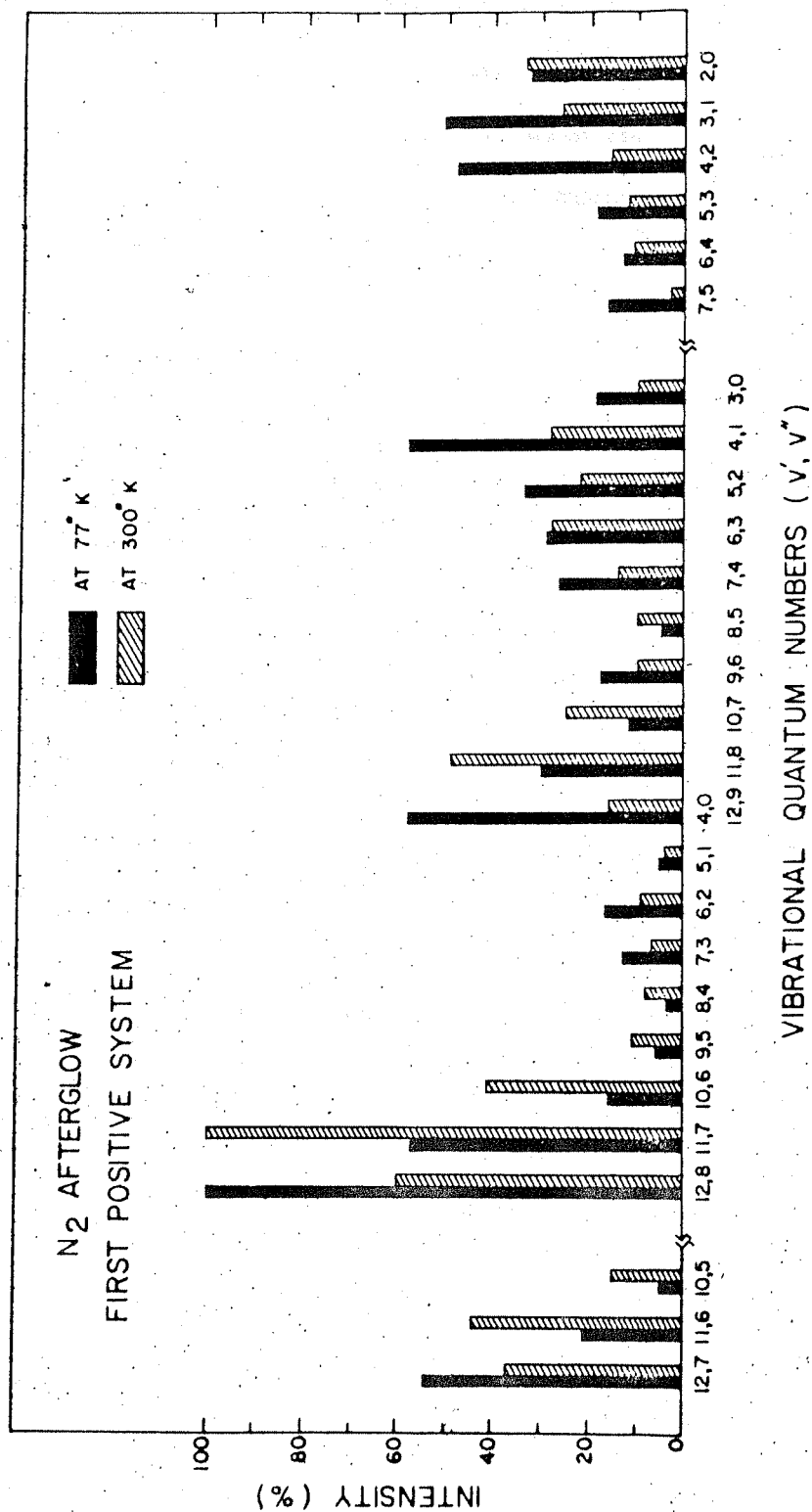
Fig. III.7   The relative intensities of vibrational bands corresponding to first positive system of nitrogen at $77^{\circ}K$. Also shown are intensities of these bands at $300^{\circ}K$.

of the first positive system could be observed at pressure from 2 to 7 Torr but at 1 Torr, spectra corresponding to (12,8) and (11,7) bands could only be observed. At pressures less than 1 Torr, the wall-recombinations increased drastically with the result that no afterglow spectra could be observed at these two temperatures.

The spectra at $300^{O}K$ and at various pressures have been shown in Fig. III.8 and Fig. III.9. The spectra correspond to $\Delta v = 4$ and $\Delta v = 3$ respectively. The peak intensities of the various bands were computed as a function of pressure of molecular nitrogen.

To ascertain whether the peak intensities of bands in the first positive system of nitrogen, had direct $[N]$ dependence or direct $[N]^{2}$ dependence, it became essential to measure the absolute atomic nitrogen concentration as a function of pressure. As has been explained in Chapter II, such measurements were made using Wrede-Harteck gauge fixed on the observation vessel near the point from where discharged products entered into the observation vessel. The dissociation effi-ciency of nitrogen, as defined by equation II.3, was measured at various pressures and has been shown in Fig. III.10. It varied from about 8 to 14% at pressures ranging from 7 Torr to 0.2 Torr. Knowing dissociation efficiency, the atomic nitrogen concentrations at various nitrogen pressures could be easily calculated. Our values of dissociation effi-ciencies are higher than those obtained by nitric oxide titration method. The values by titration method were reported to vary from 1 to 3%. However, it was observed by Ding et al. (1977) that the atomic concentra-tions measured by Wrede-Harteck gauge and mass spectrometric techniques

Fig. III.8 Afterglow spectra of some vibrational bands of first posirive system of nitrogen at 300°K corresponding to Δv = 4. The spectra have been obtained for various pressures ranging from 7 to 2 Torr.
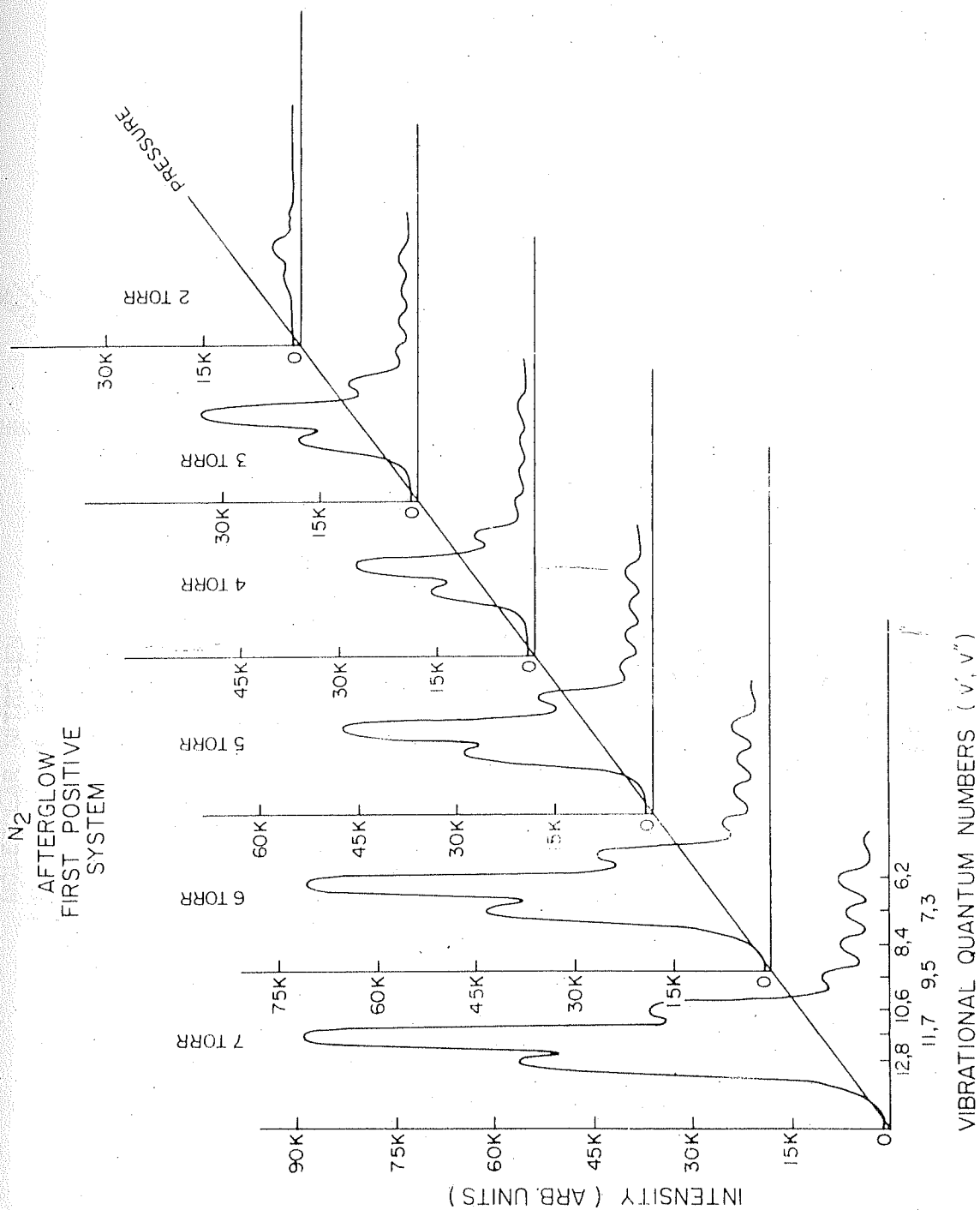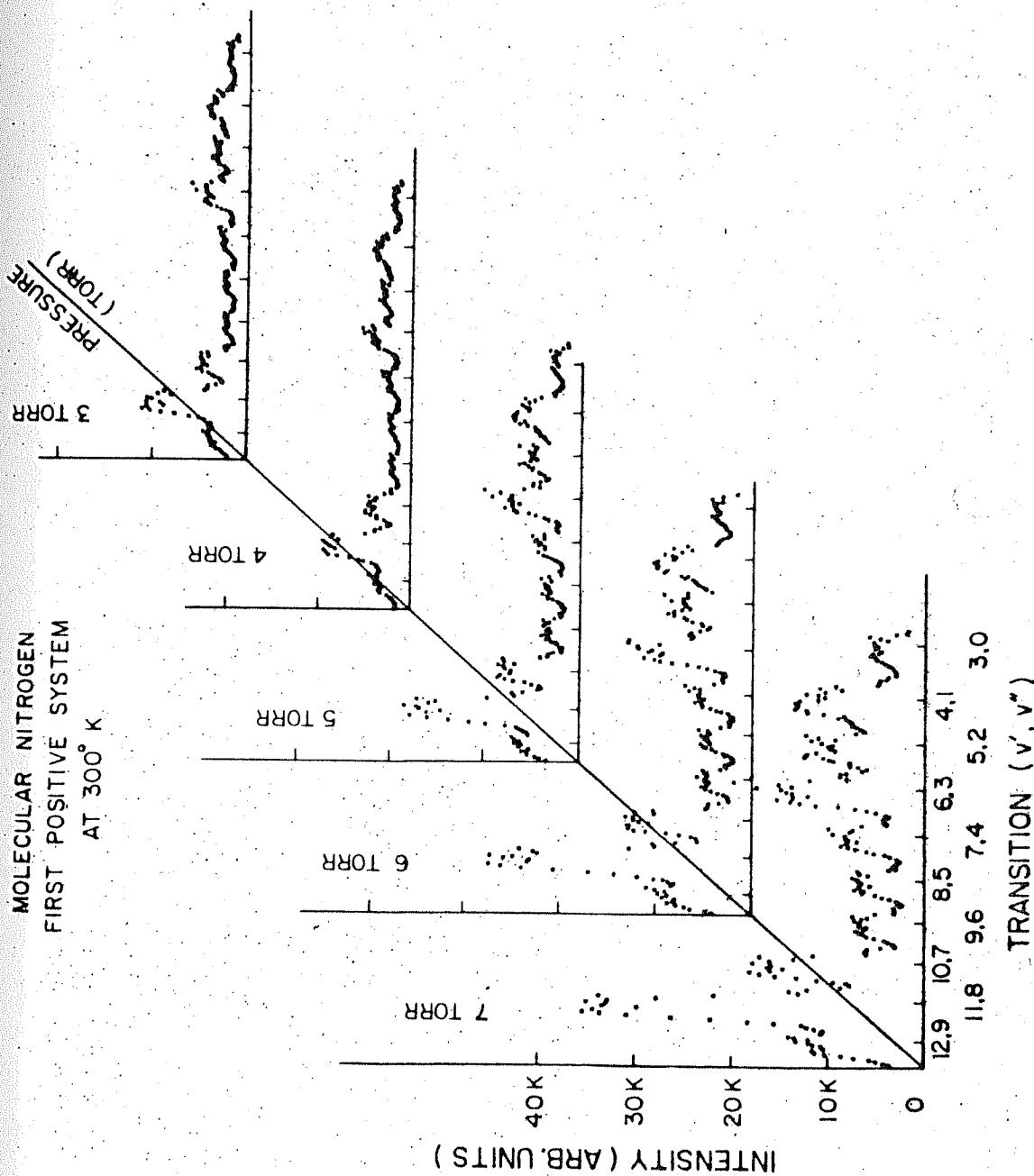
Fig. III.9   Afterglow spectra of some vibrational bands of first positive system of nitrogen at 300°K corresponding to Δv = 3. The spectra have been obtained for various pressures ranging from 7 to 3 Torr.
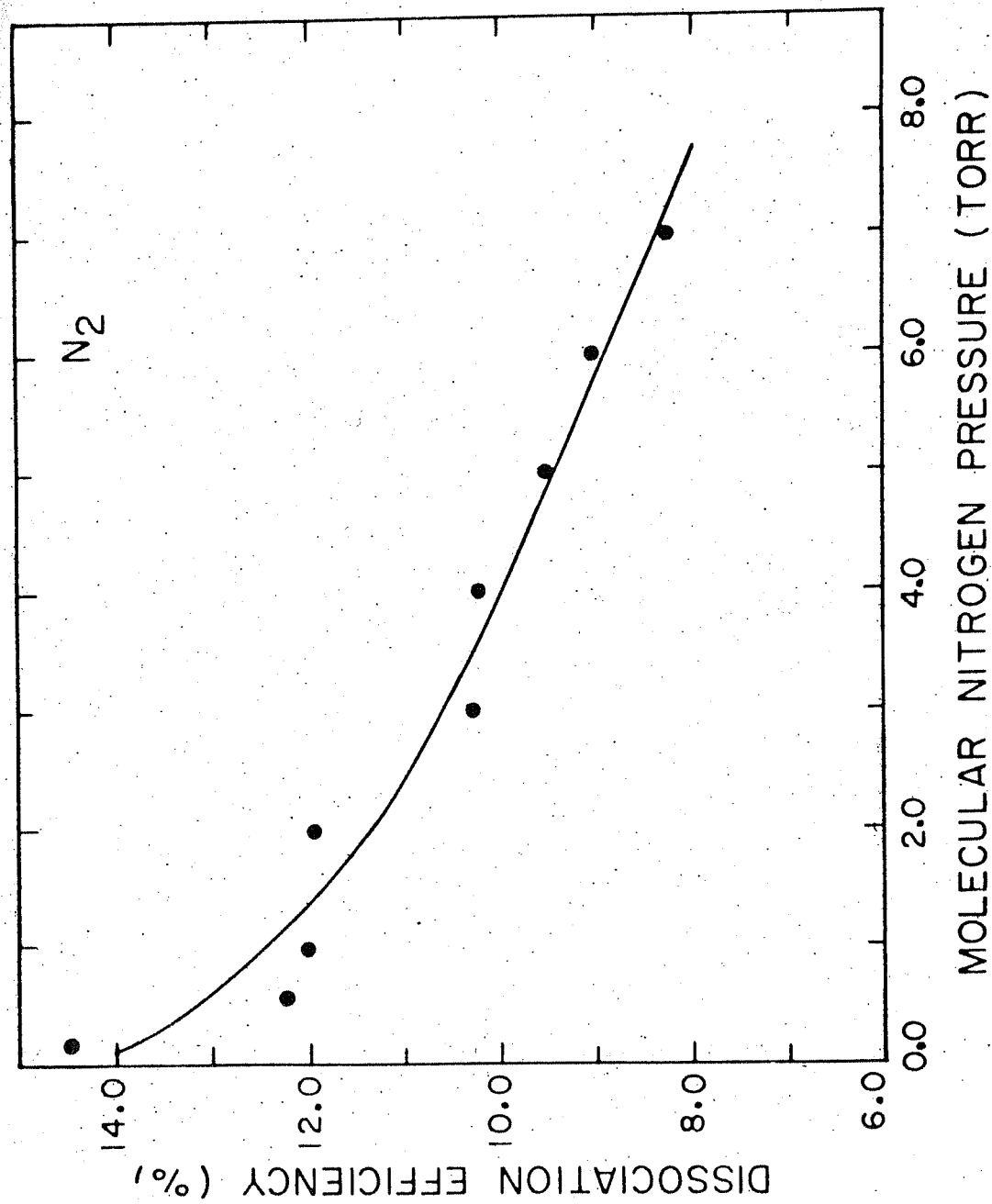
Fig. III.10   Dissociation efficiency of molecular nitrogen as a function of pressure of the parent gas from 0.2 to 7 Torr.

respectively, were relatively larger as compared to those observed by any other technique. However, a direct comparison as to which technique was superior was not possible.

In Fig. III.11 and Fig. III.12 are shown the peak intensities of various vibrational bands of the first positive system of nitrogen at 300^OK, as a function of the square of atomic nitrogen concentration i.e. $[N]^2$. The vibrational bands studied include (11,7), (12,8), (10,6), (9,5), (11,8), (10,7), (12,9), (5,2), (7,4), (9,6), (8,5) and (3,0). A linear relationship between the peak intensity and $[N]^2$ has been observed for all these bands in the pressure range 4 to 7 Torr. Between 2 and 4 Torr, $[N]^2$ dependence does not seem to hold good. Some different type of dependence may be possible in this intermediate pressure region. Our results include very few data points in this region and thus, we are not in a position to give even a qualitative picture about the type of dependence. It is suggested that this region should be re-investigated with greater care so as to yield large number of data points, using the afterglow tube of such a size that the wall-recombinations in this pressure region are appreciably reduced.

At 77^OK, the dissociation efficiencies at various pressures could not be measured because of some technical problems. It is assumed that without any serious ambiguity, the dissociation efficiency of nitrogen should be the same both at 300 and 77^OK. The peak intensities for various vibrational bands of the first positive system of nitrogen at 77^OK were plotted against square of the atomic nitrogen concentration i.e. $[N]^2$. The results are shown in Fig. III.13 for only a few
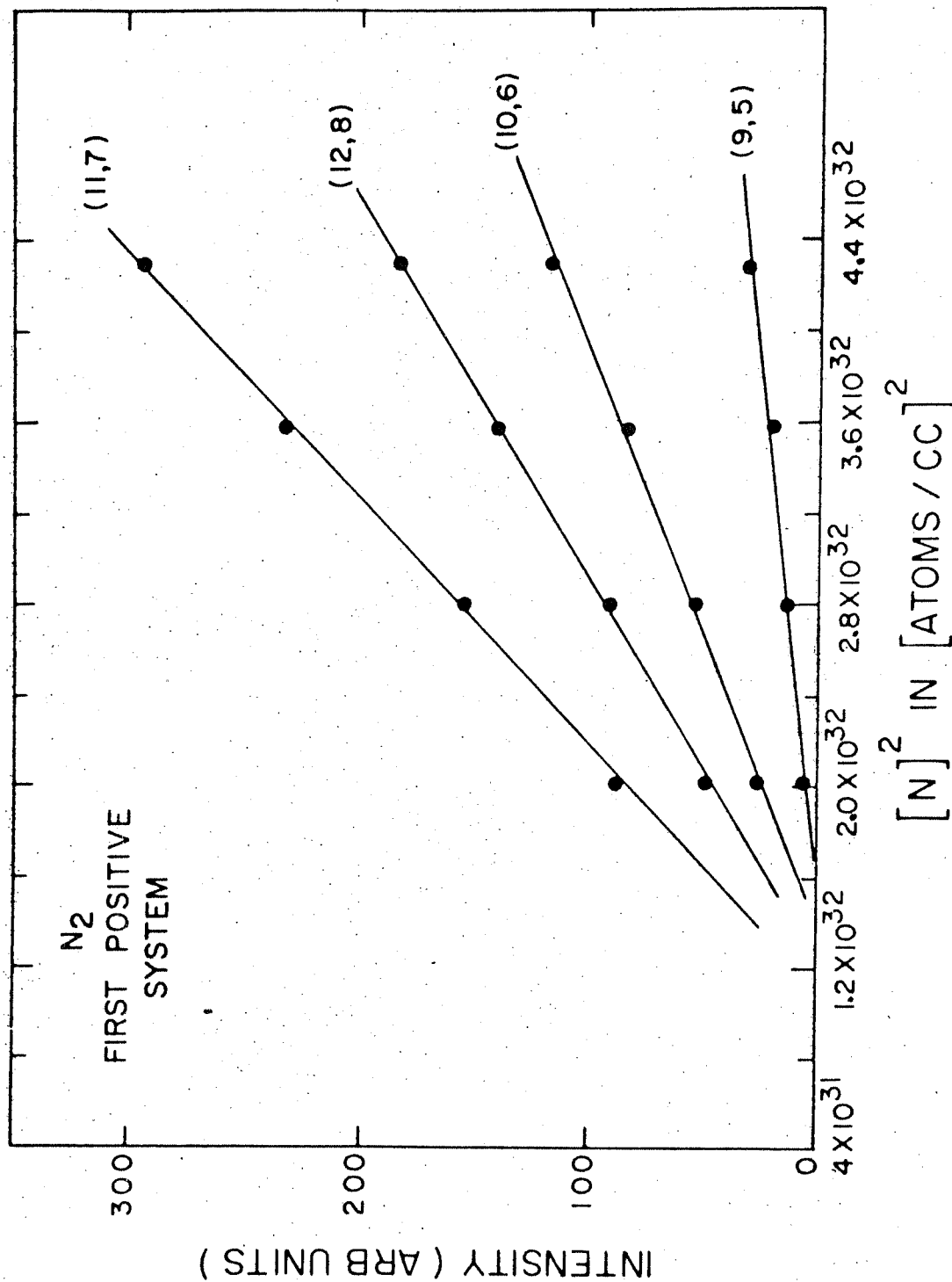
Fig. III.11 Peak intensities of (11,7), (12,8), (10,6) and (9,5) vibrational bands of the first positive system of nitrogen at 300°K as a function of square of the nitrogen atom concentration.

Fig, III,12   Peak intensities of (11,8), (10,7), (12,9), (5,2), (7,4),
(9,6), (8,5) and (3,0) vibrational bands of the first
positive system of nitrogen at $300^{\circ}K$ as a function of
square of the nitrogen atom concentration.

Fig. III.13   Peak intensities of (12,8), (11,7), (12,9), (11,8), (10,6) and (10,7) vibrational bands of the first positive system of nitrogen at $77^{\circ}K$ as a function of square of the nitrogen atom concentration.
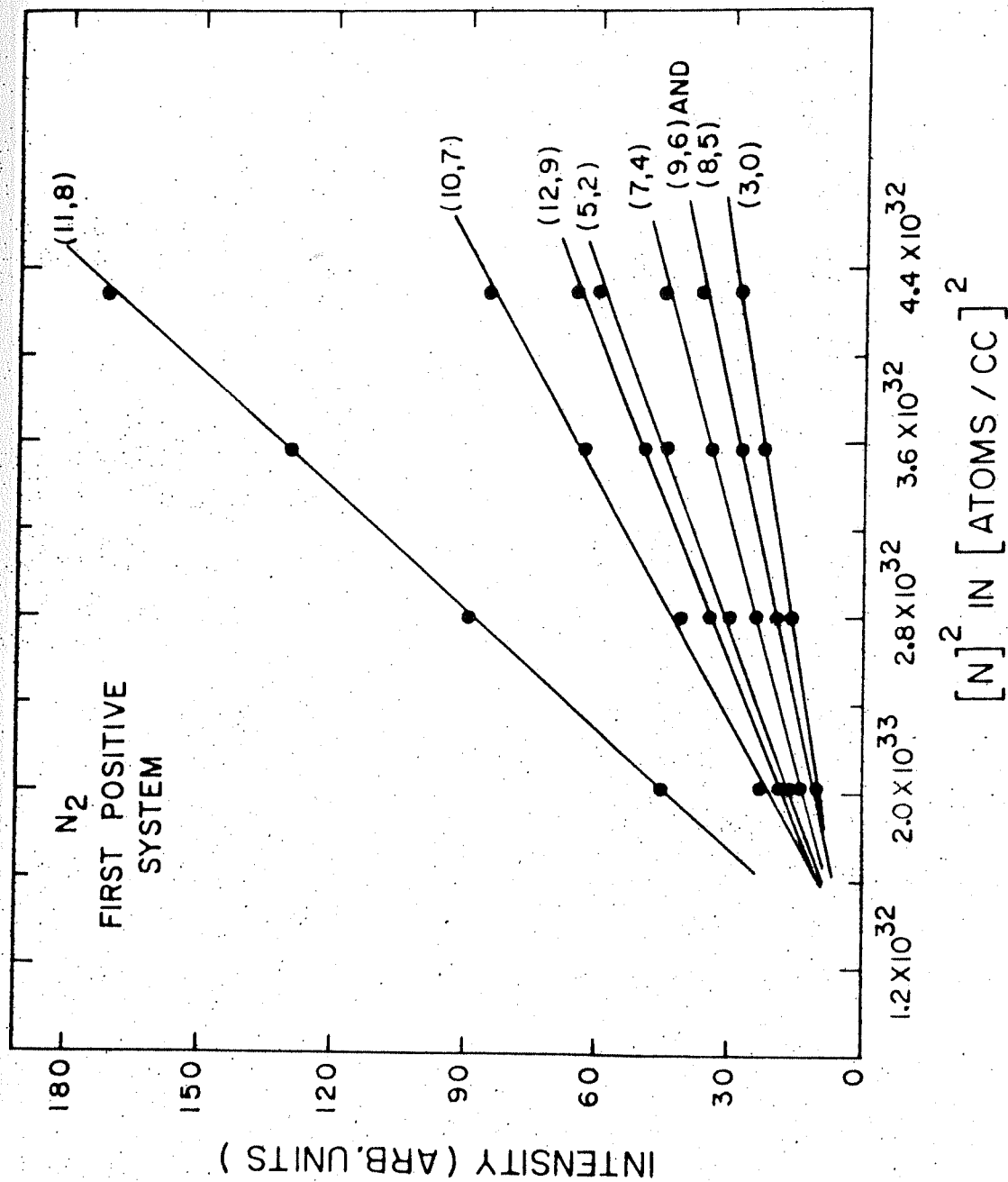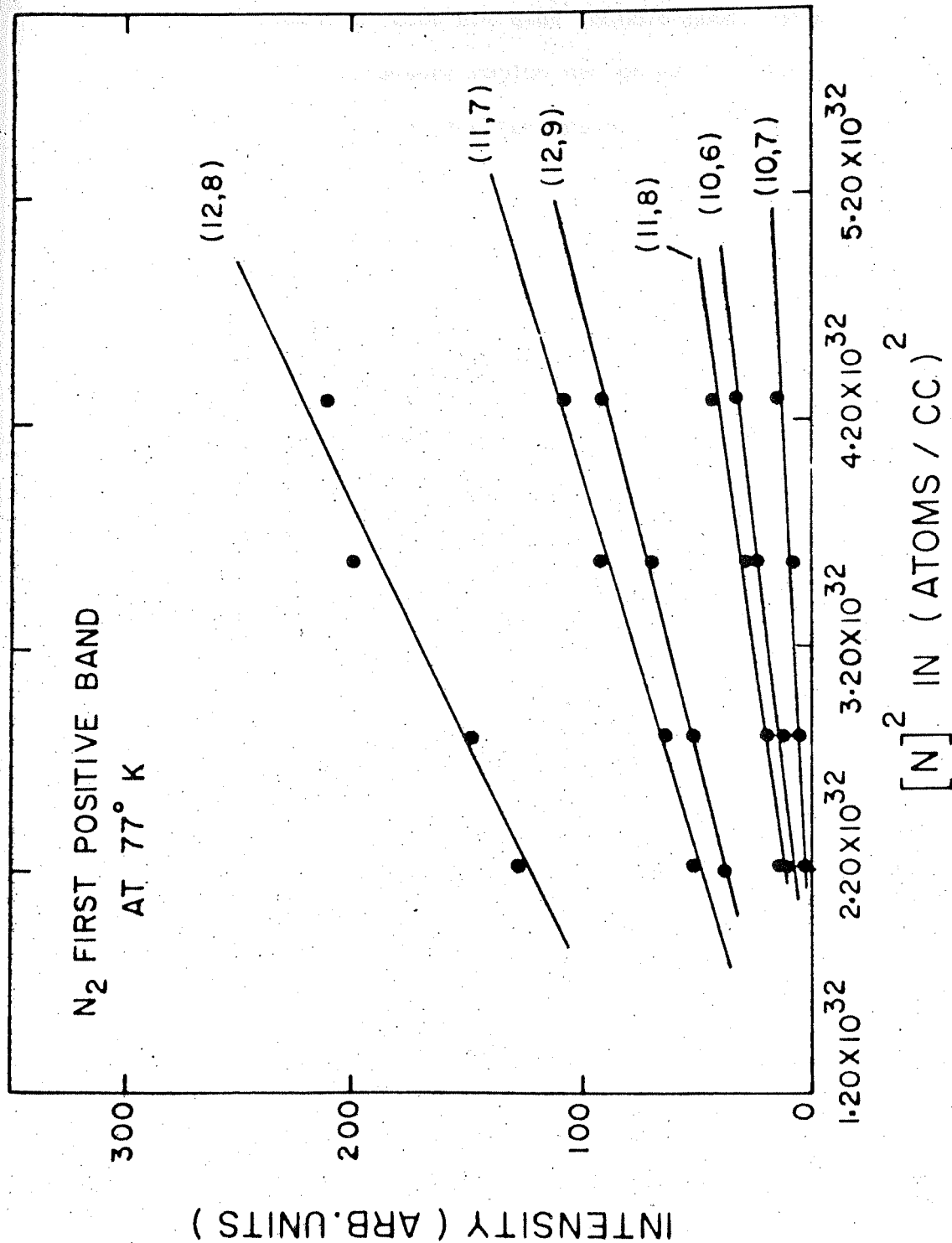
vibrational bands. A clear $[N]^2$ dependence is observed in the pressure

region between 4 and 7 Torr. Again, in the pressure region between 2 and

4 Torr, $[N]^2$ dependence does not seem to hold good. Thus, it is conclu-

ded that 2 to 4 Torr pressure region has entirely different type of

dependence, irrespective of the temperatures at which the afterglow

spectra are studied.

III.2.3. Effect of Diluent

It was reported in Section III.2.2 that no afterglow

spectrum for the first positive system of nitrogen, was observed at

pressures below 1 Torr in the present work. Even at 1 Torr, very weak

(12,8) and (11,7) bands were observed. It was found that when nitrogen

along with some carrier gas or diluent like argon was discharged, an

afterglow spectrum of first positive system of nitrogen was observed even

at very low pressures of nitrogen. In the present experiment, a fixed

pressure of 5 Torr of argon was used while the nitrogen pressure was

varied from 0.2 to 3 Torr. In all cases, the afterglow spectra could be

observed. In Fig. III.14 is shown the first positive system for nitrogen

at 300°K obtained at 5 Torr of argon and 1 Torr of nitrogen. Similar

investigations at 77°K were not undertaken. From Fig. III.14, it was

clear that in this case the various vibrational levels of the B $^3\Pi_g$

state were populated in different proportions than those observed in the

afterglow spectra without diluent at 300°K. Firstly, the most intense

band, (11,7) was about 2.3 times more intense than that without diluent

at 7 Torr pressure and 300°K temperature. Also, the intensities of all

bands are, in general, larger. In this spectrum, the vibrational levels
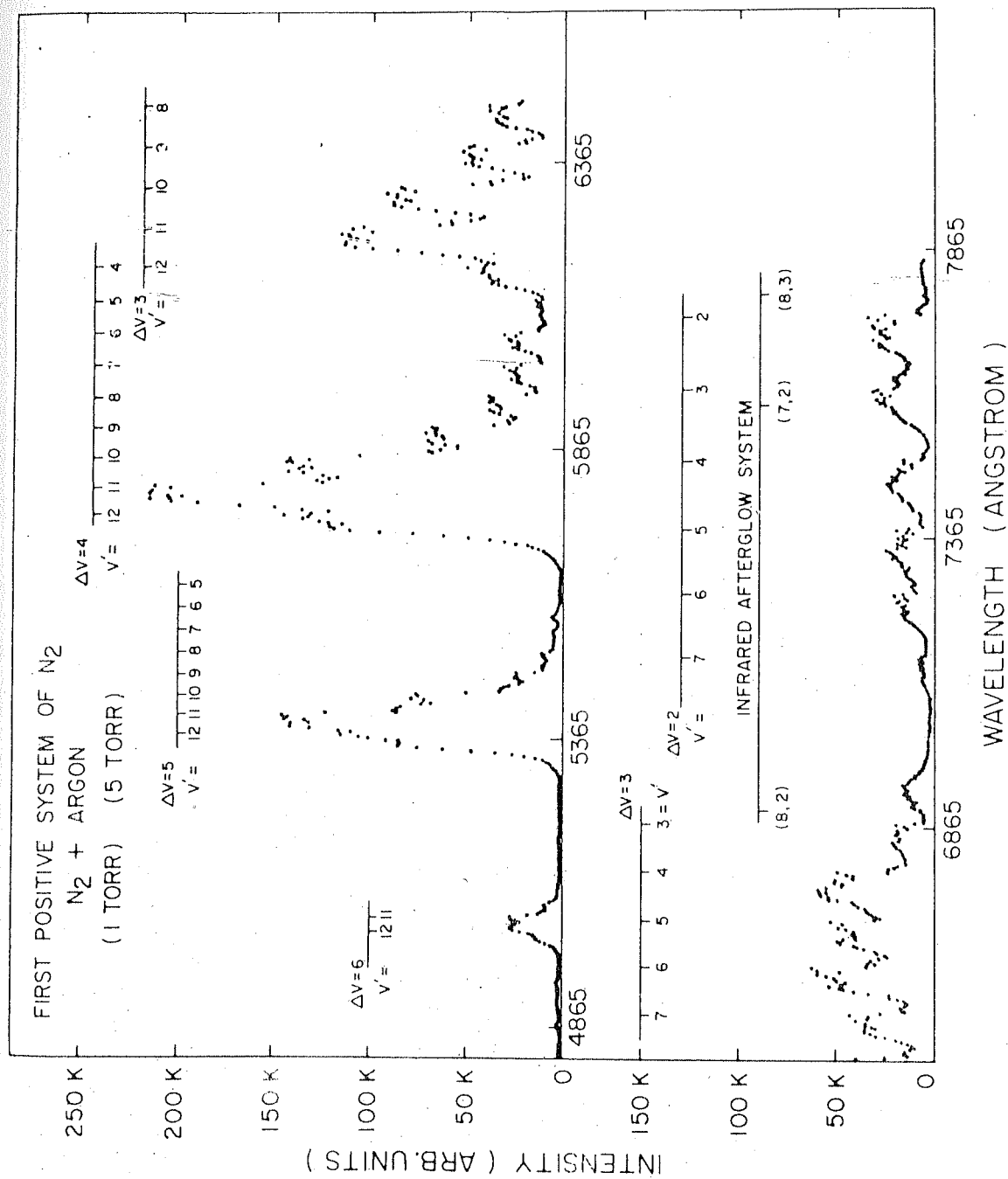
Fig. III.14   Afterglow spectra of first positive system of nitrogen at 300°K obtained at a 5 Torr pressure of argon and 1 Torr of nitrogen.

$v' = 12$ and 10 were equally populated for $\Delta v = 4$ and also for $\Delta v = 5$, but in case of $\Delta v = 3$, the level corresponding to $v' = 10$ was more populated than level at $v' = 12$. The pattern for the population of vibrational level $v' = 11$ to 8 for both $\Delta v = 4$ and 3 was entirely different than that reported for spectrum without diluent.

The existence of afterglow spectra below 1 Torr and that too with larger intensity obtained under the same experimental conditions, could only be attributed to production of large atomic nitrogen concentration in the presence of a diluent like argon. Under these conditions i.e. at 5 Torr fixed pressure of argon and nitrogen pressure varying from 0.2 to 3 Torr, the dissociation efficiency was measured by Wrede-Harteck method at entrance point of observational vessel. The results are shown in Fig. III.15. The dissociation efficiency varied from about 33% to 17% at about 0.2 to 3.0 Torr nitrogen pressure. It was obvious that atomic nitrogen concentrations were much larger when argon was used as diluent with nitrogen.

The peak intensities for the different bands of the first positive system of nitrogen were computed as a function of pressure. The plot of peak intensity against $[N]^2$ has been shown in Fig. III.16 to Fig. III.18. It did not seem to follow the $[N]^2$ dependence but is more or less a third order dependence.

In the pressure region from 0.2 Torr and above where the third order dependence on intensity of the vibrational bands has been found to exist, the quenching of N_2 (B $^3\Pi_g$) state by N_2 itself or by some
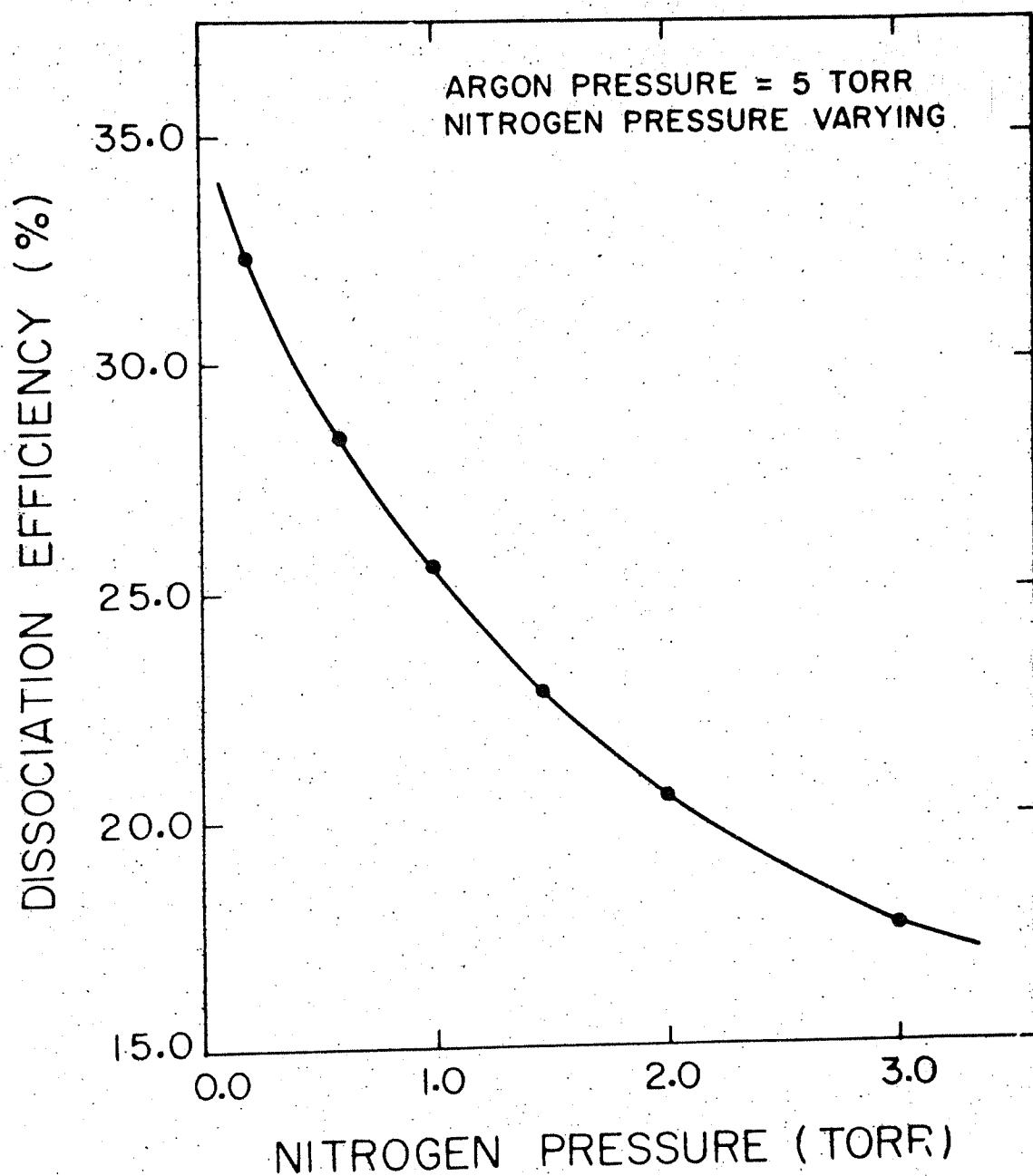
Fig. III.15   Dissociation efficiency of molecular nitrogen
at a fixed pressure of argon (5 Torr) and at
nitrogen pressure varying from 0.2 to 3 Torr.
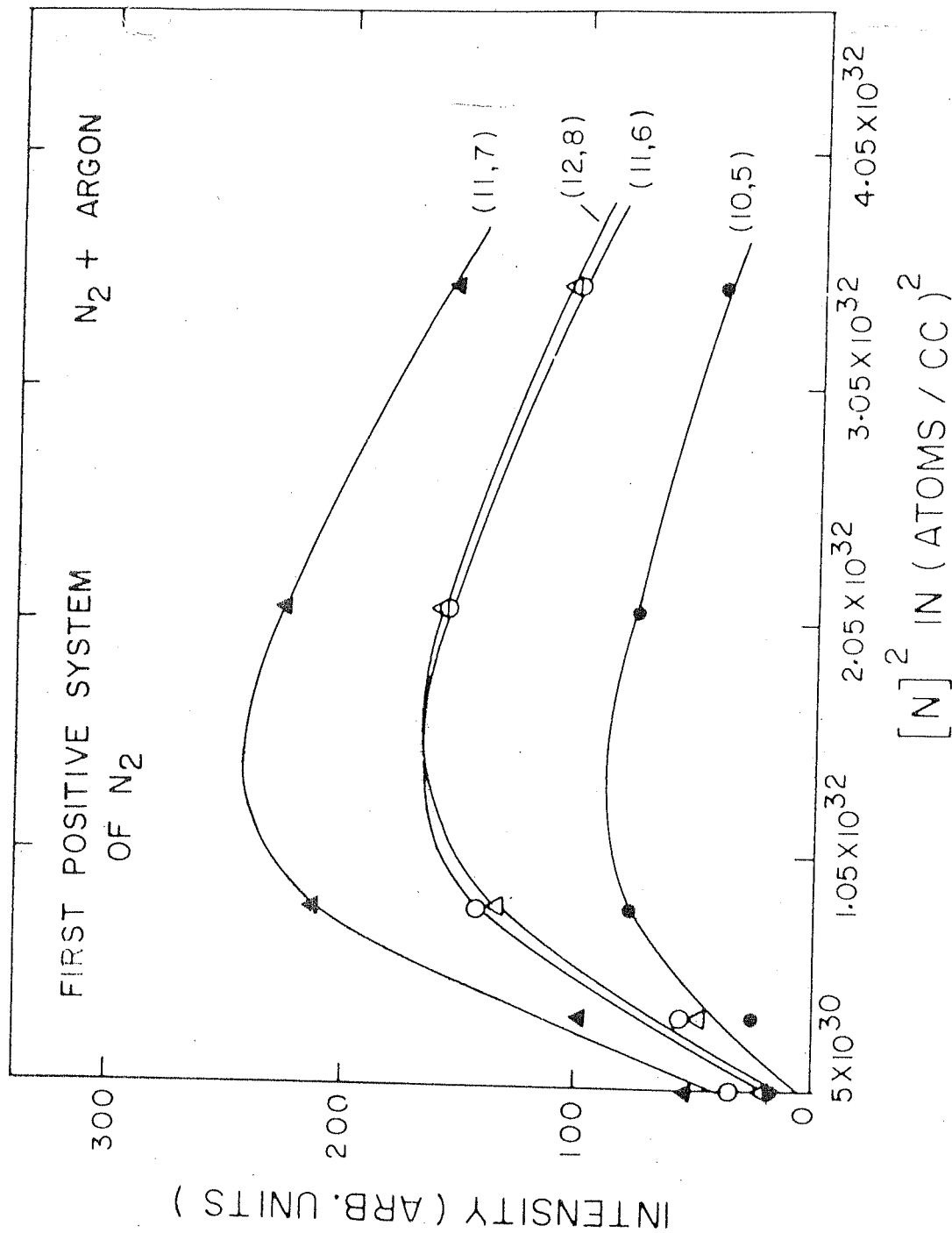
Fig. III.16 Peak intensities of (11,7), (12,8), (11,6), (10,5) vibrational bands of 1+ system of nitrogen at 300°K in the presence of a diluent, argon, as a function of $[N]^2$.
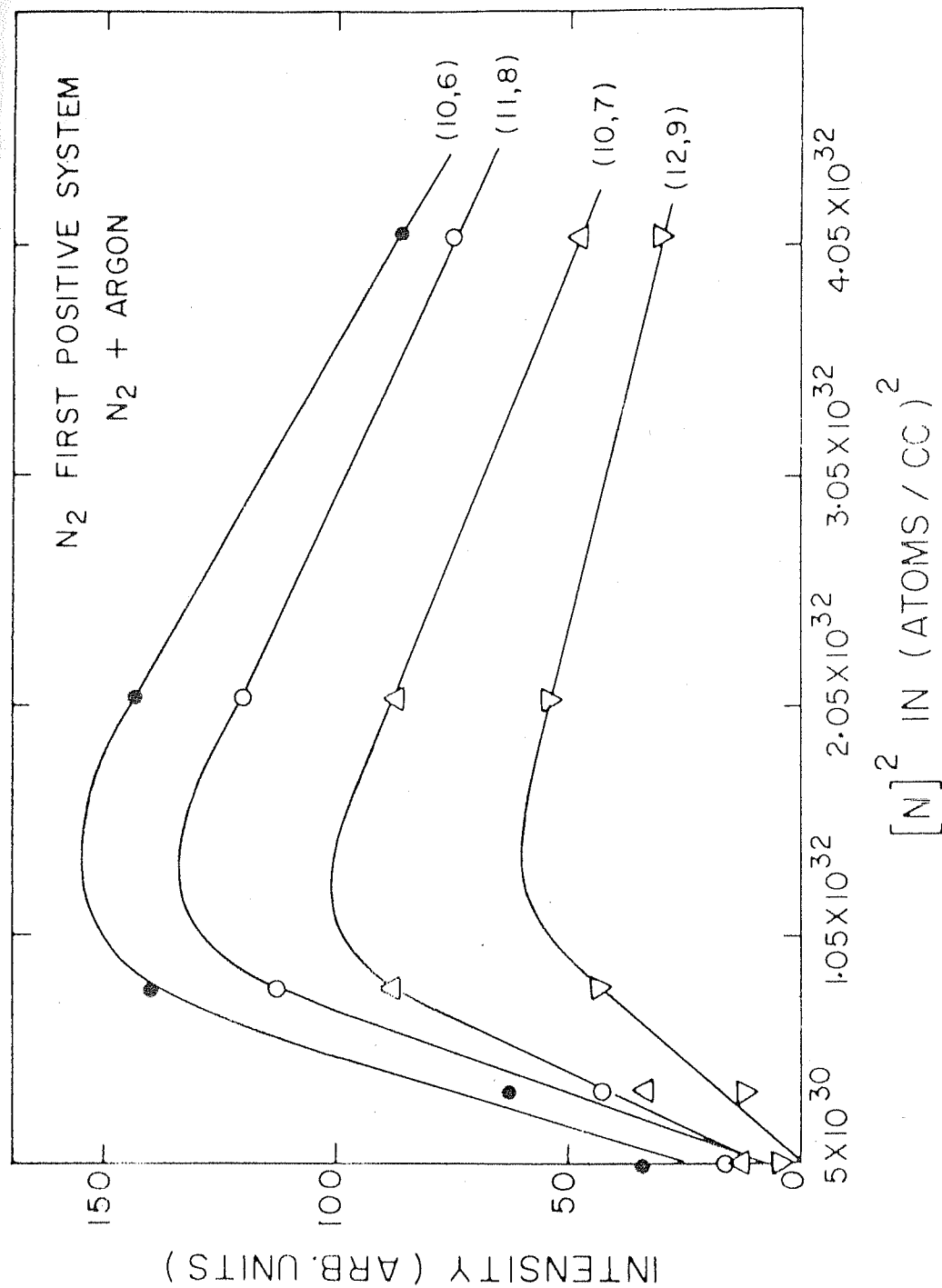
Fig. III.17 Peak intensities of (10,6), (11,8), (10,7), (12,9)
vibrational bands of 1+ system of nitrogen in the
presence of a diluent, argon, as a function of $[N]^2$.
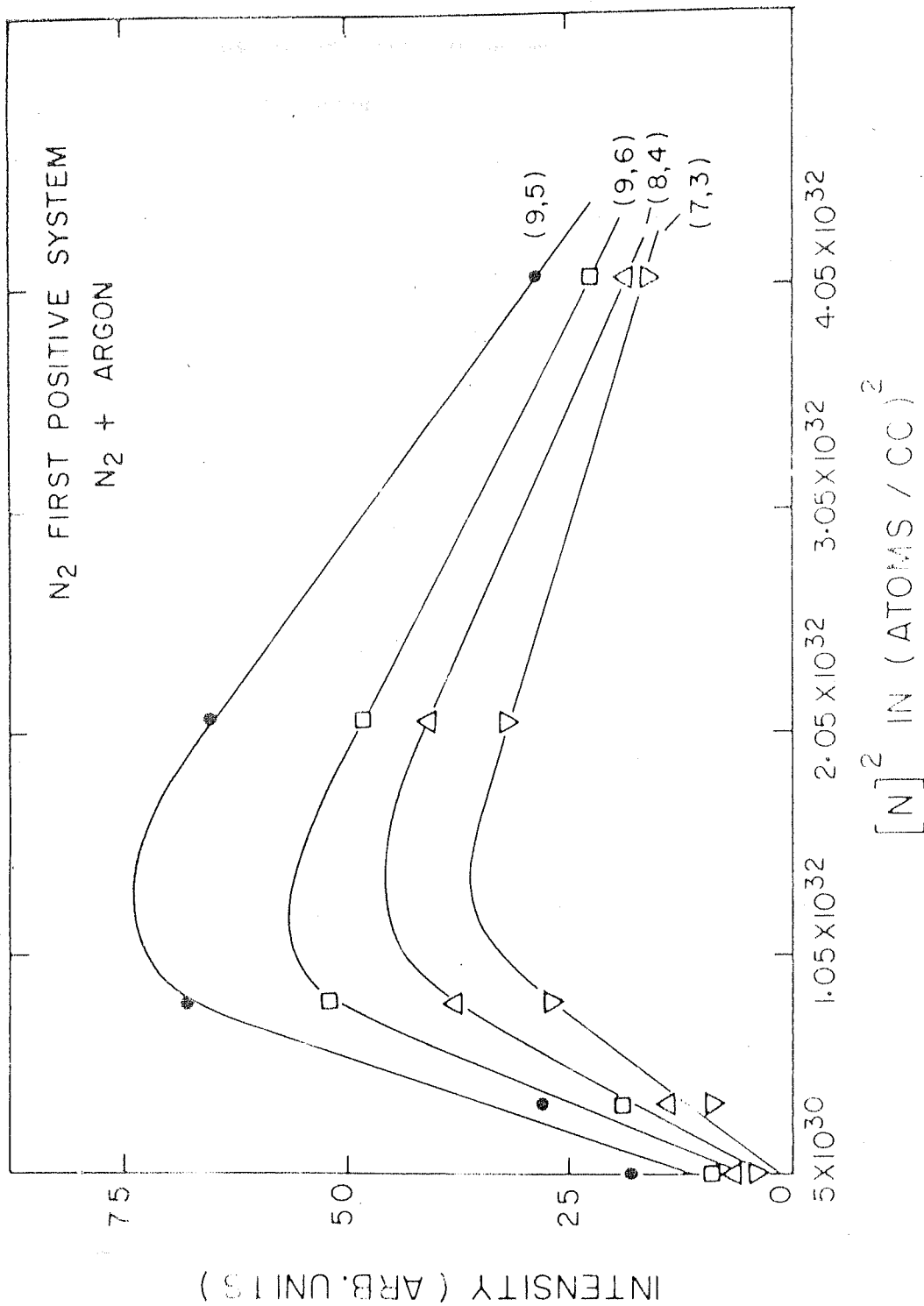
Fig. III.18   Peak intensities of (9,5), (9,6), (8,4), (7,3) vibrational bands of 1+ system of nitrogen in the presence of a diluent, argon, as a function of $[N]^2$.

diluent, is, in general, appreciable. In the present experiment, the afterglow spectra at this low pressure region without diluent could not be studied because of constraints posed by certain experimental conditions. So quenching parameters for N_2 could not be obtained. But the quenching of N_2 (B $^3\Pi_g$) state by argon at these low pressures was studied in detail. Knowing quenching parameters of N_2 (B $^3\Pi_g$) state by nitrogen from experiments reported by other scientists, similar parameters for argon were obtained in the present experiment.

At low pressures of nitrogen with no diluent, the intensity of the afterglow for different vibrational levels of the B $^3\Pi_g$ state, obeyed a rate law (Brennen and Shane (1971)) of the form

$$\frac{I}{[N]^2} = \frac{K[M]}{k\tau_B[M]+1} \qquad \text{III.2}$$

where K and k are constants for a particular diluent, τ_B is the radiative life time of the emitting state and $[M]$ is the concentration of the diluent. The half-quenching pressure is defined as $[M]_{\frac{1}{2}} = (k\tau_B)^{-1}$. In this case, the diluent is pure nitrogen alone. At two pressures 1 and 2 in the flow system, equation III.2 will be

$$\frac{I_1}{I_2} \cdot \frac{[N]_2^2}{[N]_1^2} \cdot \frac{[M]_2}{[M]_1} = \frac{k\tau_B[M]_2 + 1}{k\tau_B[M]_1 + 1} \qquad \text{III.3}$$

When at low pressure of nitrogen, a diluent, argon is added, then k becomes

$$k = k \ (Ar) \ X \ (Ar) + k \ (N_2) \ X \ (N_2) \qquad \text{III.4}$$

where X is the mole fraction of the gas and is also pressure dependent. Substituting k from equation III.4 in equation III.3, $k(Ar)\tau_B$ could be obtained provided $k(N_2)\tau_B$ is known from other experiments. The value of $k(N_2)\tau_B$ was taken as 8.6 ± 1.3 Torr^{-1} (Brennen and Shane (1971)) for $v' = 12, 11, 10$ levels of the B $^3\Pi_g$ state and the values of $k(Ar)\tau_B$ and $k(Ar)$ were calculated. The results are shown in Table III.1.

Table III.1

Half quenching pressures and quenching rates of argon for $v' = 12, 11, 10$ levels of the B $^3\Pi_g$ state of nitrogen

Level v'	Vibrational bands studied	$k(Ar)\tau_B$ in Torr^{-1}	$k(Ar)$ in cm^3 molec^{-1} sec^{-1}	Reference
12	12, 9	0.56 ± 0.15	$(3.61 \pm 0.98) \times 10^{-12}$	Present work
12	12, 8	1.5	12×10^{-12}	Jonathan and Petty (1969)
11	11, 6			
	11, 7	0.86 ± 0.13	$(5.48 \pm 0.82) \times 10^{-12}$	Present work
	11, 8			
11		1.5	12×10^{-12}	Brennen and Shane (1971)
11		1.5	12×10^{-12}	Jonathan and Petty (1969)
10	10, 5			
	10, 6	0.96 ± 0.13	$(6.16 \pm 0.84) \times 10^{-12}$	Present work
	10, 7			
10		1.5	12×10^{-12}	Brennen and Shane (1971)
10		1.5	12×10^{-12}	Jonathan and Petty (1969)

In all these calculations, τ_B for $v' = 12$, 11 and 10 of the B $^3\pi_g$ state of nitrogen, was taken as 4.4×10^{-6} sec as reported by Jeunehomme (1966). The values of k (Ar) τ_B reported by Brennen and Shane (1971) and Jonathan and Petty (1969) were larger than those reported in the present work. This could be because of the fact that these scientists used a few overlapping interference filters for peak intensity measurements while in the present work, all the afterglow spectrum was scanned by grating of the monochromator, thus avoiding the cumulative effects so inherent in the interference filters.

III.3. Discussion

The mechanisms for populating various vibrational levels from $v' = 12$ to 2 for the B $^3\pi_g$ state of nitrogen molecule would be discussed here on the basis of present results reported in the previous section as well as results from other experiments, on the afterglow spectra of first positive system at both 300 and 77°K and on pressure dependence of the peak intensities with or without diluent. The energy level diagram shown in Fig. III.19 for B $^3\pi_g$ and A $^3\Sigma_u^+$ states is based on the work reported by Benesch et al.(1965). Only vibrational levels have been shown in the diagram. Also shown in the figure are relative contributions from other excited states like B' $^3\Sigma_u^-$ and C $^3\pi_4$ to B $^3\pi_g$ state. The weak afterglow emission corresponding to (8,2) vibrational band of infra-red afterglow system (B' $^3\Sigma_u^- \rightarrow$ B $^3\pi_g$) at 300°K is shown by dotted line while moderately intense infra-red afterglow emission, (8,2) and (8,3) bands and similar (1,2) (1,4), (3,7), (4,3), (4,4) and (4,8) vibrational bands of second positive system (C $^3\pi_u \rightarrow$ B $^3\pi_g$) at
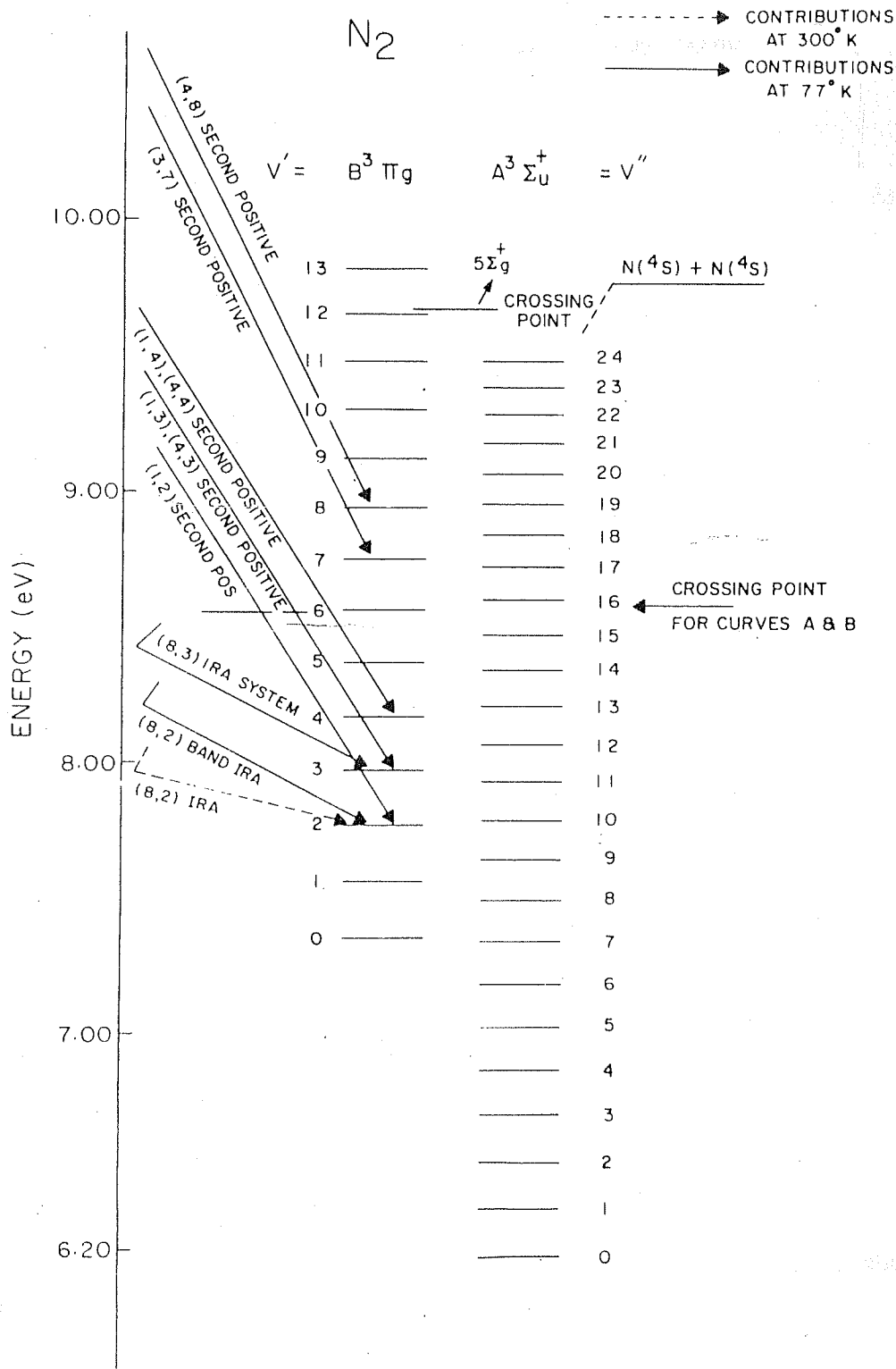
Fig. III.19   Energy level diagram of B $^3\Pi_g$ and A $^3\Sigma_u^+$ states,
Only vibrational levels have been shown in the
figure.   Also shown are radiative contribution from
some vibrational bands of IRA system and second

77^OK as reported in the present work are shown by full lines.

III.3.1. Mechanisms for populating v' = 12 to 9

In section III.2.2, we have reported that the intensity of vibrational bands with v' = 12, 11, 10 ,9 --- is proportional to $[N]^2$ for the pressure range from 4 to 7 Torr and has third order dependence in the region 0.2 to 2 Torr. The intensity of vibrational bands with v' = 12, 11, 10 ---- were found to be larger at 77^OK than at 300^OK as reported in section III.2.1. This means that first positive system of nitrogen afterglow shows negative temperature coefficient. As discussed in Chapter I, the three-body emission intensity should show a change from a second order to third order dependence at low pressures. Similar behaviour has been found for the first positive system of nitrogen afterglow. This indicates that B $^3\Pi_g$ is populated via three-body recombination.

In Chapter I, four mechanisms were considered for populating the B $^3\Pi_g$ state of nitrogen afterglow. The first mechanism, proposed by Benson (1968) is ruled out because it requires rate of vibrational relaxation at least one order of magnitude greater than collision rate (Becker 1972). Due to the position of the potential curves primarily, $^5\Sigma_g^+$ and A $^3\Sigma_u^+$ have to be considered as precursor state for B $^3\Pi_g$, v' = 9-12 in a stabilization mechanism. The simplest assumption, that a collision induced process

$$N^2 \ (^5\Sigma_g^+) + M \ \rightarrow \ N_2 \ (B^3\Pi_g \quad v' = 12\text{-}9) + M \qquad III.5$$
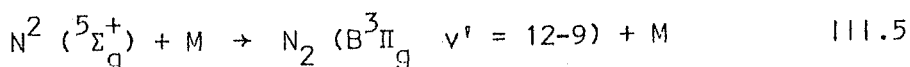
populates the v' level of the B state is consistent with our results. A $^3\Sigma_u^+$ state as precursor of B $^3\Pi_g$ state, as proposed by Campbell and Thrush (1967) is rejected on the following grounds:

1 Campbell and Thrush (1967) had chosen A $^3\Sigma_u^+$ state as a precursor state as they felt that spin conservation was important in collision induced transitions between excited triplet and singlet state of nitrogen. But involvement of $^5\Sigma_g^+$ in the preassociation of B $^3\Pi_g$, v' = 13 has clearly been established. This indicates that $\Delta S = 0$ selection rule is violated. In collisions, the selection rule g $\leftrightarrow$ u for radiationless transition is not strictly valid; thus a collision induced transition $^5\Sigma_g^+$ $\overset{M}{\to}$ B $^3\Pi_g$ might occur more readily than A $^3\Sigma_u^+$ $\overset{M}{\to}$ B $^3\Pi_g$ transition.

2 Also Campbell and Thrush (1967) mechanism failed to account for the observed change in the (v' = 11 / v' = 12) intensity ratio of B $^3\Pi_g$ state with change in temperature. Campbell and Thrush (1967) suggested that shift towards v' = 12 at low temperature was due to a reduction in the rate of predissociation of higher vibrational levels of A state. This explanation is in contradiction to what has been suggested by Golde and Thrush (1972).

On the other hand, stabilized N_2 ($^5\Sigma_g^+$, v = 0) molecules formed by reaction III.6, as suggested initially by Bayer and Kistiakowsky (1960), can be depopulated by dissociation into atoms (III.7)

$$N\,(^4S) + N\,(^4S) + M \to N_2\,(^5\Sigma_g^+,\ v = 0) + M \qquad III.6$$

$$N_2(^5\Sigma_g^+,\ v = 0) + M \to N\,(^4S) + N\,(^4S) + M \qquad III.7$$
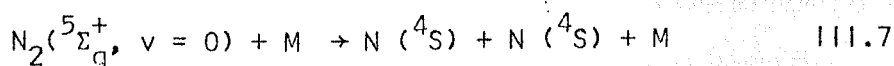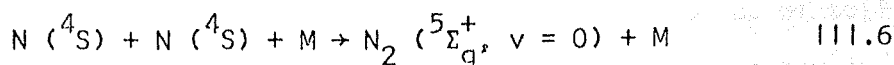
Molecules formed in stabilized $^5\Sigma_g^+$ state can also be depopulated by collision induced process

$$N_2 \, (^5\Sigma_g^+, \, v = 0) + M \rightleftharpoons N_2 \, (B \, ^3\Pi_g, \, v = 12) + M \qquad \qquad III.8$$
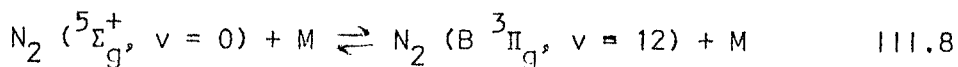
Crossing of B $^3\Pi_g$, v = 12 with $^5\Sigma_g^+$ near v = 0 of latter, together with the observed inverse predissociation of B $^3\Pi_g$, v = 13 at very low pressure (Becker et al. (1972)) from $^5\Sigma_g^+$ implies a perturbation of (B $^3\Pi_g$, v = 12) level by ($^5\Sigma_g^+$, v = 0). It can be assumed that, because of the heterogeneous perturbation, the radiationless transition between ($^5\Sigma_g^+$) $\rightleftharpoons$ (B $^3\Pi_g$, v = 12) takes place over a range of rotational levels. Rotational level analysis of this state corresponding to vibrational level v' = 12 as discussed in Chapter IV, also supports $^5\Sigma_g^+$ state as the precursor of B $^3\Pi_g$ state.

According to perturbation theory, molecules in $^5\Sigma_g^+$(v = 0) would undergo a collision-induced-radiationless transition into v' = 12 only and by no means into v' = 11 to 9 of the B $^3\Pi_g$ state. This was clear from the energy level diagram (Fig. III.19) which showed practically no energy difference between $^5\Sigma_g^+$ (v = 0) and B $^3\Pi_g$(v' = 12) level and larger energy difference for other combinations. Callear and Williams (1966) have shown that the probability of collision-induced transfer of vibrational energy falls off approximately exponentially with the amount of energy that has been converted from the vibrational to the translational form. In this case, only ΔS = 0 selection rule has been violated, which looks a weak selection rule in the presence of collisions. The level v' = 12 of B $^3\Pi_g$ thus populated, could be depopulated to some

extent by collision-induced vibrational relaxation to lower vibrational level, collision-induced electronic quenching and radiative deactivation to A $^3\Sigma_u^+$ state.

The gas kinetic collision rate is defined as

$$Z = 4 \, n \, \sigma^2 \, (\frac{\pi k T}{m})^{\frac{1}{2}}$$

III.9

where n is the number of molecules per c.c., σ is the impact parameter and k, T, m have their usual meaning. Lambert (1977) gives a value of $Z = 8.69 \times 10^9 \, sec^{-1} \, atmosphere^{-1}$ for nitrogen molecules in the ground state and at $273^\circ K$. It would be interesting to note that Z has been computed for N_2-N_2 collisions for the ground state molecules. The collision rate for molecules in excited states would possibly be different than for those in the ground state. The value of quenching rate $k(N_2)$ has been reported as $6.6 \times 10^{-11} \, cm^3 \, molec^{-1} \, sec^{-1}$ for $v' = 12$, 11 and 10 levels of the B $^3\Pi_g$ state (Brennen and Shane (1971)) at very low pressures. This would give a high value of one collision in five for quenching the higher vibrational levels at $300^\circ K$ as against a value of one out of twenty as reported by Campbell and Thrush (1967). As reported in section II.2.2, at higher pressure, there is practically negligible quenching but at pressures below 1 Torr, the quenching becomes appreciable. Also, at low pressures, there are losses due to wall recombination. That is why no afterglow spectra could be observed below 1 Torr. The spectra at low pressure was observed only in the presence of a diluent like argon which helps to increase the atomic nitrogen concentration and also reduces the wall recombination. Again,

it could be seen by comparing the spectra with and without diluent that the population of vibrational level of the B $^3\Pi_g$ state are different in the two cases.

It is clear from perturbation theory that $v' = 11$, 10 and 9 of B $^3\Pi_g$ state cannot significantly be populated directly from $^5\Sigma_g^+$ state. The perturbation effect between $^5\Sigma_g^+$, $v = 0$ and B $^3\Pi_g$, $v' = 11$, 10 and 9 will be smaller than that between $^5\Sigma_g^+$, $v = 0$ and B $^3\Pi_g$, $v' = 12$ because the energy difference for $v' = 11$, 10, 9 are greater than that for $v' = 12$ and the energy difference appears in the denominator of the perturbation term. The only possibility of populating $v' = 11$ to 9 levels of B $^3\Pi_g$ state is through vibrational relaxation from $v' = 12$ to 11, $v' = 11$ to 10 and $v' = 10$ to 9 respectively. It is possible that the probability of vibrational relaxations at high pressure is very large but no calculation has been done to prove this fact quantitatively. Similar mechanism was proposed by Anketell and Nicholls (1970) and Brennen and Shane (1971).

There is another mechanism which may be giving additional contribution to the process of populating some of the vibrational levels in this group. Some vibrational levels in the B state are very close to some levels in the A state. According to perturbation theory, the system could go from one state to the other state at B $^3\Pi_g(v' = 10)$ and A $^3\Sigma_u^+$ ($v'' = 22$) and also at B $^3\Pi_g$ ($v' = 11$) and A $^3\Sigma_u^+$ ($v'' = 24$) where these levels have approximately the same energy (Fig. III.19). The energy difference for $v' = 11$ and $v'' = 24$ is only 0.005 eV while

that for $v' = 10$ and $v'' = 22$ is only 0.02 eV. Therefore, this process would also populate $v' = 11$ and 10 levels of the B $^3\Pi_g$ state.

The picture is slightly different at 77°K where $v' = 12$ is maximum populated. The three-body recombination of nitrogen atoms has a negative temperature coefficient (Campbell and Thrush (1967)) and also, the number of collisions energetically capable of predissociating N_2 ($^5\Sigma_g^+$) state at 77°K is small (Berkowitz et al. (1956)). Also, the collision-induced vibrational relaxation to lower levels would again be small at this temperature. This would explain why the $v' = 12$ level is populated the maximum at 77°K. The $v' = 11$ and 10 levels would be populated by the second mechanism reported above.

III.3.2. Mechanism for populating B $^3\Pi_g$, $v' = 8$ to 5

The mechanism which populates the lower vibration level $v' \leqslant 8$ of B $^3\Pi_g$ state obviously cannot involve $^5\Sigma_g^+$ state. It has been emphasised before, that the curves A $^3\Sigma_u^+$ and B $^3\Pi_g$ intersect near $v'' = 16$ and $v' = 6$ respectively. The energy difference of these vibrational levels is about 0.032 eV. Thus, there is a significant probability for collision-induced radiationless transition from one level to the other. Also, the potential curves co-trace their paths above this energy along the repulsive part of the potential. There would also be collision-induced radiationless transition between A $^3\Sigma_u^+$ ($v = 19$) and B $^3\Pi_g$ ($v = 8$), the energy difference being 0.014 eV between the two. (It may be important to note that we have taken energies of vibrational energy levels as

reported by Benesch et al. (1965) which are probably the latest. There is some difference between these values and those taken by Campbell and Thrush (1967). This way the levels corresponding to $v' = 8$ and 6 would be populated, $v' = 6$ being populated much more. There would be a collision-induced vibrational relaxation from levels $v' = 8$, 6 to $v' = 7$ and 5 respectively. The net effect would be that all levels in this group would be populated, though $v' = 6$ would be populated the maximum. The above picture corresponds well to the experimental results reported at 300°K (section III.2)

At 77°K, there would be less vibrational relaxation. But as shown in Fig. III.19, 8 and 7 levels of B state would have some contribution from the radiative transition ($C\ ^{3}\Pi_{u} \rightarrow B\ ^{3}\Pi_{g}$), (4,8) and (3,7) vibrational bands of the second positive system of nitrogen.

III.3.3. Mechanisms for populating $v' = 4$ to 2

The first positive emission from $v' = 4$ to 0 levels of the $B\ ^{3}\Pi_{g}$ state covers the spectral range from 7000 to 11000 $\overset{\circ}{A}$ but in our experiment, we could observe upto 8000 $\overset{\circ}{A}$ only. This corresponds to emission from $v' = 4$ to 2 levels. At room temperature (300°K), the levels $v' = 4$ to 2 could be populated through the following radiative transitions:

1   A weak (8,2) band of infra-red afterglow system has been observed by us as reported in section III.2.1. Level $v' = 2$ could be weakly populated by this radiative transition.

2   The strong observed transition corresponding to (4,2), (5,2) and
(6,3) bands of the $^3\Delta_u \rightarrow B\ ^3\Pi_g$ system have been reported by Wu and
Benesch (1968). This would be another agency to populate $v' = 2$ and
3 levels of the $B\ ^3\Pi_g$ state.

3   The (7,4), (7,3) bands of the $B'\ ^3\Sigma_u^- \rightarrow B\ ^3\Pi_g$ system in the near
infra-red region (not reported in our work) could moderately
populate $v' = 4,3$ levels of $B\ ^3\Pi_g$ state.

The net result of the three above processes would be to
populate $v' = 4$ to 2 levels of the $B\ ^3\Pi_g$ state. The extent of populating
any level by one of these processes is not known to us. Also, the levels
$v' = 3$ and 2 may be populated to some extent, by collision-induced vibra-
tional relaxation from $v' = 4$ and 3 levels respectively.

At 77°K, the levels $v' = 2$ and 3 are intensely populated by
emission corresponding to (8,2) and (8,3) bands of the infra-red after-
glow system. Also, (1,4), (4,4), (1,3), (4,3) and (1,2) bands corres-
ponding to second positive system contribute significantly to $v' = 2,3$
and 4 levels. All these transitions have been observed by us in the
afterglow spectra of nitrogen at 77°K.

CHAPTER IV

MEASUREMENT OF DISSOCIATION ENERGY OF MOLECULAR NITROGEN

IV.1. Introduction

The lowest dissociation limit, N (^{4}S) + N (^{4}S), for molecular nitrogen, would theoretically lead to electronic states of the type X $^1\Sigma_g^+$, A $^3\Sigma_u^+$, $^5\Sigma_g^+$ and $^7\Sigma_u^+$. Out of these, X $^1\Sigma_g^+$, A $^3\Sigma_g^+$ and $^5\Sigma_g^+$ have been observed experimentally since long. A large number of values for the dissociation energy corresponding to the lowest dissociation limit have been reported (Gaydon (1968)); these vary from 5 to 17 eV. Most of the previous work in this field is only of historical importance, though some reliable values are available from work on emission spectroscopy, predissociation and electron impact studies of molecular nitrogen.

Herman and Herman (1942), in their observation of Lyman-Birge-Hopfield system in emission, reported, possibly the first reliable values of dissociation energy for the ground state of molecular nitrogen. This value for the dissociation energy of 9.8 ± 0.5 eV was close to that of Lozier (1933) (9.73 eV) reported from the measurements of appearance potential of N^+ by electron-impact study. Douglas and Herzberg (1951) observed the predissociation of a $^1\Pi_g$ state in emission near the sixth vibrational level. This gave a value of 78828 cm^{-1} or 9.77 eV for the lowest dissociation limit for molecular nitrogen. A value of 9.76 eV was given by Gaydon (1968) in the study of predissociation of B $^3\Pi_g$ state which required the existence of a curve $^5\Sigma_g^+$ type cutting B $^3\Pi_g$ near or below the dissociation limit. A series of multi-reference double-excitation configuration-interaction calculations for three lowest dissociation limits have been reported in relatively recent times (Butscher et al. (1977)).

The object of the present study is to determine accurately the dissociation energy of molecular nitrogen by high resolution after-glow spectroscopy. The vibrational bands (12,8), (11,7), (12,9) and (11,8) of the first positive system of nitrogen have been studied with a beam resolution of about 1 $\overset{O}{A}$ at two temperatures, 300 and 77°K. The rotational spectra of these vibrational bands have been studied exten-sively and mechanism for populating the rotational levels in the v' = 12 level of the B $^3\Pi_g$ state has been discussed.

IV.2. Results

The vibrational band (12,8), (11,7), (12,9) and (11,8) of
the first positive system of nitrogen have been studied by high resolu-
tion afterglow spectroscopy at two temperatures, $300^{O}K$ and $77^{O}K$. In
Fig. IV.1 and Fig. IV.2 are shown the afterglow spectra of (12,8) and
(11,7) bands at $300^{O}K$ and $77^{O}K$ respectively in the spectral range from
5685 $\overset{O}{A}$ to 5800 $\overset{O}{A}$ at a wavelength resolution corresponding to FWHM of
about 1.1 $\overset{O}{A}$. Similar afterglow spectra have been observed for the
vibrational bands (12,9) and (11,8) at $300^{O}K$ and $77^{O}K$ (Fig. IV.3 and
Fig. IV.4) respectively, in the wavelength range between 6112 $\overset{O}{A}$ and
6240 $\overset{O}{A}$. In this case, the wavelength resolution corresponded to a FWHM
of about 2.3 $\overset{O}{A}$. The afterglow spectra, in general, showed a large
number of peaks corresponding to P(J), Q(J) and R(J) rotational transi-
tions, with some peaks clearly resolved while some other peaks were
merged together. Also, the peaks in the afterglow spectra at $77^{O}K$ were
found to be much more intense than those in the spectra at $300^{O}K$.
Another general feature observed was the presence of almost the same
number of peaks corresponding to rotational transitions at both the
temperatures, $300^{O}K$ and $77^{O}K$. This was contrary to what is generally
observed in normal collisionless emission and absorption spectroscopy
where less number of peaks having much larger intensity are observed
at lower temperature. This favours the well known conclusion that
afterglow is a collision-induced phenomenon.

Fig. IV.1   High resolution afterglow spectra of (12,8) and
(11,7) vibrational bands of first positive system
of N_2 at 300°K.   Here integration time for data
~~collection for each channel was 20 sec~~
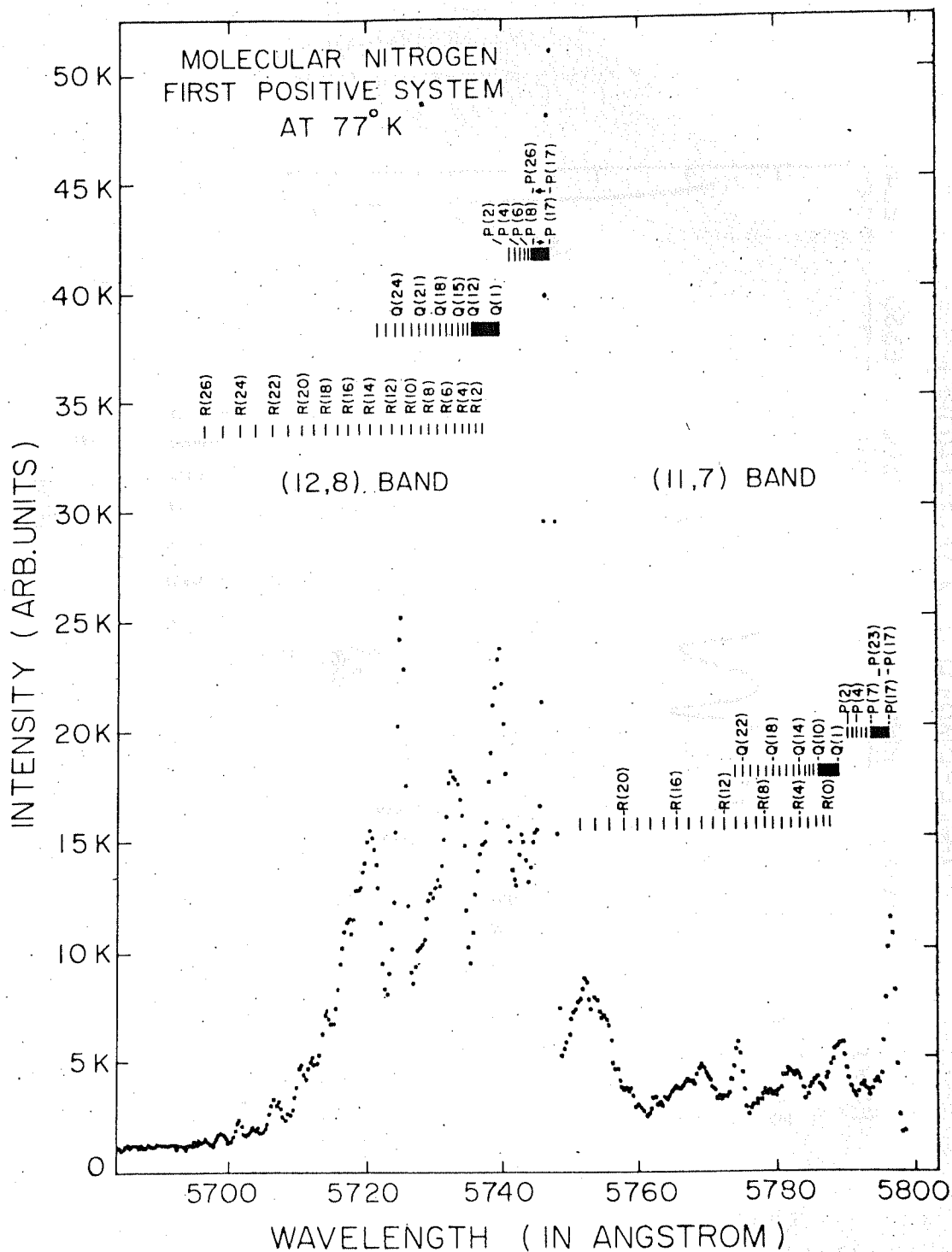
Fig. IV.2   High resolution afterglow spectra of (12,8) and
(11,7) vibrational bands of first positive system
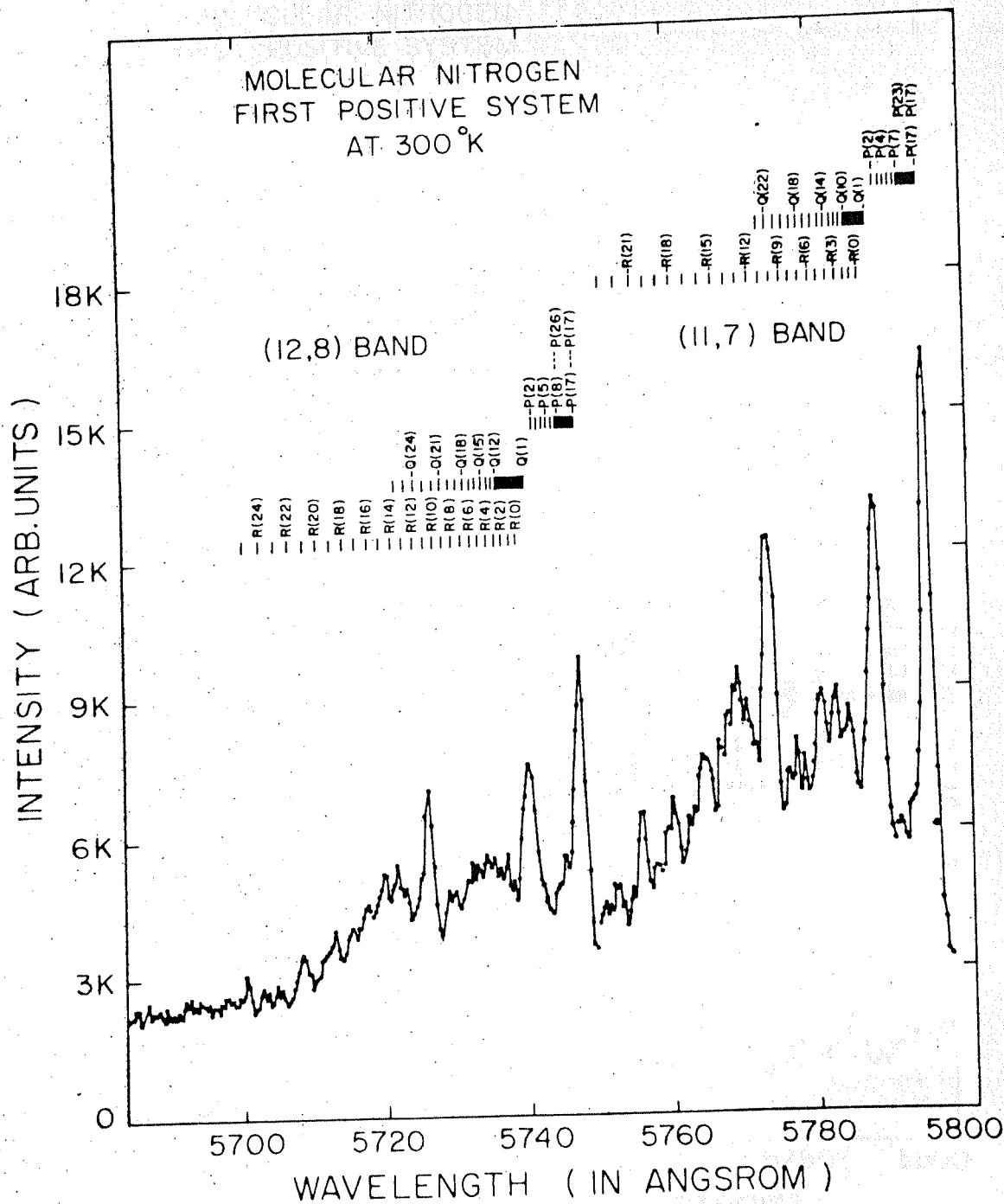of N_2 at 77°K.   Here integration time for data
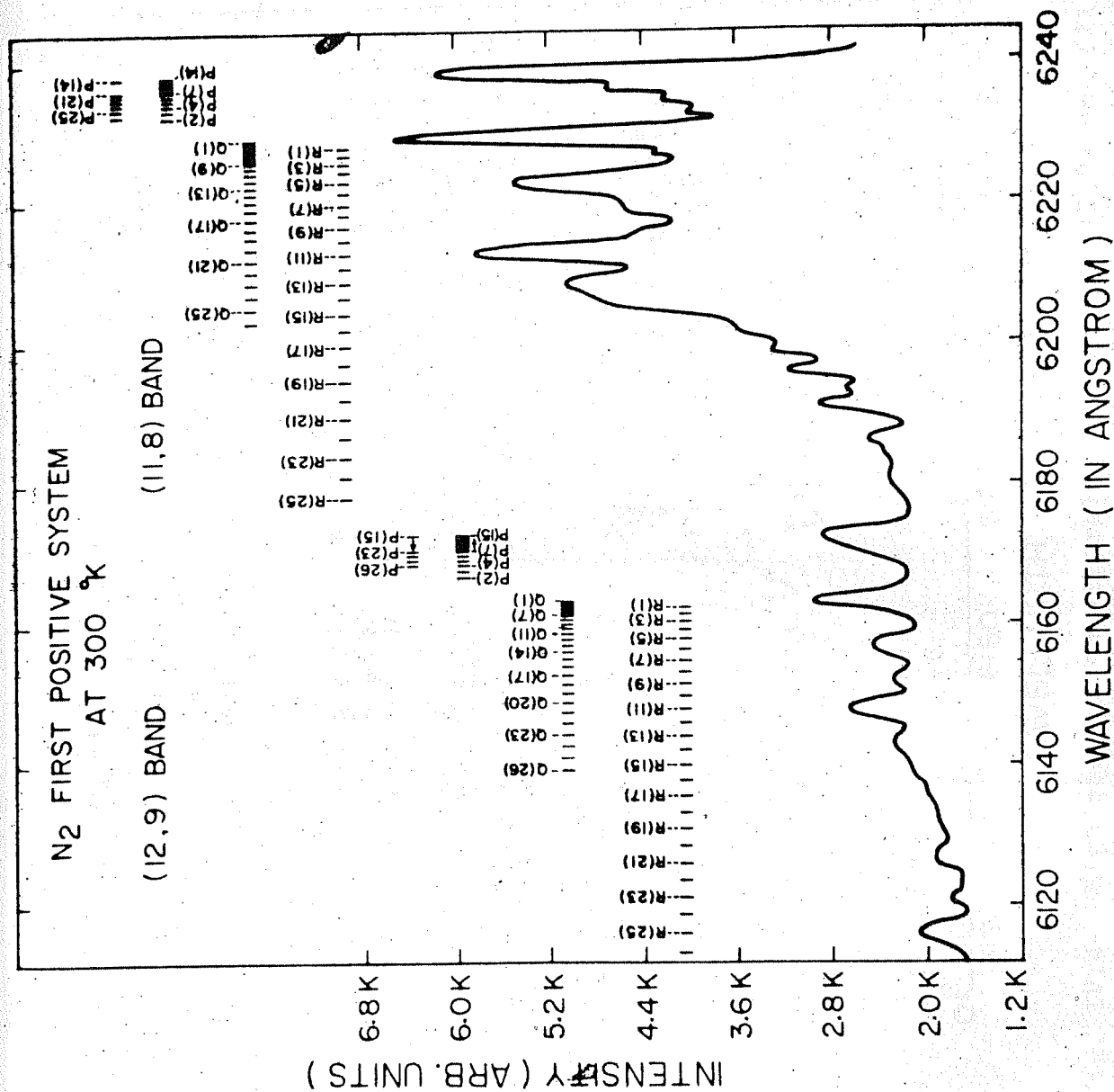
Fig. IV.3 High resolution afterglow spectra of (12,9) and (11,8) vibrational bands of first positive system of N_2 at $300°$ K.
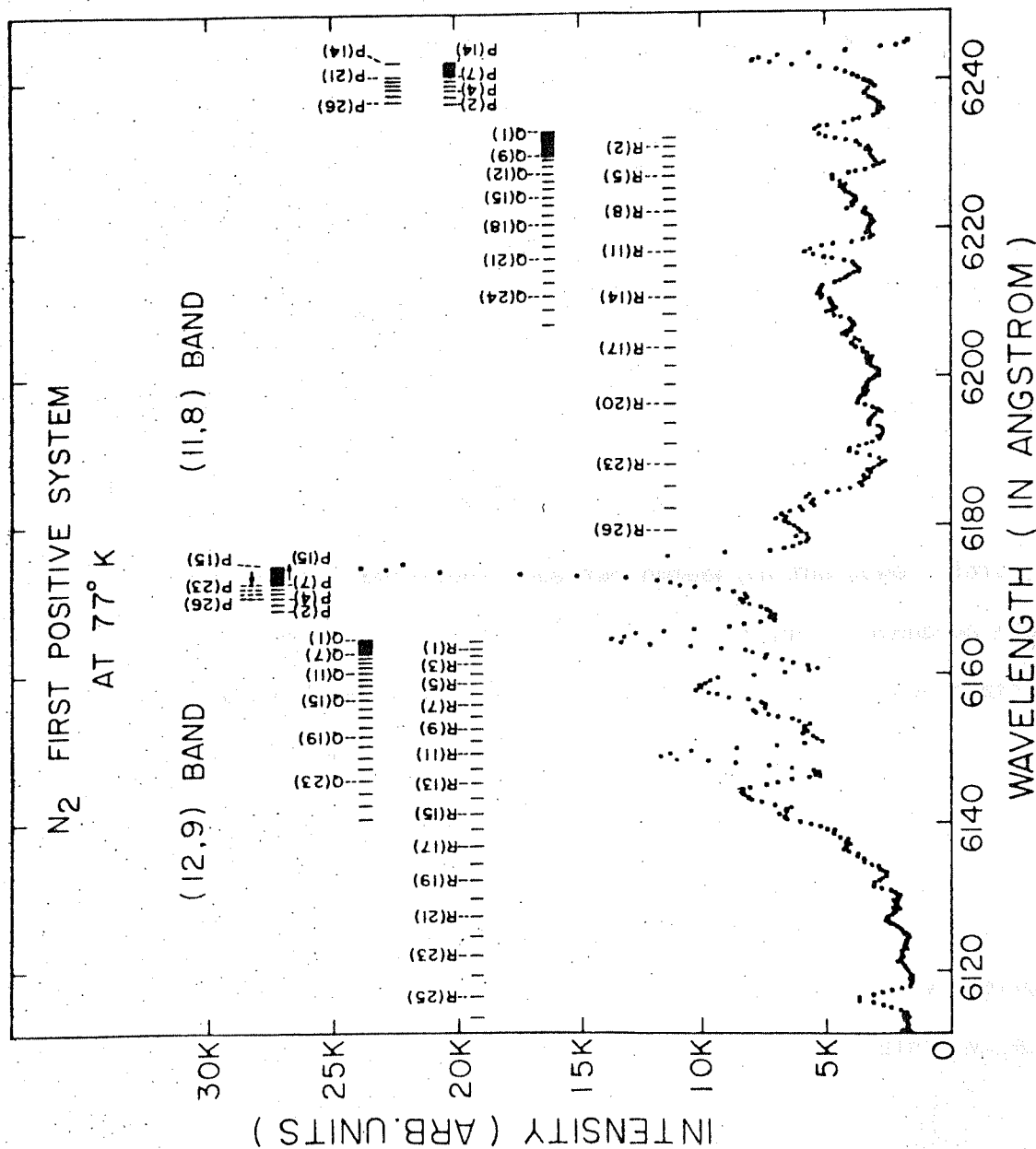
Fig. IV.4 High resolution afterglow spectra of (12,9) and (11,8) vibrational bands of first positive system of N_2 at $77^\circ K$.

IV.2.1. Identification of Spectra

Here the first task is to identify the rotational transi-
tions for different vibrational bands of B $^3\Pi_g \rightarrow$ A $^3\Sigma_u^+$ nitrogen system.
For this transition, difference in electronic angular momentum is not
equal to zero. Thus we would expect three series of lines (branches)
in the rotational-vibration spectra respectively whose wave numbers are
given by the following formulae:

R branch: $\nu = \nu_0 + B_v' + (2B_v' - B_v'')J + (B_v' - B_v'')J^2$ .. R(J)

Q branch: $\nu = \nu_0 \qquad + (B_v' - B_v'')J + (B_v' - B_v'')J^2$ .. Q(J) $\qquad$ IV.1

P branch $\nu = \nu_0 \qquad - (B_v' + B_v'')J + (B_v' - B_v'')J^2$ .. P(J)

Here the J's are the rotational quantum number in the lower state. $\Delta J = 0$
gives Q branch while $\Delta J = +1$ and -1 would give R and P branches respecti-
vely. B_v' and B_v'' are rotational constants in the vibrational state v'
and v" and are given by

$$B_v = B_e - \alpha_e (V + 1/2) + \ldots \qquad\qquad IV.2$$

Here B_e and α_e are constants for electronic state and their values are
given by Herzberg (1952). B_v' and B_v'' are calculated, for vibrational
state v' = 12 and 11 of B $^3\Pi_g$ state and for vibrational state v" = 7, 8
and 9 of A $^3\Sigma_u^+$ state, and are given in Table IV.1.

In expression IV.1, ν_0 which is called the band origin is
given by $\nu_0 = \nu_e + \nu_v$ and it is a constant for a specific vibrational

transition.   Here ν_e and ν_v represent the wave number corresponding to transition between electronic state and vibrational state respectively without taking account of rotation.

The wave number ν can be represented as difference between two quantities called term values.   So wave number ν_e can be written as $\nu_e = T_e' - T_e''$ where T_e' and T_e'' are term values of the corresponding upper and lower electronic states involved in the transition. ν_e is a constant for a given electronic transition.   Wave number of the pure vibrational transition ν_v without taking account of rotation ($J' = J'' = 0$) will be $\nu_v = G(v') - G(v'')$.   Here $G(v')$ and $G(v'')$ are term values corresponding to vibrational quantum number v' and v''. $G(v)$ is defined as

$$G(v) = \omega_e(v+1/2) - \omega_e X_e(v+1/2)^2 + \omega_e Y_e(v+1/2)^3 + \ldots \ldots \qquad \text{IV.3}$$

So wave number corresponding to band origin can be calculated from the expression

$$\nu_e = (T_e' - T_e'') + [\{\omega_e'(v'+1/2) - \omega_e' X_e'(v'+1/2)^2 +$$
$$\omega_e' Y_e'(v'+1/2)^3\} - \{\omega_e''(v''+1/2) - \omega_e'' X_e''(v''+1/2)^2 + \qquad \text{IV.4}$$
$$\omega_e'' Y_e''(v''+1/2)^3\}]$$

Taking values of constants T_e', T_e'', ω_e', $\omega_e' X_e'$, $\omega_e' Y_e'$, ω_e'', $\omega_e' X_e'$ and $\omega_e'' Y_e'$ from Herzberg (1952), ν_e is calculated for (12,8), (12,9), (11,7) and (11,8) vibrational bands of first positive system of nitrogen and values obtained are given in Table IV.2.

Table IV.1

Rotational constants B_v for different vibrational levels of B $^3\Pi_g$ and A $^3\Sigma_u^+$ states

v'	B_v' (in cm^{-1})	v''	B_v'' (in cm^{-1})
12	1.4080	7	1.3425
11	1.4264	8	1.3295
		9	1.3165

For B $^3\Pi_g$ state (Herzberg (1952))

$B_e = 1.6380$ cm^{-1}

$\alpha_e = 0.0184$ cm^{-1}

For A $^3\Sigma_u^+$ states (Herzberg (1952))

$B_e = 1.440$ cm^{-1}

$\alpha_e = 0.013$ cm^{-1}

Table IV.2

ν_o and J- Vertex values for some vibrational bands of (B $^3\Pi_g \rightarrow$ A $^3\Sigma_u^+$) transition.

Vibrational band	ν_o (in cm^{-1})	J- Vertex for P-branch
(12,8)	17422.91	17
(12,9)	16215.58	15
(11,7)	17277.20	17
(11,8)	16039.08	14

Values of constant (Herzberg (1952)) used

For B $^3\Pi_g$ $T_e' = 59626.3$ cm^{-1}, $\omega_e' = 1734.11$ cm^{-1}, $\omega_e'X_e'' = 17.08$ cm^{-1}

For A $^3\Sigma_u^+$ $T_e'' = 50206.0$ cm^{-1}, $\omega_e'' = 1460.37$ cm^{-1}, $\omega_e''X_e'' = 13.891$ cm^{-1}

Substituting value of ν_0 from Table IV.2 and values of B_v' and B_v'' from Table IV.1 in expression IV.1, wave numbers corresponding to P, Q, R branches of rotational transitions for vibrational bands (12,8), (11,7), (12,9) and (11,8) have been calculated and are given in Tables IV.3 and IV.4.

Fortrat diagram, which is a plot of rotational quantum numbers against corresponding wave numbers of all the three branches, is plotted for nitrogen (12,8) vibrational band of the first positive system and is shown in Fig. IV.5. From figure it is clear that the band head lies in the P branch. It is known that a head is formed in the P branch if $B_v' > B_v''$. $B_v' > B_v''$ means that the internuclear distance in the upper state is smaller than that in the lower state and band will be shaded (degraded) towards the violet (towards shorter wavelength). The J value corresponding to the vertex of the Fortrat parabola, i.e., to the band head is obtained by putting $\frac{d\nu}{dJ} = 0$ in (IV.1). The J-vertex values are also given in Table IV.2.

On the basis of values thus computed for R(J), Q(J) and P(J) for (12,8), (11,7), (12,9) and (11,8) vibrational bands, given in Table IV.3 and Table IV.4, the peaks in Fig. IV.1 to Fig. IV.4 were identified and correspondingly, assignment was made to each peak.

IV.2.2. Characteristic Features of the Spectra

The afterglow spectra of (12,8) and (11,7) bands at 300°K shows three distinct sharp peaks, one each in P,Q and R branches (Fig. IV.1). These sharp peaks, however, did not correspond to single
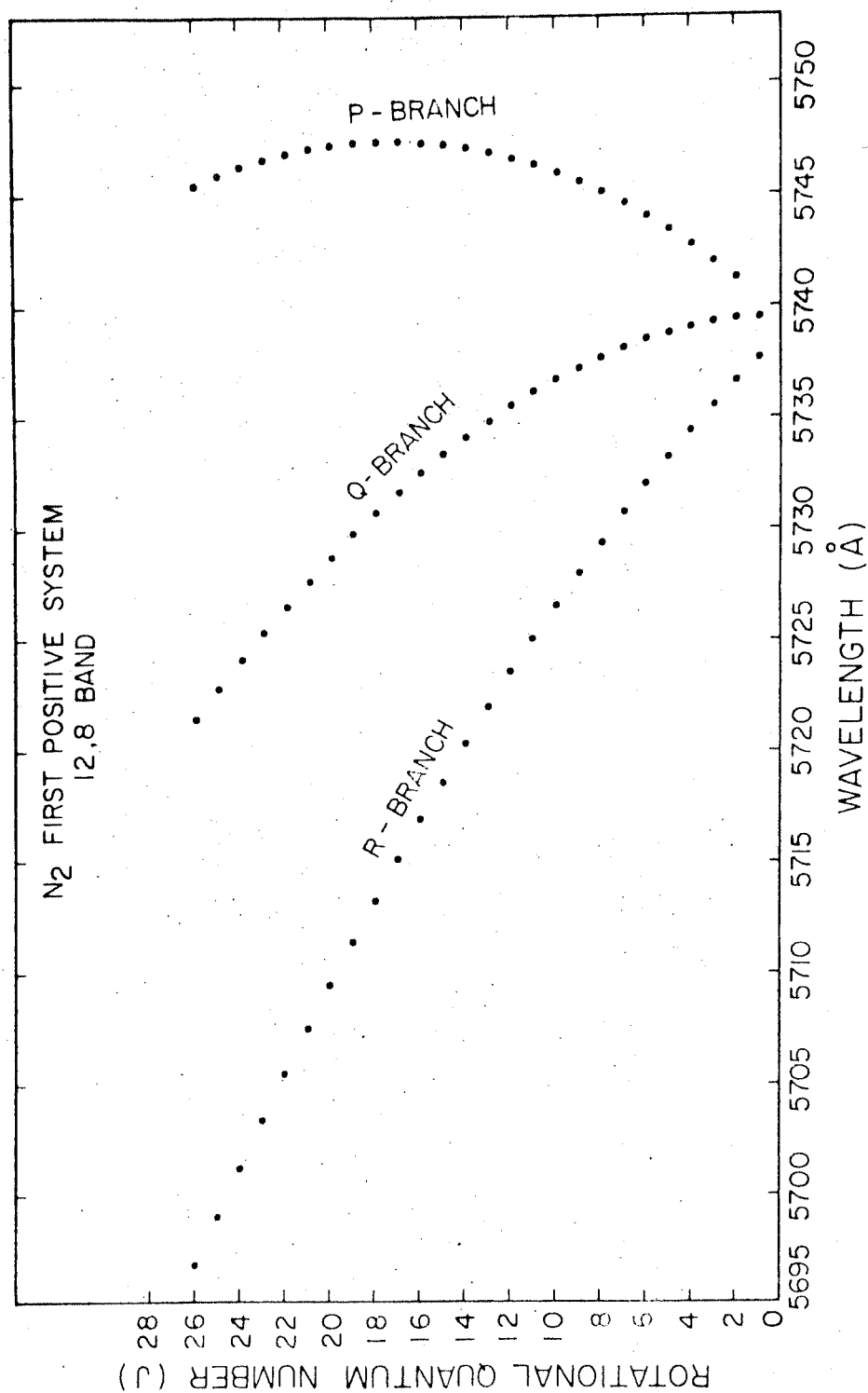
Fig. IV,5 Fortrat diagram for (12,8) vibrational band of B $^3\Pi_g \rightarrow$ A $^3\Sigma_u^+$
system of nitrogen.

Table IV.3

Wavelength (in Ångström units) of R, Q, P-branches, corresponding to rotational transition in (12,8) and (11,7) vibrational bands of first positive system.

Rotational quantum number	For (12,8) vibrational band			For (11,7) vibrational band		
J	R(J)	Q(J)	P(J)	R(J)	Q(J)	P(J)
0	5738.60			5787.02		
1	5737.66	5739.52		5786.01	5787.92	
2	5736.63	5739.41	5741.27	5784.94	5787.81	5789.72
3	5735.55	5739.26	5742.04	5783.82	5787.64	5790.51
4	5734.42	5739.05	5742.76	5782.64	5787.41	5791.24
5	5733.23	5738.79	5743.43	5781.41	5787.13	5791.91
6	5732.00	5738.48	5744.05	5780.12	5786.79	5792.53
7	5730.71	5738.12	5744.60	5778.77	5786.40	5793.10
8	5729.38	5737.71	5745.13	5777.37	5785.95	5793.60
9	5727.99	5737.24	5745.60	5775.91	5785.45	5794.05
10	5726.55	5736.73	5746.01	5774.40	5784.88	5794.45
11	5725.06	5736.16	5746.37	5772.84	5784.27	5794.79
12	5723.52	5735.54	5746.68	5771.22	5783.59	5795.07
13	5721.93	5734.87	5746.93	5769.54	5782.86	5795.29
14	5720.29	5734.14	5747.14	5767.81	5782.08	5795.46
15	5718.56	5733.37	5747.29	5766.02	5781.24	5795.57
16	5716.86	5732.54	5747.39	5764.18	5780.34	5795.63
17	5715.06	5731.67	5747.44	5762.29	5779.39	5795.63
18	5713.22	5730.74	5747.43	5760.34	5778.38	5795.57
19	5711.33	5729.76	5747.38	5758.33	5777.31	5795.46
20	5709.39	5728.73	5747.27	5756.28	5776.19	5795.29
21	5707.39	5727.65	5747.11	5754.16	5775.02	5795.07
22	5705.35	5726.51	5746.90	5752.00	5773.79	5794.79
23	5703.26	5725.33	5746.64	5749.78	5772.50	5794.45
24	5701.12	5724.10	5746.33			
25	5698.93	5722.81	5745.96			
26	5696.69	5721.45	5745.54			

Table IV.4

Wavelength (in Ångström units), of R, Q, P-branches, corresponding to rotational transition in (12,9) and (11,8) vibrational bands of first positive system.

Rotational quantum number	For (12,9) vibrational band			For (11,8) vibrational band		
J	R(J)	Q(J)	P(J)	R(J)	Q(J)	P(J)
0	6165.84			6233.66		
1	6164.70	6166.84		6232.48	6234.70	
2	6163.49	6166.70	6168.84	6231.22	6234.55	6236.76
3	6162.21	6166.49	6169.71	6229.89	6234.32	6237.65
4	6160.86	6166.21	6170.50	6228.48	6234.02	6238.46
5	6159.45	6165.86	6171.22	6227.00	6233.64	6239.19
6	6157.96	6165.45	6171.88	6225.44	6233.19	6239.85
7	6156.41	6164.96	6172.46	6223.81	6232.66	6240.43
8	6154.79	6164.40	6172.98	6222.10	6232.06	6240.94
9	6153.10	6163.78	6173.43	6220.33	6231.38	6241.37
10	6151.34	6163.08	6173.80	6218.47	6230.63	6241.73
11	6149.51	6162.32	6174.10	6216.55	6229.80	6242.01
12	6147.62	6161.48	6174.34	6214.54	6228.90	6242.21
13	6145.66	6160.58	6174.51	6212.47	6227.92	6242.34
14	6143.63	6159.61	6174.60	6210.32	6226.87	6242.40
15	6141.53	6158.57	6174.63	6208.10	6225.74	6242.37
16	6139.36	6157.46	6174.59	6205.81	6224.54	6242.28
17	6137.13	6156.28	6174.48	6203.44	6223.27	6242.11
18	6134.83	6155.03	6174.29	6201.00	6221.92	6241.86
19	6132.46	6153.71	6174.04	6198.49	6220.49	6241.54
20	6130.03	6152.33	6173.72	6195.91	6218.99	6241.14
21	6127.52	6150.87	6173.33	6193.25	6217.42	6240.66
22	6124.96	6149.35	6172.87	6190.52	6215.77	6240.11
23	6122.32	6147.76	6172.34	6187.72	6214.05	6239.49
24	6119.62	6146.10	6171.74	6184.85	6212.25	6238.79
25	6116.85	6144.37	6171.07	6181.91	6210.38	6238.01
26	6114.02	6142.58	6170.33	6178.89	6208.44	6237.16

rotational transition but were mixture of large number of such transi-
tions. For example, the sharp peak in P-branch was due to transitions
which included P(8) to P(17) and P(17) to P(26) member in case of (12,8)
band. In comparison, sharp peaks in Q and R branches were mixture of
very few rotational transitions. There were a few broad peaks corres-
ponding to R series while some of the R(J) members with large J values
were nicely resolved. The last member of the R(J) series which could be
identified unambiguously corresponded to $J = 25$ for (12,8) band. Peak
due to J value higher than 25 could not be identified because of bad sta-
tistics in this region of the afterglow spectrum. The intensities of the
peak of (11,7) band were, in general, larger than those of peaks of (12,8)
band. The ratio of intensities of sharp peaks in P, Q, R branches of
(11,7) and (12,8) bands were found to be of the order of 1.65, 1.73 and
1.76 respectively.

The afterglow spectra of (12,8) and (11,7) vibrational bands
at $77^{\circ}K$ are shown in Fig. IV.2. The intensities of the peaks were, in
general, much larger at $77^{\circ}K$ than those of peaks at $300^{\circ}K$. Also the
largest peak in the P-branch of (12,8) band at $77^{\circ}K$ was about 6.4 times
larger than the most intense peak in P-branch of (11,7) band at $300^{\circ}K$
(Fig. IV.1). Again, it was clear from Fig. IV.2 that the most intense
peak in the P-branch of (12,8) band was about 4.5 times larger than that
in the P-branch of (11,7) band in the afterglow spectra at $77^{\circ}K$. Another
characteristic feature of the spectra was that the statistics was much
better as a result of which the R(J) member with higher J values were
nicely resolved in the (12,8) band. Even the peak corresponding to R(26)

could be observed. However, the intensity of R(26) was very small.
It may be recalled that R(26) was not observed in the (12,8) band in the
afterglow spectra at 300°K as the intensity in this region was poorer
and the statistics was bad.

The afterglow spectra of (12,9) and (11,8) vibrational bands
at 300°K and 77°K are shown in Fig. IV.3 and Fig. IV.4 respectively.
The peaks corresponding to different P, Q and R branches have been identi-
fied and assigned in the same way as described before in the same section.
At 300°K, the intensity of (11,8) band was observed to be much larger
than that of (12,9) band but the reverse was true in the spectra at 77°K.
The spectra at 77°K was much sharper than at 300°K. Many members of the
R(J) series corresponding to larger values were nicely resolved in the
spectra at 77°K. One characteristic feature of (12,9) band, both at 300°K
and 77°K was the presence of a well-resolved sharp and intense peak corres-
ponding to J = 25 of the R(J) series. In comparison, the R(25) peaks of
(12,8) band, both at 300°K and 77°K, were much weaker. Another revealing
feature was the absence of the R(26) peaks in the (12,9) band, both at
300°K and 77°K while R(26) peak in the (12,8) band was found to be present
in the afterglow spectra at 77°K only , though it was relatively very weak.

IV.3. Discussion

The results presented in the previous section about the rota-
tional transitions in the (12,8) and (12,9) vibrational bands of the
first positive system of nitrogen, give a fair idea about the quanti-
tative evaluation of dissociation energy of the neutral molecule, leading

to the lowest dissociation limit. Before this part is discussed, it would be a good idea to discuss about the possible mechanism for populating the emitting rotational levels corresponding to $v' = 12$ of the $B\,^3\Pi_g$ state of nitrogen.

The population mechanism for rotational levels could be explained as discussed below. The $N\,(^4S)$ atoms would undergo three-body recombination into the $^5\Sigma_g^+$ state, which is in near equilibrium with $N\,(^4S)$ atoms. This could be represented by

$$N\,(^4S) + N\,(^4S) + M \rightleftharpoons N_2\,(^5\Sigma_g^+,\ v = 0,\ J_{Higher\ Values}) + M \qquad IV.5$$
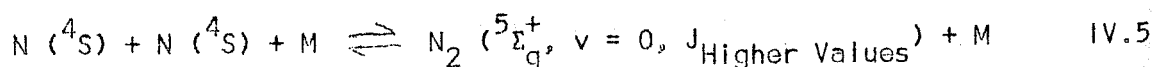
Energetically possible rotational levels of $v = 0$ state of $^5\Sigma_g^+$ below the dissociation limit would be populated according to equation (IV.5). As the two electronic states $^5\Sigma_g^+$ and $B\,^3\Pi_g$ intersect near $v = 12$ of $B\,^3\Pi_g$ state, because of perturbation, molecules in $^5\Sigma_g^+$ ($v = 0$, $J_{Higher\ Values}$) would undergo collision-induced radiationless transition into $v = 12$ vibrational state of $B\,^3\Pi_g$. It can be assumed that because of heterogenous perturbation, radiationless transition will take place over a range of rotational levels. This phenomena could be represented by the following equation

$$N_2\,(^5\Sigma_g^+,\ v = 0,\ J_{Higher\ Values}) + M \rightarrow N_2\,(B\,^3\Pi_g,\ v = 12,\ J_{Higher\ Values}) + M \qquad IV.6$$
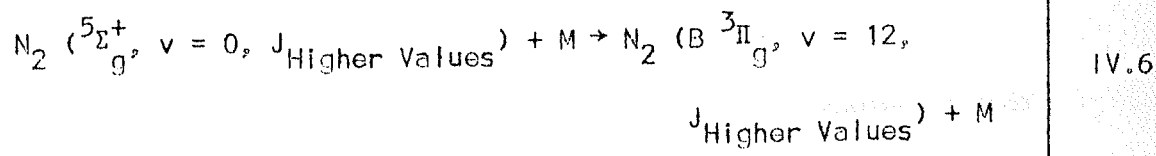
The molecules, thus populated in the rotational levels of $v = 12$ of $B\,^3\Pi_g$ state would also undergo rotational relaxation which is much more

efficient than the vibrational relaxation. So lower rotational levels would also be populated to some extent by rotational relaxation from higher J levels to lower values.

The dissociation energy of molecular nitrogen corresponding to the first dissociation limit could be determined from the high reso- lution afterglow spectra of (12,8) and (12,9) vibrational bands at both 300^OK and 77^OK. It has already been mentioned earlier that peaks upto R(25) could be observed in the spectra of (12,9) band at 77^OK and 300^OK and in the spectra of (12,8) band at 300^OK. A weak peak corresponding to R(26) member of the (12,8) band was found at 77^OK. The rotational transitions R(25) and R(26) correspond to J levels of 26 and 27 of v = 12 vibrational level of B $^3\Pi_g$ state, respectively. However, rotational levels upto J = 30 are energetically possible, in accordance with the computation made from molecular constants (Herzberg(1952)). The rota- tional levels for which transitions are not observed in the afterglow spectra, must be lying above the first dissociation limit of nitrogen. Molecules in such high rotational levels would undergo predissociation.

From the above arguments, it is clear that the rotational levels corresponding to J = 26 or 27 (v = 12 of B $^3\Pi_g$ state) may be lying very close to the first dissociation limit. This would give dissociation energy of 9.77 or 9.78 eV depending upon whether J = 26 or J = 27 lies close to the dissociation limit. We strongly feel that the presence of transition R(26) of (12,8) band at 77^OK starting from J = 27 level cannot be ignored inspite of the fact that this peak was very weak (Fig. IV.2). Peaks corresponding to R(26) transition

could not be observed in the spectrum of (12,8) band at 300°K and (12,9) band at both 300°K and 77°K because of certain reasons explained in the previous section. We, therefore, believe that the right value out of the two for dissociation energy corresponding to the first dissociation limit is 9.78 eV. Our value is in good agreement with the generally accepted value of 9.76 eV proposed by Gaydon (1968) in relatively recent times. In Table IV.5 are shown values of dissociation energy as reported by other scientists using different experimental and theoretical methods. These compare very well with our results.

Table IV.5

Values for dissociation energy of nitrogen

Dissociation Energy	Reference	Method
9.78 eV	Present work	High resolution afterglow spectroscopy
9.77 eV	Douglas and Herzberg (1951)	Predissociation in the emission spectra
9.73 eV	Lozier (1933)	Electron-impact
9.76 eV	Gaydon (1968)	Predissociation in the emission spectra
9.8 ± 0.5 eV	Herman and Herman (1942)	Lyman-Birge-Hopfield system in emission spectra
9.19 eV	Butscher et al. (1977)	Configuration interaction calculations

CHAPTER   V

QUENCHING OF (12,8) AND (11,7) BANDS OF B $^3\Pi_g \to A\ ^3\Sigma_u^+$ SYSTEM

OF NITROGEN BY NO AT 88°K

V.1.   Introduction

Mechanism for populating some of the emitting states in the

nitrogen afterglow, have been known for quite some time while controversy

still exists for populating a large number of other states. However, it

has been discussed in Chapter III that the B $^3\Pi_g$ state for molecular

nitrogen is populated by collision-induced recombination of two nitrogen

atoms in the ground state in the presence of a third body, through a

precursor, $^5\Sigma_g^+$ state (Bayes and Kistiakowsky (1960)). Also, it is now

known that the intensities of different vibrational bands of the first

positive system of nitrogen have a second order dependence ($I \alpha [N]^2$)
at pressures larger than 1 Torr (Young and Sharpless (1963), Campbell
and Thrush (1967), Jonathan and Petty (1969)). But in Chapter III,
we have reported that the second order dependence seemed to exist at
pressures between 4 and 7 Torr or higher. Also, it was observed
(Brennen and Shane (1971), Jonathan and Petty (1969), and also by us)
that there was practically negligible quenching of the radiation in
the first positive band by the third body, N_2, itself at higher
pressures while there was appreciable quenching by nitrogen at
pressures between 0.1 and 1 Torr. The quenching of the first positive
system of nitrogen by NH_3, CO, CO_2, CH_4 etc. has been studied exten-
sively (Bayes and Kistiakowsky (1960)). However, to the best of our
knowledge, there has been no systematic investigation of quenching by
NO so far. In view of this, a systematic study of quenching of some
of the vibrational bands of the $B\ ^3\Pi_g \rightarrow A\ ^3\Sigma_u^+$ system by NO at about $88^\circ K$,
has been undertaken by us.

The quenching in general leads to reducing the population
of the emitting state. The quenching agent, NO, reacts with nitrogen
atoms and removes some of these through a chemical reaction. This
results in less number of nitrogen atoms getting involved in collision-
induced radiationless transition leading to populating the $B\ ^3\Pi_g$ state,
through a precursor, $^5\Sigma_g^+$. In the present work, nitric oxide quenching
rates for the (12,8) and (11,7) vibrational bands of the first positive
system of nitrogen have been measured at about $88^\circ K$.

V.2. Production of Quenching Agent, NO

While taking the afterglow spectra of nitrogen at any of the pressures varying from 1 to 7 Torr at liquid nitrogen temperature, it was observed that the nitrogen pressure increased with time as measured from M.K.S. Baratron capacitance manometer using 10 Torr head. In a fast flow system, this could not be explained until and unless a new product was formed by a chemical reaction and this new product was getting solidified at liquid nitrogen temperature. It is well-known that inspite of further purification of IOLAR-II nitrogen, atomic oxygen may be formed in very small quantities because of microwave discharge of impurity oxygen. The reaction

$$N + O + M \rightarrow NO^* + M \hspace{3cm} V.1$$

is responsible for the production of NO in different electronic states. NO, thus formed, gets solidified on the walls of the afterglow tube. NO vapours in equilibrium with the solid NO may be responsible for the increase in pressure observed in the tube. With time, more and more NO would be formed by reaction (V.1) and it would get solidified. After some time, the NO vapour would be in complete equilibrium with solid NO and any additional NO produced would be pumped out in the fast flow system. This would correspond to the initial increase and then saturation of pressure as observed in the MKS capacitance manometer. This yields a method to measure the vapour pressure of solid NO at very low temperatures.

It may be interesting to view these arguments in terms of the afterglow spectra of N_2 at $300^{\circ}K$ and $77^{\circ}K$ respectively. The after-glow spectra of N_2 at these two temperatures have previously been reported in Chapter III. The spectra from 1900 to 4800 Å at $300^{\circ}K$ showed a few very small peaks corresponding to beta bands of impurity NO while no member of the gamma bands could be observed at this temperature in the spectra at various pressures (1 to 7 Torr) of N_2. In comparison, a large number of very intense beta and gamma bands of NO were observed in the afterglow spectra at $77^{\circ}K$. These observations give credence to the statements regarding production of NO as discussed above.

The vapour pressure of solid NO near liquid nitrogen temperature has been measured as a function of various N_2 pressures. In Fig. V.1 are shown observation of total absolute pressure as a function of time. Each time interval is of 15 minutes duration. At time $t = 0$, the pressure corresponds to molecular nitrogen and its dissociated products. As time increases, the total absolute pressure increases but after a lapse of certain time, the total pressure starts saturating. The vapour pressure of solid NO would be given by the saturated pressure minus the pressure at $t = 0$. The observations have been recorded for six nitrogen pressures at time $t = 0$, from 1 to 4 Torr and at 6 and 7 Torr.

Once the vapour pressures of solid NO are measured in the presence of N_2 at a certain pressure, the temperature of the saturated vapour could be determined. The variation of vapour pressure with temperature is given by (Hand Book of Chemistry and Physics, 1979-1980)
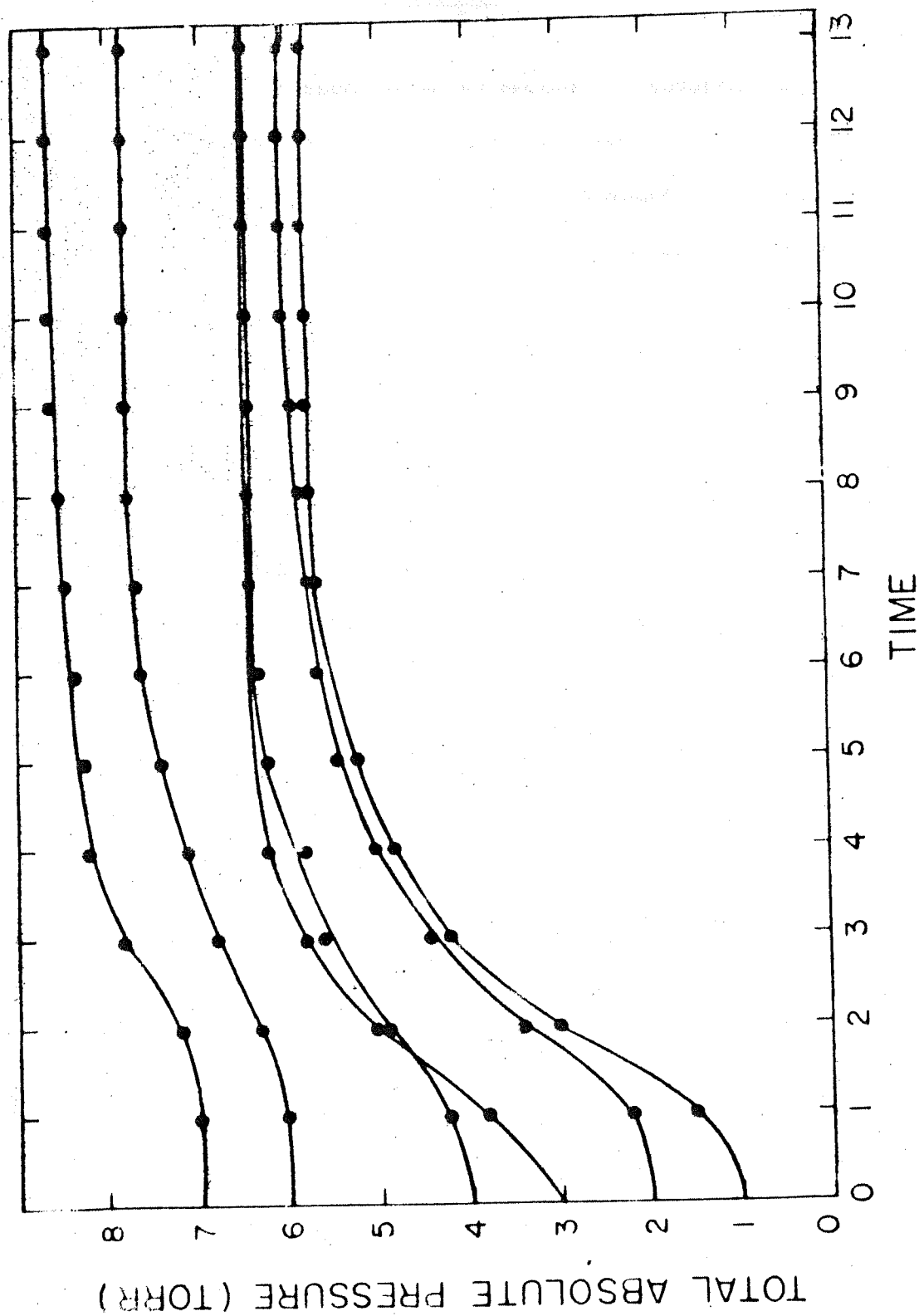
EACH INTERVAL IS OF 15 MINTS. DURATION

Fig. V.1   Total absolute pressure of the system (N_2 + NO) as a function of time.
Each time interval is of 15 minutes.

$$\log_{10} p = -\frac{0.05223}{T} a + b \qquad\qquad V.2$$

where p is the pressure in mm of mercury of saturated vapour at the

absolute temperature, T. For solid NO from $73^\circ K$ to $112^\circ K$, a = 16423 and

b = 10.048. Using equation (V.2), the temperature of the saturated

vapour could be determined for various N_2 pressures. This is shown in

Fig. V.2. From the figure, it is clear that at higher nitrogen pressures,

the temperature of the saturated vapour is less while the temperature

is larger at low N_2 pressures. Higher pressure of nitrogen would mean

larger number of molecules in the flow tube which would offer larger

conductance to the transfer of heat energy from the outer jacket to the

center of the tube. So the losses would be more at higher pressure of

N_2 than at lower pressure with the result that the temperature of the

saturated vapour inside the tube would be less at higher pressures than

at low pressures.

The nitric oxide molecules in equilibrium with the solid NO

could be used for measuring quenching rates of different vibrational

bands of the first positive system of nitrogen at temperatures ranging

from $87^\circ K$ to about $92^\circ K$. The quenching rates have been measured for

(12,8) and (11,7) vibrational bands.

V.3. Results and Discussion

In Fig. V.3 are shown the afterglow spectra of two bands,

(12,8) and (11,7), taken at a fixed nitrogen pressure but at varying

total pressure which is the sum of partial pressures of nitrogen and
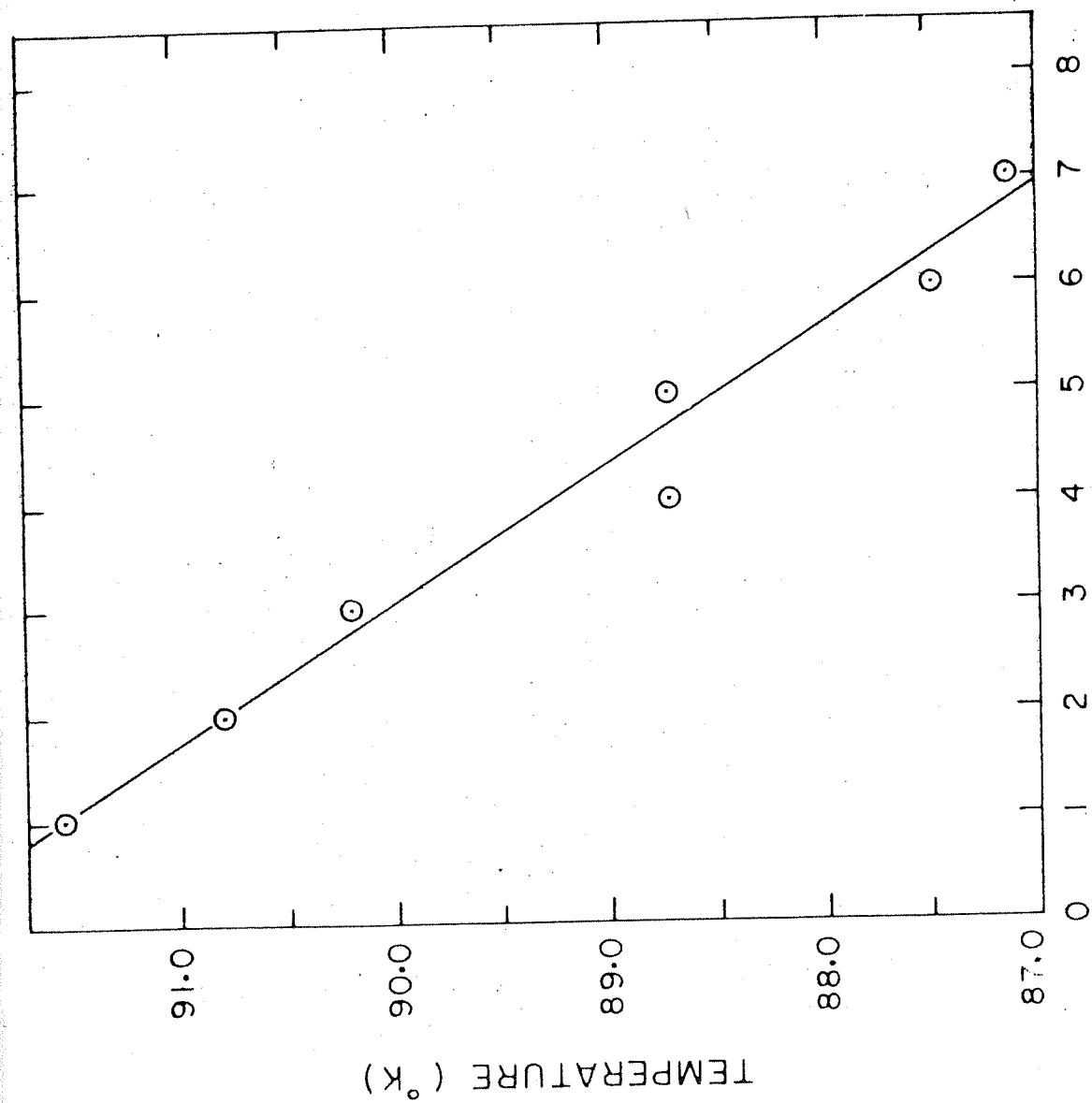
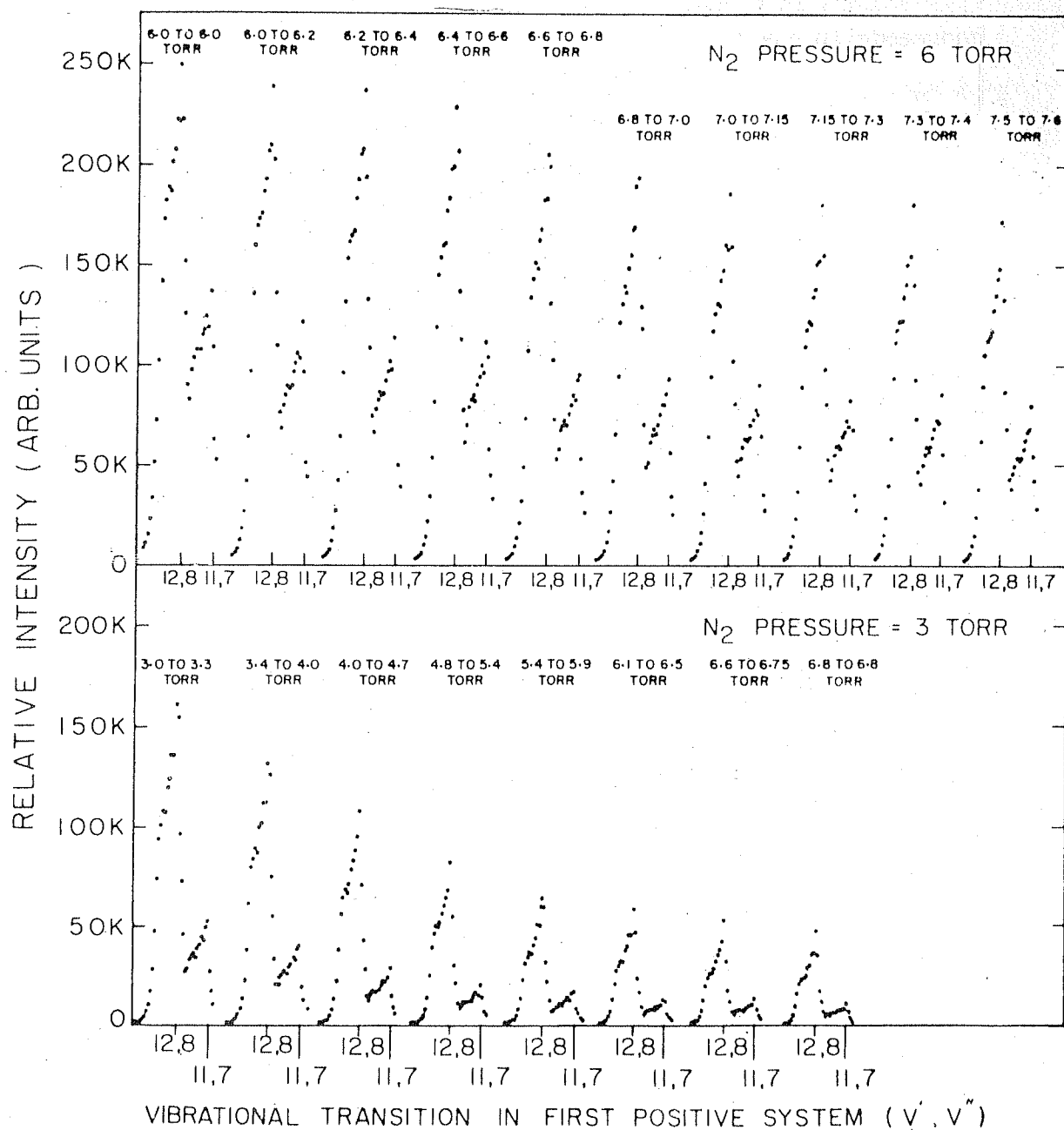Fig. V.2 Temperature of the saturated vapour of NO as a function of nitrogen pressure.

Fig. V.3 Afterglow spectra of (12,8) and (11,7) bands
corresponding to first positive system of nitrogen
at fixed pressures of 6 and 3 Torr respectively.
The peak intensities of these bands are shown to
vary with quenching agent NO at different pressures.

saturated vapours of NO. The spectra are taken at fixed N_2 pressures ranging from 1 to 7 Torr in 1 Torr interval. In Fig. V.3 only two sets of afterglow spectra are shown at fixed N_2 pressures of 6 and 3 Torr respectively.

In the spectra at the fixed nitrogen pressure of 6 Torr, the total pressure did not vary during the period of taking the first spectrum. During the second spectrum, the total pressure changed from 6.0 to 6.2 Torr. Thus, on the average, the total pressure varied by 0.1 Torr which is the partial pressure of saturated vapour of NO. Similarly, other spectra were taken at different partial pressures of NO. The quenching of both (12,8) and (11,7) vibrational bands was clearly seen in Fig. V.3 as the intensity of both peaks decreased with higher NO partial pressure. In these spectra, (12,8) band is much more intense than the (11,7) band as the spectra is being taken at near liquid nitrogen temperature. Also, the intensity of the (12,8) band decreased by approximately 1.5 times at total pressures of 6 Torr and 7.55 Torr, which correspond to NO partial pressure of 0 and 1.55 Torr respectively. The intensity of (12,8) band observed at a fixed N_2 pressure of 3 Torr decreased by about 3.4 time at total pressures of 3.15 Torr and 6.8 Torr which correspond to NO partial pressure of 0.15 Torr and 3.8 Torr respectively. It may be pointed out here that once the quenching studies at one fixed N_2 pressure are complete, the liquid nitrogen in the jacket is completely evaporated and the remnant NO evacuated from the afterglow chamber. The quenching studies at a different fixed N_2 pressure are started only after the system has been pumped for a long time.

The intensities of the (12,8) and (11,7) bands were measured as a function of partial pressure of NO at different fixed N_2 pressures. In Fig. V.4 and Fig. V.5 are shown plots of I_O/I against NO partial pressures at N_2 fixed pressures of 4, 5, 6 Torr for (12,8) and (11,7) vibrational bands respectively. I_O is the intensity at time $t = 0$ and I is the intensity of the vibrational band after the quenching by NO has taken place. From Fig. V.4 and Fig. V.5, it is obvious that there is a linear relationship between I_O/I and NO concentration - at fixed nitrogen pressures of 6, 5, and 4 Torr only. At other pressures of nitrogen i.e. at 3, 2 and 1 Torr, I_O/I and NO concentration are not linearly related but some other dependence like near exponential dependence seems to exist. Such measurements have been made both for (12,8) and (11,7) vibrational bands but the measurements for only (12,8) band are being shown in Fig. V.6.

It has been pointed out earlier that the intensities of various vibrational bands of the first positive system of nitrogen have a linear second order dependence ($I \alpha [N]^2$) at pressures larger than 1 Torr (Young and Sharpless (1963), Campbell and Thrush (1967), Jonathan and Petty (1969)). Also we have reported (in Chapter III) that $I \alpha [N]^2$ dependence seems to exist at pressures between 4 Torr and 7 Torr. In view of that when afterglow spectra is taken in this pressure region and there is no other quenching agent present, the intensity of the vibrational band would be given by

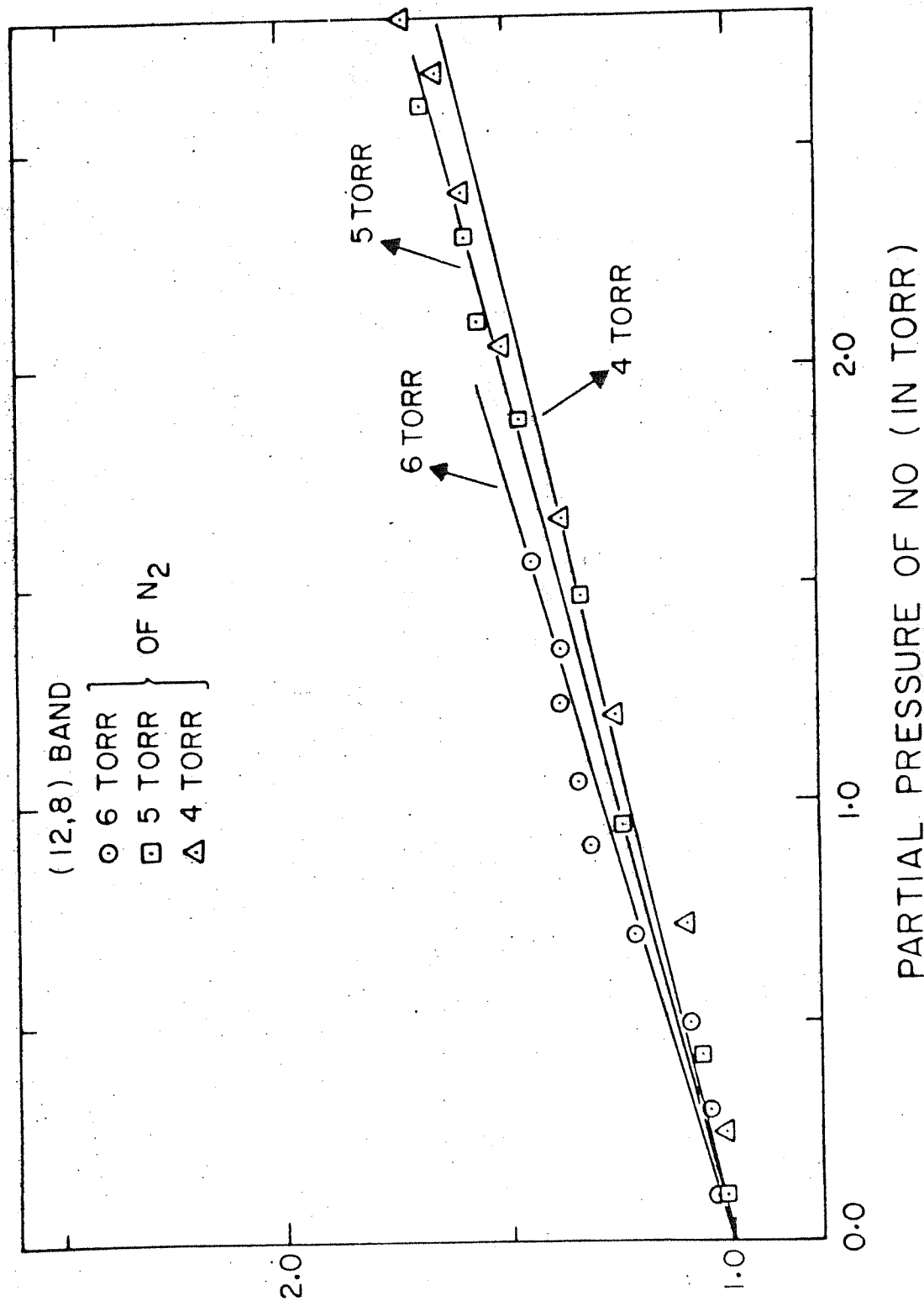$$I = K[N]^2 \qquad\qquad\qquad V.3$$

Fig. V.4 I_0/I as a function of partial pressures of NO at three N_2-pressures (4, 5 and 6 Torrs). The quenching measurements have been reported for (12,8) band of first positive system of nitrogen.
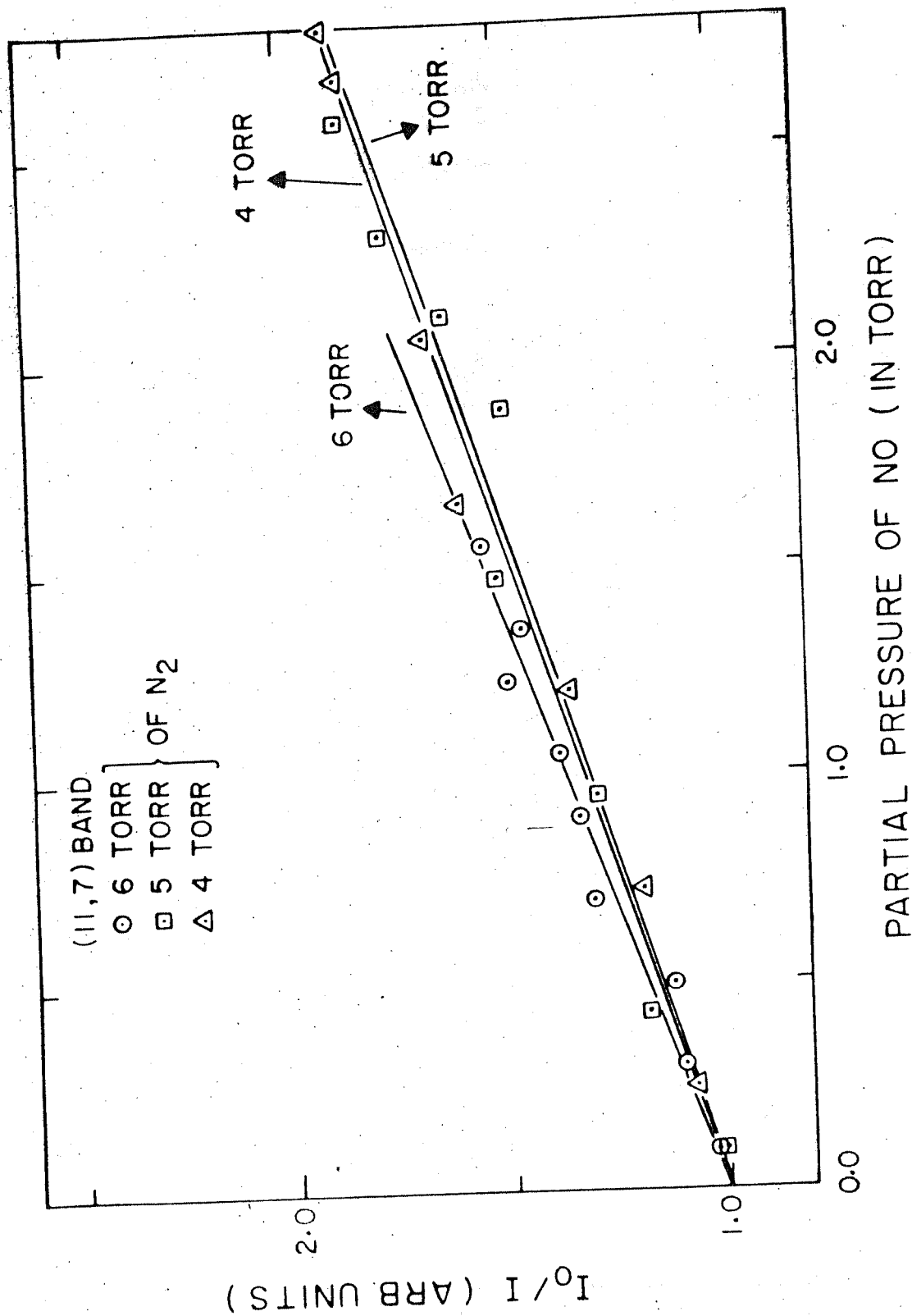
Fig. V.5 I_0/I as a function of partial pressures of NO at three N_2-pressures (4, 5 and 6 Torrs). The quenching measurements have been reported for (11,7) band of first positive system of nitrogen.
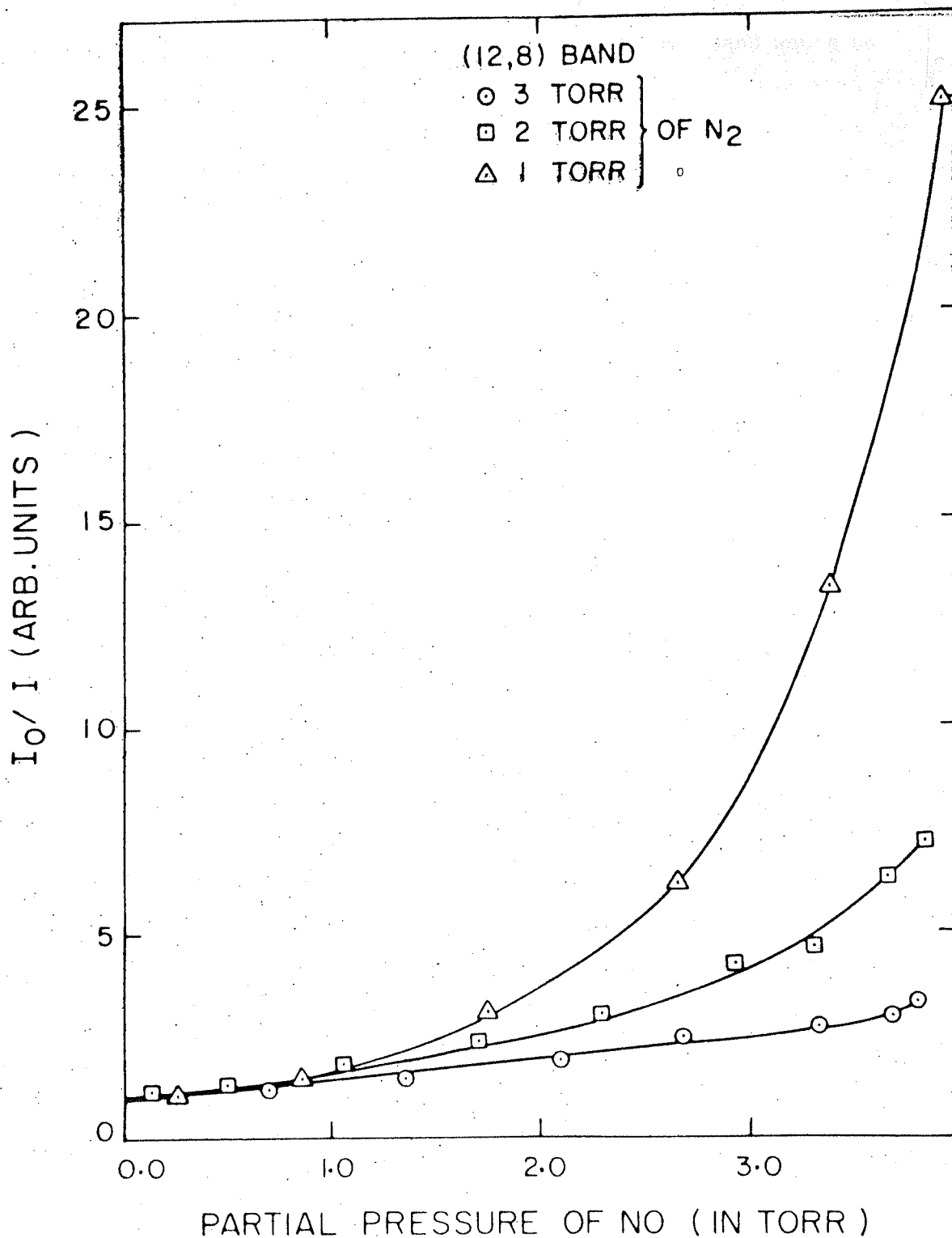
Fig. V.6 I_0/I as a function of partial pressures of NO at N_2
pressure of 1,2 and 3 Torr respectively. The quench-
ing measurements have been shown for (12,8) band of

where k is reaction rate constant for this reaction. When the quench-
ing agent NO is present, then the intensity of the band would be
decreased according to the following equation

$$I = \frac{k\,[N]^2}{k_{NO}\,\tau\,[NO] + 1} \qquad\qquad V.4$$

where k_{NO} is the quenching rate by NO, τ is the radiative life time of
$v = 12$, 11 levels of B $^3\Pi_g$ state. In these calculations, τ has been
taken as 4.4×10^{-6} sec. for both the vibrational levels as reported by
Jeunehomme (1966). From equations V.3 and V.4, the quenching rate of NO
can easily be determined.

$$k\,(NO)\,\tau = \frac{1}{[NO]}\left(\frac{I_o}{I} - 1\right) \qquad\qquad V.5$$

The quenching rates for (12,8) and (11,7) vibrational bands by NO have
been calculated for different fixed N_2 pressures. The temperatures of
the saturated NO vapour are given corresponding to N_2 pressures
(Fig. V.2). In Table V.1 are given quenching rate at different tempera-
tures.

Table V.1

Quenching rates of (12,8) and (11,7) bands by NO at different temperatures

Temperature $^\circ$K	k(NO) in $cm^3\,moloc^{-1}\,sec^{-1}$	
	(12,8) Band	(11,7) Band
87.7	$(1.97 \pm 0.37) \times 10^{-12}$	$(2.61 \pm 0.26) \times 10^{-12}$
88.5	$(1.57 \pm 0.14) \times 10^{-12}$	$(2.19 \pm 0.24) \times 10^{-12}$
89.2	$(1.46 \pm 0.18) \times 10^{-12}$	$(2.14 \pm 0.26) \times 10^{-12}$

The quenching rates as given in Table V.1 are for tempera-
tures varying from about $87^{\circ}K$ to $89^{\circ}K$. The temperature interval is too
small and therefore, from this, temperature dependence of the quenching
rate cannot be determined authentically. Instead, an average quenching
rate at a fixed temperature should be reported. For (12,8) band, the
average quenching rate as calculated from the above table, is
$(1.67 \pm 0.23) \times 10^{-12}$ cm^3 $molec^{-1}$ sec^{-1} at an average temperature of
$88.5^{\circ}K$ while for (11,7) band, the average quenching rate is
$(2.20 \pm 0.25) \times 10^{-12}$ cm^3 $molec^{-1}$ sec^{-1}. To the best of our knowledge,
there are no other measurements reported in the literature for the NO
quenching rates. Therefore, no comparison is possible.

CHAPTER VI

DEACTIVATION OF A $^3\Sigma_u^+$ STATE OF OXYGEN BY OXYGEN, ARGON AND

HELIUM

VI.1 Introduction

The importance of studying deactivation of A $^3\Sigma_u^+$ state of

oxygen by oxygen itself has been discussed in Chapter I. Such a

measurement requires kinetic study of Herzberg I emission band, in

oxygen afterglow, with or without the presence of a diluent like argon

and helium. Kinetics for Herzberg I band has been studied in detail by

Young and Sharpless (1962, 1963), Young and Black (1966) and Campbell

and Thrush (1967 b). However, no laboratory afterglow measurements

have been made to study quantitatively the deactivation of A $^3\Sigma_u^+$ state

by oxygen, argon and helium.

In this chapter, we present the afterglow spectra of mole-
cular oxygen with diluents, argon and helium, and without any diluents
in the spectral range from about 2400 to 4250 Å. A large number of
Herzberg I vibrational bands and a few very weak Herzberg II bands have
been observed in this region. The afterglow spectra has been studied
as a function of oxygen pressure from 2 to 7 Torr when there is no
diluent and from 0.2 to 1 Torr when diluents like argon and helium are
used at a fixed diluent pressure of 6 Torr. The quenching rates for
the vibrational bands (5, 4), (4, 4) and (4, 3) of the Herzberg I
system by oxygen, argon and helium have been measured.

VI.2   Results and Discussions

VI.2.1   Afterglow Spectra

The afterglow spectra of oxygen has been studied at $300^{\circ}K$ in
the spectral region from about 2400 to 4250 Å. The spectrum at 4 Torr
oxygen pressure is shown in Fig. VI.1. Many vibrational bands corres-
ponding to Herzberg I spectrum have been nicely resolved while a few
could not be completely resolved. Most of the vibrational bands have
been identified and proper assignment has been given to these with
reference to the spectra observed by Broida and Gaydon (1954). The
(0, 3), (0, 4) vibrational bands corresponding to Herzberg II could not
be properly identified in this spectra while (0, 3), (0, 4) and (0, 5)
vibrational bands could barely be recognized in the afterglow spectra
of oxygen in presence of diluents like argon and helium. In Fig. VI.2
and Fig. VI.3 are shown spectra at pressure of 6 Torr of argon and
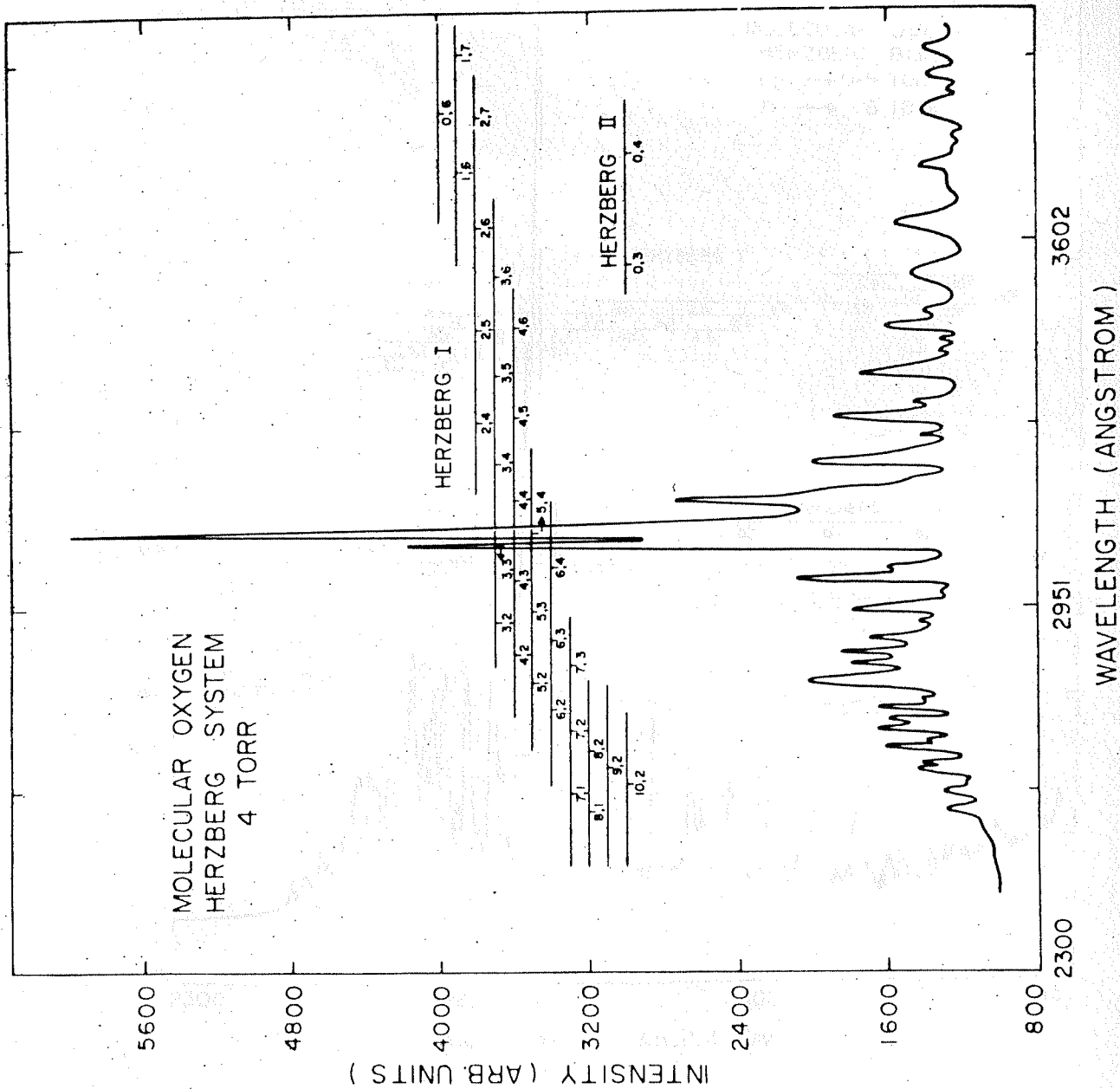
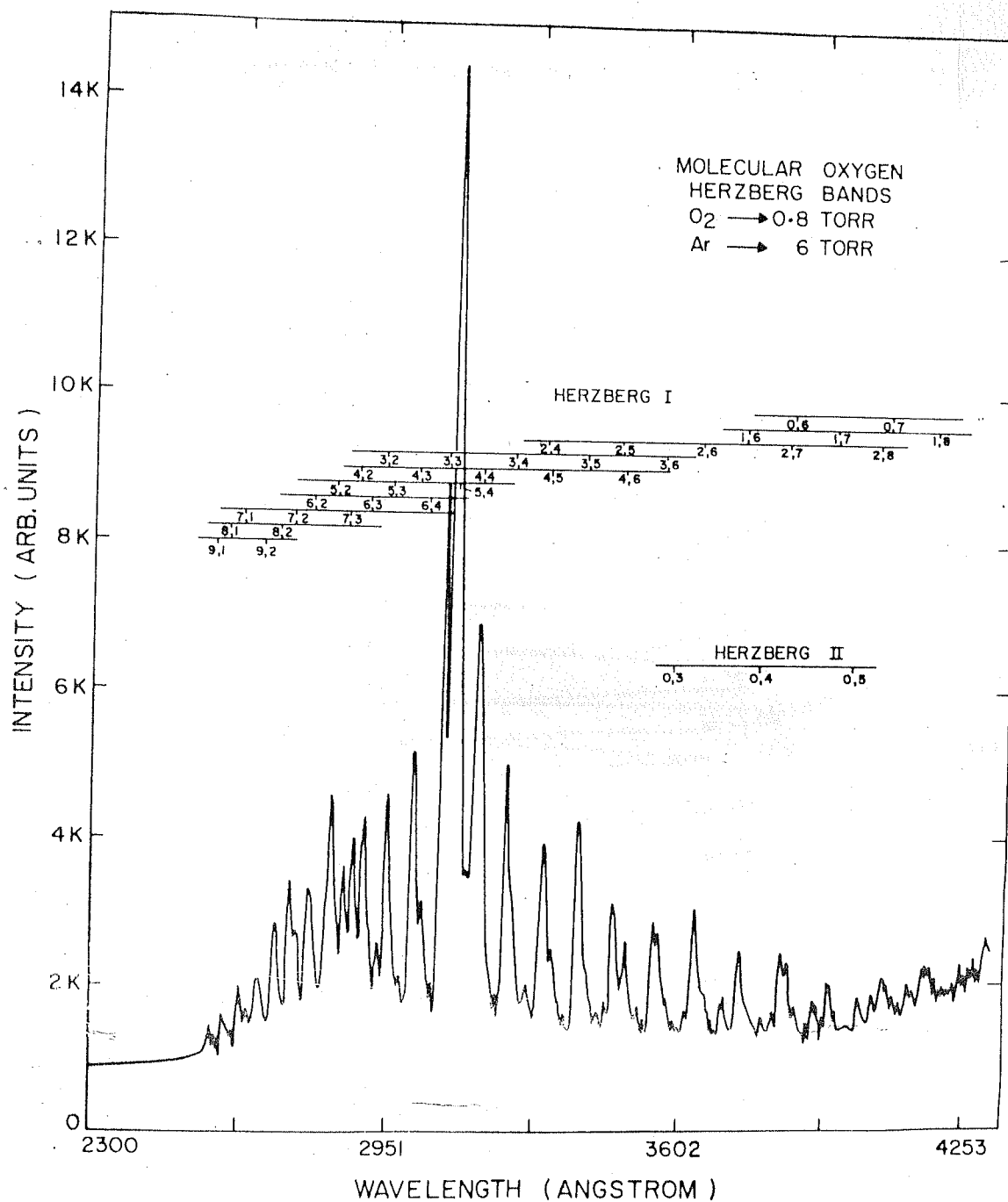Fig. VI.1 Afterglow spectra of oxygen at $300^\circ K$ from 2400 to 4250 Å.

Fig. VI.2. Afterglow spectra of oxygen at $300^{O}K$ obtained at a 6 Torr pressure of argon and 0.8 Torr of oxygen.
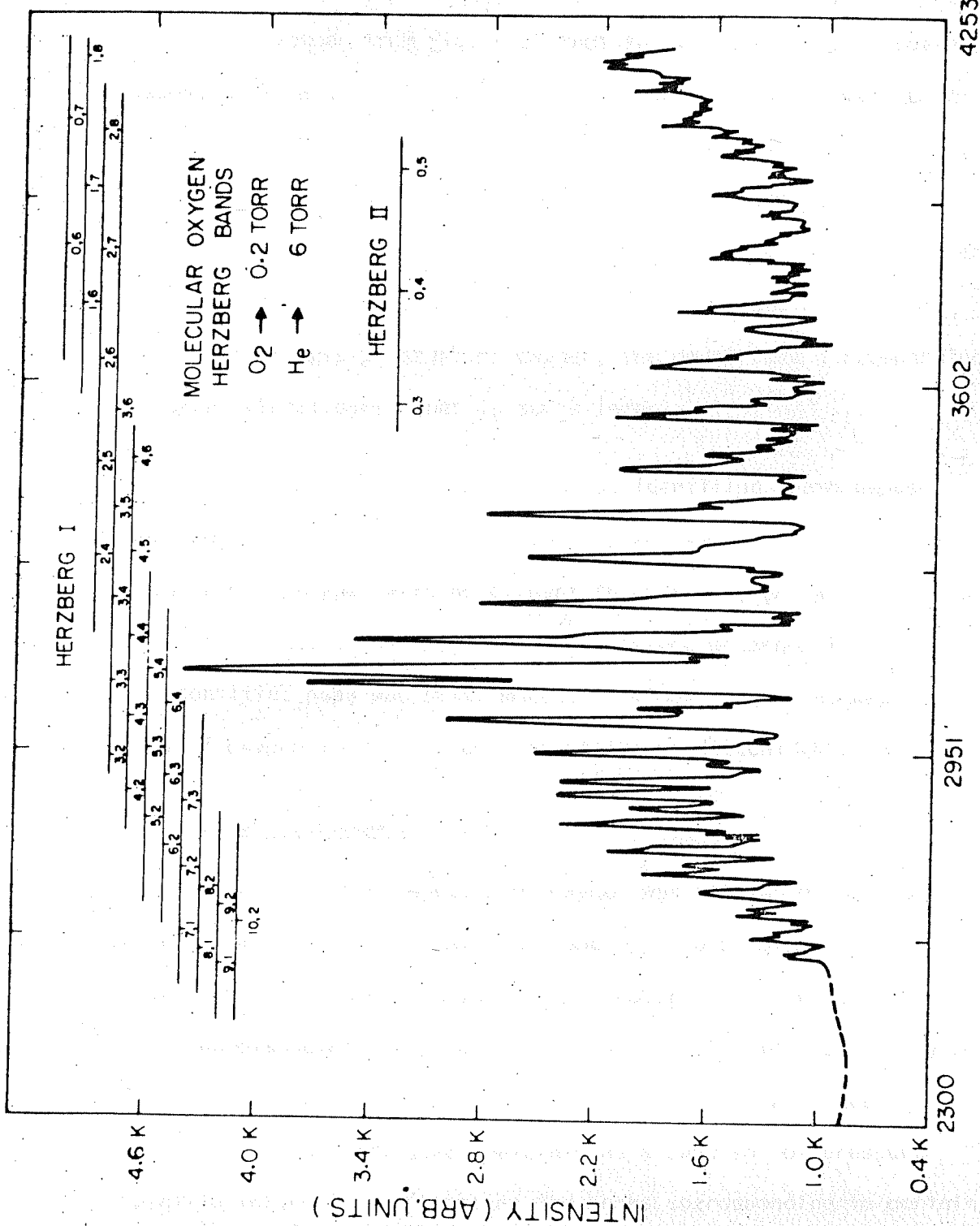
Fig. VI.3 Afterglow spectra of oxygen at 300°K obtained at a 6 Torr pressure of helium and 0.2 Torr of oxygen.

0.8 Torr of oxygen and 6 Torr of helium and 0.2 Torr of oxygen, respectively. It is clear from Fig. VI.2 that the vibrational band peaks corresponding to argon plus oxygen spectrum are relatively much more intense than those observed in the spectra of oxygen without any diluent (Fig. VI.1). A similar behaviour has also been noticed in the spectra for helium and oxygen mixture at various oxygen pressures. The spectrum in Fig. VI.3 is shown for 6 Torr of helium and 0.2 Torr of oxygen. Even at this pressure of oxygen, the count rate corresponding to different vibrational bands is quite large.

Some of the peaks could not be identified unambiguously. One such peak at the wavelength of 3704 $\overset{O}{A}$, was very weak in the afterglow spectrum of oxygen with no diluent (Fig. VI.1), but was relatively strong in the spectrum of oxygen in the presence of argon (Fig. VI.2). This unidentified peak was still more predominant in the afterglow spectrum of oxygen in the presence of helium as diluent (Fig. VI.3).

VI.2.2 Pressure Dependence

The afterglow spectra of oxygen was studied at various pressures from 2 to 7 Torr. Also, at each pressure, dissociation efficiency of parent oxygen molecules was determined by Wrede-Harteck method. The dissociation efficiency varied from 7.2 to 8.2% at oxygen pressure varying from 7 to 2 Torr respectively. This way, absolute atomic oxygen concentration was obtained as a function of pressure. The relative intensities of some of the peaks corresponding to certain vibrational bands of Herzberg I system were measured and plotted

against the square of atomic oxygen concentration. In Fig. VI.4 are shown plots of intensity versus $[0]^2$ for (5,4), (4,4), (4,3) and (3,3) vibrational bands of the Herzberg I system. It is clear that there is a marked departure from the second order pressure dependence. Also it is obvious that the A $^3\Sigma_u^+$ state is being deactivated by the third body which, in this case, is molecular oxygen.

The afterglow spectra of oxygen was also studied in the presence of diluents like argon and helium at fixed diluent pressure of 6 Torr and at oxygen pressure varying from 0.2 to 1 Torr. The oxygen-helium or oxygen-argon mixtures were allowed to undergo the microwave discharge. At all these pressures, dissociation efficiency was determined using Wrede-Harteck method. The dissociation efficiency varied from 21 to 29% in both cases at oxygen pressures varying from 0.2 to 1 Torr. The dissociation efficiency measured in the latter case is much larger than that obtained without any diluent. This was expected because both the diluents reduced the wall-recombination and increased the three-body volume recombination. The relative intensity of the peaks corresponding to vibrational bands, (5,4), (4,4) and (4,3) of Herzberg I system were measured and plotted against $[0]^2$. The results obtained are similar to what has been reported in Fig. VI.4. The departure from the second order pressure dependence shows that the A $^3\Sigma_u^+$ state is not only being deactivated by oxygen itself but by the diluents like argon and helium, also.
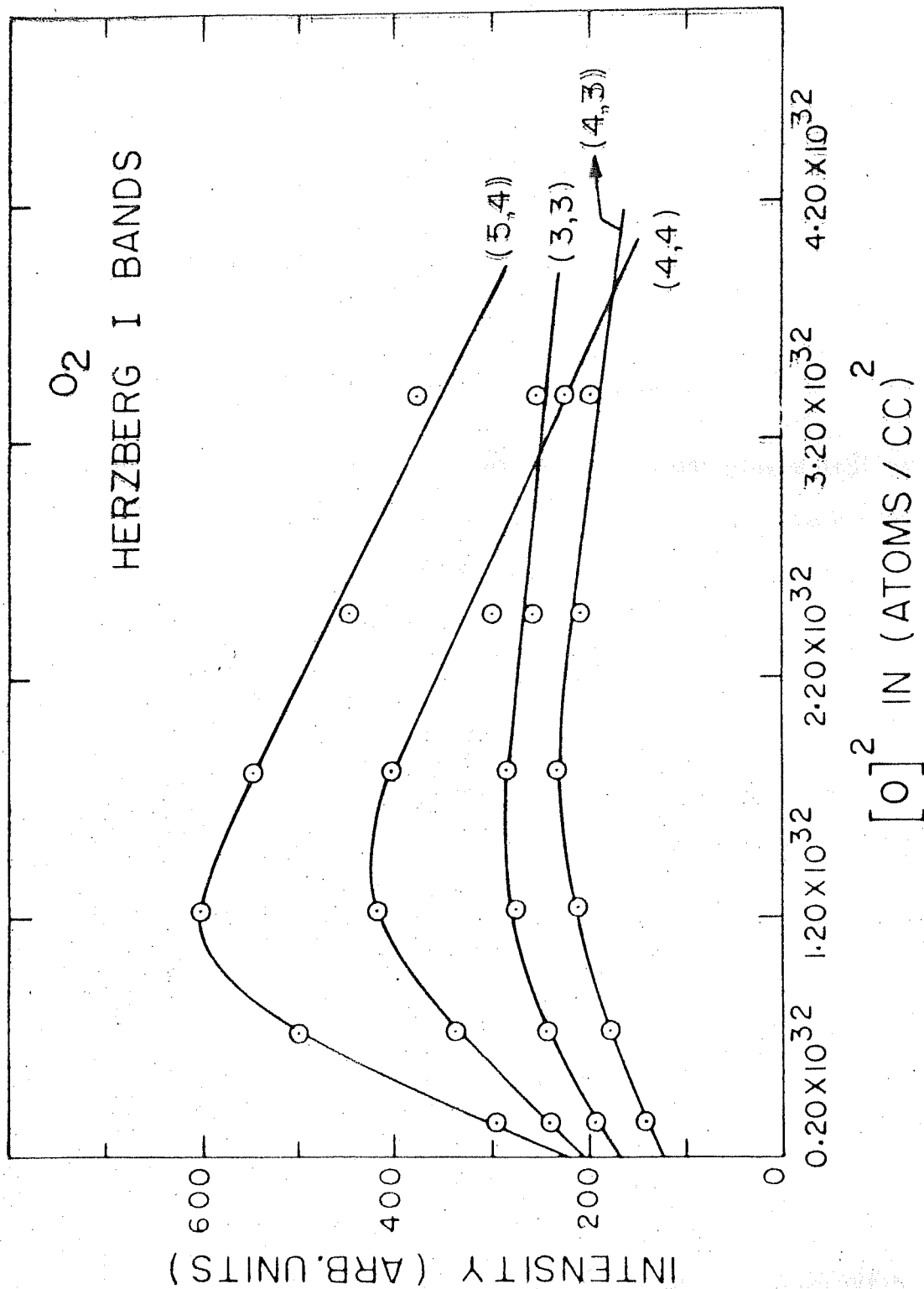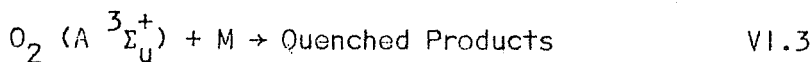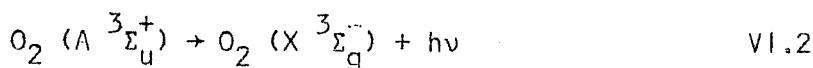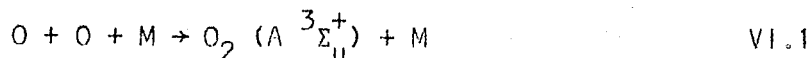
Fig. VI.4   Peak intensities of (5,4), (3,3), (4,3) and (4,4) vibrational bands of Herzberg I system of oxygen as a function of square of the oxygen atom concentration.

VI.2.3 Quenching Studies

It is generally agreed that the Herzberg I bands $(A\ ^3\Sigma_u^+ \rightarrow X\ ^3\Sigma_g^-)$ are produced by the following mechanism:

$$O + O + M \rightarrow O_2\ (A\ ^3\Sigma_u^+) + M \qquad\qquad VI.1$$

$$O_2\ (A\ ^3\Sigma_u^+) \rightarrow O_2\ (X\ ^3\Sigma_g^-) + h\nu \qquad\qquad VI.2$$

$$O_2\ (A\ ^3\Sigma_u^+) + M \rightarrow Quenched\ Products \qquad\qquad VI.3$$

These reactions explained the atmospheric night glow emissions in Herzberg I bands as reported by Bates (1957), Chamberlain (1961) and Barth (1964). The kinetics of formation of A $^3\Sigma_u^+$ state appears to be quite complex as the emitting state itself is deactivated rapidly (Golde and Thrush (1973)). The quenching rates for A $^3\Sigma_u^+$ state by oxygen molecules could be determined if the change in peak intensity, I, of the vibrational bands is known as a function of oxygen pressure and atomic oxygen concentration. From Equation VI.1 to Eq. VI.3,

$$I = \frac{K\ [O]^2\ [O_2]}{1 + k_{O_2}\cdot\tau\ [O_2]} \qquad\qquad VI.4$$

where K is the reaction rate constant of equation (VI.1), k_{O_2} is the quenching rate of A $^3\Sigma_u^+$ state by O_2 and τ is the radiative life time of A $^3\Sigma_u^+$ state. At any two pressures of parent molecular oxygen, the intensity ratio would be given by

$$\frac{I_1}{I_2} = \frac{[O]_1^2}{[O]_2^2}\cdot\frac{[O_2]_1}{[O_2]_2}\cdot\frac{1 + k_{O_2}\tau\ [O_2]_2}{1 + k_{O_2}\tau\ [O_2]_1} \qquad\qquad VI.5$$

The quenching rate k_{O_2} and half-quenching pressure $(k\tau)^{-1}$ could be determined from equation (VI.5) as all other quantities are known (section VI.2.2). The radiative life time τ has been deduced from the absolute absorption coefficient (Hasson et al. (1970)) and relative emission band strength data (Degen and Nicholls (1969) and Jarmain (1972)) and for A $^3\Sigma_u^+$, this has been reported to be approximately 1/6 sec. It has been assumed here that the radiative life time for all the vibrational levels of the A $^3\Sigma_u^+$ state is the same. The quenching rates and inverse half-quenching pressure for (5,4), (4,4) and (4,3) vibra-tional bands of Herzberg I system have been calculated for quenching agent oxygen from equation (VI.5) and these are given in Table VI.1. For all the three vibrational bands (5,4), (4,4) and (4,3) the values for quenching rate and inverse half-quenching pressure are practically the same. It could be thus assumed that for all other vibrational bands in the Herzberg I system, the values of k_{O_2} and $k_{O_2}\tau$ may be practically the same. It is not easy to compare our results with those reported elsewhere. This is because not much laboratory work has been carried out in this direction. A value of 10^{-15} cm^3 molec^{-1} sec^{-1} has been reported for k_{O_2} by Young and Sharpless (1962), assuming a value of 10^{-3} sec for the radiative life time of the O_2 (A $^3\Sigma_u^+$) state. However, the latest value for τ, as discussed before is 1/6 sec. Taking this value for τ, k_{O_2} value given by Young and Sharpless (1962) would be modified to 6×10^{-18} cm^3 molec^{-1} sec^{-1}. This value is about an order less than that measured by us.

The quenching rate for quenching A $^3\Sigma_u^+$ state by oxygen has been determined from the afterglow spectra at various oxygen pressures

from 2 to 7 Torr. The A $^3\Sigma_u^+$ state was also effectively quenched by

mixtures of oxygen, argon and oxygen, helium. This was evident from

the afterglow spectra of oxygen with diluents like argon and helium at

a fixed diluent pressure (6 Torr) and varying oxygen pressure (from

0.2 to 1 Torr). Knowing the quenching rates for oxygen, those for

argon and helium could also be determined. Equation (VI.5) would get

modified when mixture of oxygen/argon or oxygen/helium are used. For

argon and oxygen mixtures, the total quenching rate would become

$$k = k_{Ar} \cdot X~(Ar) + k_{O_2} \cdot X~(O_2) \qquad\qquad VI.6$$

where X is the mole fraction of the gas and it would be pressure

dependent. Using equation (VI.5) and equation (VI.6), k_{Ar} or k_{He} could

be calculated by using

$$k_{Ar}\tau = \cfrac{-k_{O_2}\tau\{\dfrac{I_1}{I_2} \cdot \dfrac{[O]_2^2}{[O]_1^2} \cdot [O_2]_2 \, X_1(O_2) - X_2(O_2)[O_2]_2\} + \{1 - \dfrac{I_1}{I_2}\dfrac{[O]_2^2}{[O]_1^2} \cdot \dfrac{[O_2]_2}{[O_2]_1}\}}{\dfrac{I_1}{I_2} \cdot \dfrac{[O]_2^2}{[O]_1^2} \cdot [O_2]_2 \, X_1(Ar) - X_2(Ar)\,[O_2]_2} \qquad VI.7$$

The values of quenching rates and inverse half-quenching pressures

for argon and helium have been computed for the vibrational bands (5,4),

(4,4) and (4,3) of the Herzberg I system. These values have been

reported in Table VI.2. To the best of our knowledge, no other

laboratory measurements about the quenching rates of A $^3\Sigma_u^+$ state by

Table VI.1

Quenching rates and inverse half-quenching pressures for quenching agent oxygen

(v',v") band of Herzberg I system	$k_{O_2}\tau$ (in Torr^{-1})	k_{O_2} (in cm^3 molec^{-1} sec^{-1})
(5,4)	0.31 ± 0.05	$(5.29 \pm 0.86) \times 10^{-17}$
(4,4)	0.33 ± 0.05	$(5.60 \pm 0.84) \times 10^{-17}$
(4,3)	0.32 ± 0.05	$(5.49 \pm 0.84) \times 10^{-17}$

Table VI.2

Quenching rates and inverse half-quenching pressures for argon and helium

	(v',v") band of Herzberg I system		
	(5,4)	(4,4)	(4,3)
$k_{Ar}\tau$ in Torr^{-1}	3.23 ± 0.53	2.87 ± 0.38	2.82 ± 0.31
k_{Ar} in cm^3 molec^{-1} sec^{-1}	$(5.47 \pm 0.90) \times 10^{-16}$	$(4.86 \pm 0.64) \times 10^{-16}$	$(4.77 \pm 0.53) \times 10^{-16}$
$k_{He}\tau$ in Torr^{-1}	2.95 ± 0.25	2.95 ± 0.16	2.89 ± 0.15
k_{He} in cm^3 molec^{-1} sec^{-1}	$(5.01 \pm 0.43) \times 10^{-16}$	$(5.00 \pm 0.27) \times 10^{-16}$	$(4.90 \pm 0.26) \times 10^{-16}$

argon and helium have been reported in the literature. That is why no comparison with other data is possible.

From Table VI.1 and Table VI.2, it may be interesting to note that k_{O_2} values are much smaller than k_{Ar} or k_{He} values for the same vibrational band. In fact, this should be exactly opposite to what has been observed. It may be recalled that no afterglow spectrum for oxygen alone could be obtained at pressure below 1 Torr while afterglow spectra of oxygen in the presence of diluents like argon and helium was observed at very low oxygen pressures. This is a clear evidence that k_{O_2} should have been larger than k_{Ar} or k_{He}. From this, it is clear that there is an additional quenching by some other agency which has not been taken into account while calculating k_{Ar} or k_{He}. It is assumed that this additional quenching agent may have negligible quenching rate at higher pressures ($\gtrsim 1$ Torr) of molecular oxygen but may have sufficiently larger quenching rates at pressures below 1 Torr. Such a quenching agent for deactivating O_2 (A $^3\Sigma_u^+$) state could be O (^3P) atoms which are produced in larger quantities at lower pressures ranging from 0.2 to 1 Torr.

Inverse Predissociation (Preassociation)

Two atoms approach each other on one potential surface and then make a radiationless transition from the continuous range of energy levels to one of the discrete levels of the emitting state of molecule. This transition occurs when the energy of molecule in continuous range of energy levels, coincides with that of one of the discrete levels. The molecule thus formed could again predissociate until and unless it loses its energy during the life time by emission of radiation. Here all cases of predissociation occur in reverse.

Selection Rules

The radiationless transition from the unstable to the stable state is subject to certain selection rules which must be satisfied if the transition is to occur with appreciable probability. These selection rules differ in some respects from those for radiative transition, being the same as those for perturbation (Kronig, 1928, 1930). These selection rules have been enunciated below:

For state with Hund's case a or b coupling, (Herzberg, 1950), the spin, S, must remain unchanged ($\Delta S = 0$) for strong inverse pre-dissociation or perturbation; that is the multiplicity of the two states must be the same.

Λ, the quantum number of the angular momentum of the electron about the internuclear axis, changes by 0 or ± 1. When the two states have the same Λ and S, the strength of inverse predissociation or perturbation is independent of the rotational energy. When $\Delta\Lambda = \pm 1$, the strength of the inverse predissociation or perturbation increases with increasing rotational quantum number.

In Hund's case **c**, (Herzberg, 1950), the multiplicity and Λ are no longer defined and we have the single rule $\Delta\Omega = 0, \pm 1$.

For transition between Σ or $\Omega = 0$ states the $+ -$ symmetry must be the same.

For individual energy levels the $+ -$ symmetry also remains unchanged.

The rotational quantum number must be the same. This rule has usually been expressed as $\Delta J = 0$. In case b coupling, the rotational energy is determined by K, the quantum number of total angular momentum apart from spin, which is a rigid quantum number, and for transition between two states in case b coupling the additional rule $\Delta K = 0$ is to be expected. In cases a or c, K is no longer a rigid quantum number and the selection rule for K drops out.

These selection rules may be summarized:

(i) $\Delta S = 0$

(ii) $\Delta\Lambda = 0, \pm 1$ case a or b: $\Delta\Omega = 0, \pm 1$ case c

(iii) $\Delta J = 0$, $\Delta K = 0$ (case b only)

(iv) $+ \rightarrow -$, $- \rightarrow -$, $+ \nleftrightarrow -$.

(v) $g \rightarrow g$, $u \rightarrow u$, $g \nleftrightarrow u$. For indentical nucleii.

(iii), (iv) and (v) are strong selection rules, while (i) is an approximate rule whose strength depends inversely on the interaction between S and Λ.

REFERENCES

1   Anketell, J., and Nicholls, R.W., 1970, Rep. Prog. Phys., 33, 269.

2   Barth, C.A., 1964, Ann. Geophys., 20, 182.

3   Bates, D.R., 1951, Mon. Notic. Roy. Astron. Soc., 111, 303.

4   Bates, D.R., 1957, The Threshold of Space, Ed. M. Zelikoff
    (New York : Pergamon), p.14.

5   Bayes, K.D., and Kistiakowsky, G.B., 1960, J. Chem. Phys., 32, 992.

6   Becker, K.H., Fink, E.H., Groth, W., and Kley, D., 1972, Faraday
    Disc. Chem. Soc., 53, 35.

7   Benesch, W., Vanderslice, J.T., and Wilkinson, P.G., 1965,
    Astrophys. J., 142, 1227.

8   Benson, J.M., 1952, J. Appl. Phys., 23, 757.

9   Benson, S.W., 1968, J. Chem. Phys., 48, 1765.

10 Berkowitz, J., Chupka, W.A., and Kistiakowsky, G.B., 1956,
    J. Chem. Phys., 25, 457.

11 Borst, W.L., and Zipf, E.C., 1971, Phys. Rev. A, 3, 979.

12 Brennen, W., and Shane, E.C., 1971, J. Phys. Chem., 75, 1552.

13 Brennen, W., and Shuman, M.E., 1977, J. Chem. Phys., 66, 4248.

14 Broida, H.P., and Gaydon, A.G., 1954, Proc. R. Soc. A, 222, 181.

15 Brown, R.L., 1970, J. Chem. Phys., 52, 4604.

16 Butscher, W., Shih, S., Buekner, R.J., and Peyerimhoff, S.D., 1977,
    Chem. Phys. Lett., 52, 457.

17   Callear, A.B. and Williams, G.J., 1966, Trans. Faraday Soc.,
      62, 2030.

18   Campbell, I.M., and Thrush, B.A., 1967, Proc. R. Soc. A, 296,
      201.

19   Campbell, I.M., and Thrush, B.A., 1967b, Proc. R. Soc. A, 296,
      222.

20   Carrington, T., 1972, J. Chem. Phys., 57, 2033.

21   Chamberlain, J.W., 1961, Phys. of the Aurora and Airglow
      (New York : Academic Press)

22   Chow, K.W., and Smith, A.L., 1971, J. Chem. Phys., 54, 1556.

23   Clyne, M.A.A., Stedman, D.H., 1967, J. Phys. Chem., 71, 3071.

24   Degen, V., 1968, Can. J. Phys., 46, 783.

25   Degen, V., and Nicholls, R.W., 1969, J. Phys. B : Atoms. Molec. Phys.,
      2, 1240.

26   Ding, A., Karlau, J., and Weise, J., 1977, Rev. Sci. Instrum.,
      48, 1002.

27   Dodd, R.W., and Robinson, P.L., 1957, Experimental Inorganic
      Chemistry (New York : Elsevier), p.166.

28   Douglas, A.E., and Herzberg, G., 1951, Can. J. Phys., 29, 294.

29   Gaydon, A.G., 1968, Dissociation Energies and Spectra of Diatomic
      Molecules, 3rd edn. (London : Chapman and Hall), p.184.

30   Gilmore, F.R., 1965, J. Quantue. Spectrosc. Radiat. Transfer,
      5, 369.

31   Golde, M.F., and Thrush, B.A., 1972, Faraday Disc. Chem. Soc.,
      53, 52.

32   Golde, M.F., and Thrush, B.A., 1973, Rep. Prog. Phys., 36, 1285.

33   Greaves, J.C., and Linnett, J.W., 1959, Trans. Faraday Soc., 55, 1338.

34.   Gross, R.W.F., 1968, J. Chem. Phys., 48, 1302.

35   Hand Book of Chemistry and Physics, 1979-1980, Ed. R.C. Weast, 60th edn (Florida : CRC Press, Inc.), p.D-219.

36   Hasson, V., Nicholls, R.W., and Degen, V., 1970, J. Phys. B., 3, 1192.

37   Herman, R., and Herman, L., 1942, Ann. d'Astrophys., 5, 1.

38   Herzberg, G., 1950, 1952, Spectra of Diatomic Molecules (New York : Van Nostrand).

39   Herzberg, G., 1966, Electronic Spectra of Polyatomic Molecules (New York : Van Nostrand).

40   Jarmain, W.R., 1972, J. Quant. Spectrosc. Radiat. Transfer, 12, 603.

41   Jennings, K.R., 1961, Q. Rev. Chem. Soc., 15, 237.

42   Jeunehomme, M., 1966, J. Chem. Phys., 45, 1805.

43   Jonathan, N., and Petty, R., 1969, J. Chem. Phys., 50, 3804.

44   Kaufman, F., and Kelso, J.R., 1957, J. Chem. Phys., 27, 1209.

45   Kaufman, F., and Kelso, J.R., 1958, J. Chem. Phys., 28, 510.

46   Kronig, R. de L., 1928, Z. Physik, 50, 347.

47   Kronig, R. de L., 1930, Z. Physik, 62, 300.

48   Knudsen, M., 1910, Ann. Phys., 31, 205; ibid., 31, 633.

49   Lambert, J.D., 1977, Vibrational and Rotational Relaxation in Gases (Oxford : Clarendon Press), p.4.

50   Lawrence, G.M., Barth, C.A., and Argabright, V., 1977, Science, 195, 537.

51   Lewis, E.P., 1900, Astrophys. J., 12, 8.

52   Lozier, W.W., 1933, Phys. Rev., 44, 575.

53   Meyer, J.A., Stedman, D.H., and Setser, D.W., 1969, Astrophys. J., 157, 1023.

54   Morren, M.A., 1865, Ann. Chem. Phys., 4, 293.

55   Nickerson, J.L., 1935, Phys. Rev., 47, 707.

56   Noxon, J.F., 1962, J. Chem. Phys., 36, 926.

57   Palmer, H.B., 1967, J. Chem. Phys., 47, 2116.

58   Pearse, R.W.B., and Gaydon, A.G., 1965, The Identification of Molecular Spectra, 3rd edn. (London : Chapman and Hall).

59   Rayleigh, R.J.S., 1911, Proc. R. Soc. A, 85, 219.

60   Saxon, R.P., and Liu, B., 1977, J. Chem. Phys., 67, 5432.

61   Shui, V.H., Appleton, J.P., and Keck, J.C., 1970, J. Chem. Phys., 53, 2547.

62   Slanger, T.G., 1978a, Science, 202, 751.

63   Slanger, T.G., 1978b, J. Chem. Phys., 69, 4779.

64   Slanger, T.G., and Black, G., 1981, J. Chem. Phys., 74, 6517.

65   Smith, A.L., and Meriwether, J.W., 1965, J. Chem. Phys., 42, 2984.

66   Smith, F.T., 1962, Disc. Faraday, Soc., <u>33</u>, 183.

67   Tanaka, Y., and Yoshino, K., 1963, J. Chem. Phys., <u>39</u>, 3081.

68   Ung, A.Y.M., 1976, J. Chem. Phys., <u>65</u>, 2987.

69   Ung, A.Y.M., 1980, J. Chem. Phys., <u>72</u>, 3731.

70   Wu, H.L., and Benesch, W., 1968, Phys. Rev., <u>172</u>, 31.

71   Young, R.A., and Black, G., 1966, J. Chem. Phys., <u>44</u>, 3741.

72   Young, R.A., and Sharpless, R.L., 1962, J. Geophys. Res., <u>67</u>, 3871.

73   Young, R.A., and Sharpless, R.L., 1963, J. Chem. Phys., <u>39</u>, 1071.

LIST OF PUBLICATIONS

1. Afterglow spectra of nitrogen at different temperatures
   and pressures

   Vijay Kumar and Ajai Kumar

   Submitted for publication to

   J. Chem. Phys.

2. Measurement of dissociation energy of molecular nitrogen

   Vijay Kumar and Ajai Kumar

   Submitted for publication to

   J. Chem. Phys.

3. Quenching of (12,8) and (11,7) bands of B $^3\Pi_g \to$ A $^3\Sigma_u^+$
   system of nitrogen by NO at 88°K

   Vijay Kumar and Ajai Kumar

   Submitted for publication to

   J. Chem. Phys.

4. Deactivation of A $^3\Sigma_u^+$ state of oxygen by oxygen, argon
   and helium

   Vijay Kumar and Ajai Kumar

   Submitted for publication to

   J. Chem. Phys.